36518

NATIONAL LIBRARY
OTTAWA

CANADA

BIBLIOTHÈQUE NATIONALE
OTTAWA

NAME OF AUTHOR....YANNIS FAINEKOS.....

TITLE OF THESIS....Synchronization of Earth Stations to a Switching Satellite using Non-Coherent Frequency shift keying

UNIVERSITY....McMaster, Hamilton, Ont.

DEGREE FOR WHICH THESIS WAS PRESENTED....M. Engineering

YEAR THIS DEGREE GRANTED....1977.....

(Signed)....Fainekos.....

PERMANENT ADDRESS:

1310 Pinecrest Rd #1510
Ottawa, K2C 3N8

.....

DATED. April 25th 1977

NL-91 (10-68)

NOTICE

The quality of this microfiche is heavily dependent upon the quality of the original thesis submitted for microfilming. Every effort has been made to ensure the highest quality of reproduction possible.

If pages are missing, contact the university which granted the degree.

Some pages may have indistinct print especially if the original pages were typed with a poor typewriter ribbon or if the university sent us a poor photocopy.

Previously copyrighted materials (journal articles, published tests, etc.) are not filmed.

Reproduction in full or in part of this film is governed by the Canadian Copyright Act, R.S.C. 1970, c. C-30. Please read the authorization forms which accompany this thesis.

THIS DISSERTATION
HAS BEEN MICROFILMED
EXACTLY AS RECEIVED

AVIS

La qualité de cette microfiche dépend grandement de la qualité de la thèse soumise au microfilmage. Nous avons tout fait pour assurer une qualité supérieure de reproduction.

S'il manque des pages, veuillez communiquer avec l'université qui a conféré le grade.

La qualité d'impression de certaines pages peut laisser à désirer, surtout si les pages originales ont été dactylographiées à l'aide d'un ruban usé ou si l'université nous a fait parvenir une photocopie de mauvaise qualité.

Les documents qui font déjà l'objet d'un droit d'auteur (articles de revue, examens publiés, etc.) ne sont pas microfilmés.

La reproduction, même partielle, de ce microfilm est soumise à la Loi canadienne sur le droit d'auteur, SRC 1970, c. C-30. Veuillez prendre connaissance des formules d'autorisation qui accompagnent cette thèse.

LA THÈSE A ÉTÉ
MICROFILMÉE TELLE QUE
NOUS L'AVONS REÇUE

SYNCHRONIZATION OF EARTH STATIONS

SYNCHRONIZATION OF EARTH STATIONS TO A SWITCHING SATELLITE USING NON-COHERENT FREQUENCY SHIFT KEYING

By

Yannis Fainecos, B.Sc.

A Thesis

Submitted to the Faculty of Graduate Studies

in Partial Fulfilment of the Requirements

for the Degree

Master of Engineering

McMaster University

February 1977

Master of Engineering (1977) McMaster University
Hamilton, Ontario

TITLE: Synchronization of Earth Stations to a Switching Satellite using Non-Coherent Frequency Shift Keying

AUTHOR: Yannis Fainecos, B.Sc.
National University of Athens.

SUPERVISOR: Dr. S. S. Haykin

NUMBER OF PAGES: viii, 161

ABSTRACT

In a space division multiple access/spacecraft switched-time division multiple access (SDMA/SS-TDMA) satellite system, precise synchronization between the satellite switching sequence and the earth stations is required. Fine synchronization can be achieved by transmitting non-coherent frequency shift keying (FSK) signals. The timing error between the satellite and the earth station time bases is defined on-board the satellite by the sync-window modulation of the sync bursts (FSK signals). A measure of the timing error, i.e. the error voltage, is obtained at the receiver and fed to the timing circuits. Depending on the value of the error voltage, the timing circuits shift the earth station time base accordingly so as to reduce the timing error. This procedure is repeated until synchronization is achieved, i.e., the timing error becomes zero.

Two sources of noise (uplink and downlink) are considered in this synchronization loop. The noise affects the number of iterations required to achieve synchronization as well as the accuracy of the synchronization in the steady state. The study is supported by a digital computer simulation of the envelope-detected signal in the receiver.

ACKNOWLEDGEMENTS

The author wishes to express his appreciation and sincere thanks to his supervisor Dr. S.S. Haykin for his helpful guidance throughout this work.

He also greatfully acknowledges the numerous discussions and valuable suggestions and remarks given by Dr. C.R. Carter.

The financial support by the National Research Council is also appreciated.

TABLE OF CONTENTS

LIST OF ILLUSTRATIONS

CHAPTER I

INTRODUCTION

Communications via satellites have experienced a rapid growth over the past ten years and are also expected to continue to grow rapidly in the future. To meet the future needs in high capacity communication satellite systems, new efficient modulation and multiple-access techniques must be introduced [1]. This is all the more so because the presently used spectrum for satellite communications is becoming overcrowded and inadequate. A lot of study has been devoted to make possible the expansion of this spectrum towards higher frequencies [1],[2]. Microwave technology seems to be ready to supply the satellite designers with the necessary antennas, tubes and components so that future satellite systems will make wider use of frequencies above 10 GHz [3].

The use of millimeter wavelengths might also enable the optimum multiple-access technique for high-capacity satellite channels to be developed. Indeed, by using shorter wavelengths, the size of microwave antennas is reduced and it is feasible to employ highly-directive antennas producing spot-beam zones, thereby enabling the realization of a multiple-access system called space-division multiple-access (SDMA) [4].

In SDMA systems, portions of the spectrum can be reused by the various spot-beam zones and bandwidth conservation can be achieved. To realize the full benefits of frequency reuse, SDMA must be combined with a multiple-access modulation technique (e.g., time-division, frequency

division).

If time-division multiple-access (TDMA) is used, the satellite must be provided with a high-speed microwave switching matrix to rapidly rearrange the connections among receiving and transmitting beams [2],[5]. This combination of space and time division multiple-accesses is called Space Division Multiple Access/Satellite Switched — Time Division Multiple-Access (SDMA/SS-TDMA).

In SDMA/SS-TDMA a high-degree of synchronization between the satellite and the earth stations is required, so that signals do not overlap at the satellite transponder.

In this thesis, a synchronization technique using non-coherent Frequency-Shift-Keying (FSK), suitable for use in any SDMA/SS-TDMA system, is studied.

1.1 DIFFERENT METHODS OF MULTIPLE-ACCESS

The purpose of multiple-access is that many user-earth stations can access the same satellite transponder simultaneously without interfering with each other.

The efficiency, capacity, and cost of a given satellite network are directly related to the M/A (multiple-access) scheme being used. Thus, the selection of a M/A technique is a system -analysis problem and involves various areas of communication technology, operational doctrines and systems economics. Fig. 1.1 shows some of the areas which contribute to the analysis and selection of the multiple-access system [6].

Multiple-access modulation systems can be divided into the following broad areas [7],[8]:

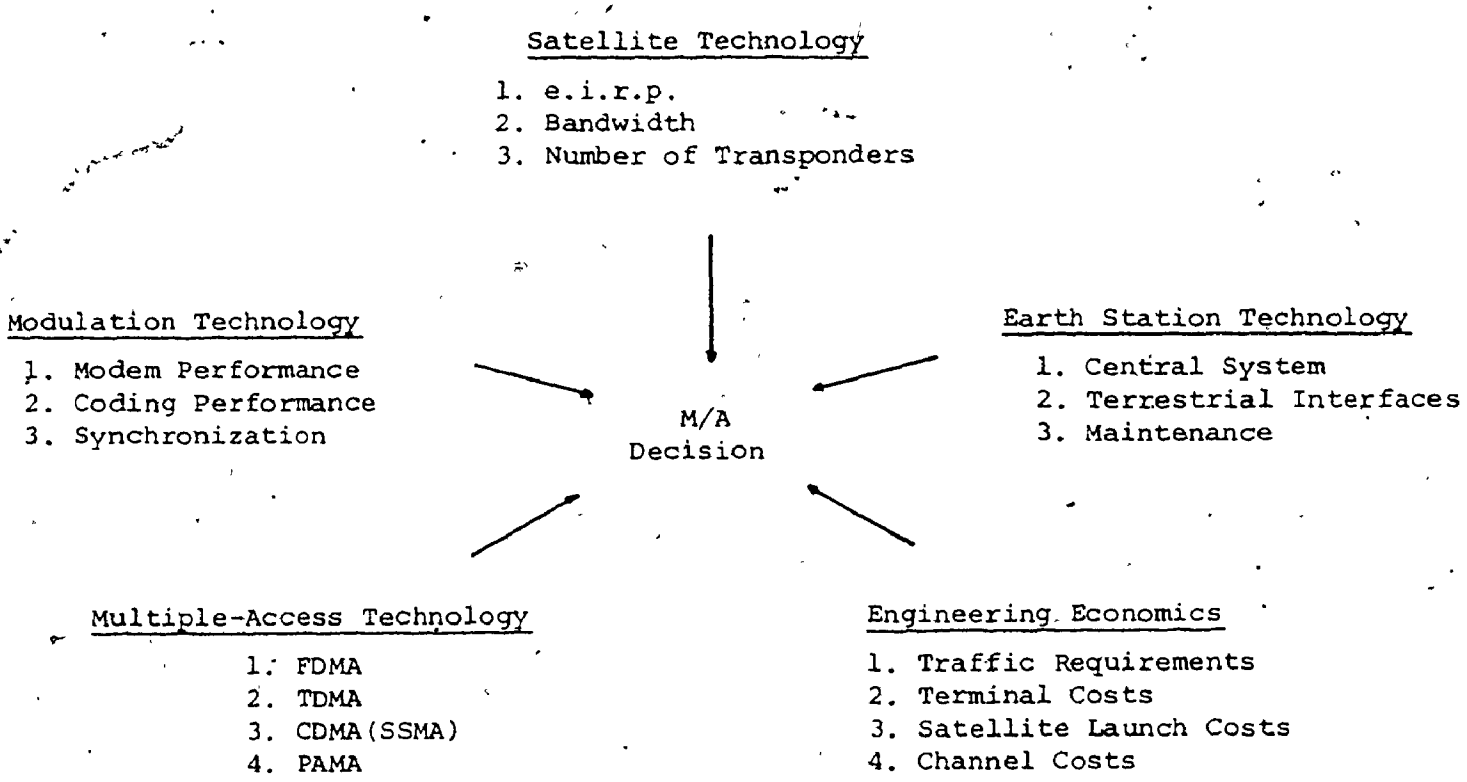

Fig. 1.1 Multiple-access: system design and considerations

1. Frequency Division Multiple Access (FDMA)
2. Time Division Multiple Access (TDMA)
3. Pulse (or Packet) Address Multiple Access (PAMA)
4. Code Division Multiple Access (CDMA)
   (a. constant-envelope spread-spectrum and
   b. frequency hopping)

Comparing the above M/A techniques, FDMA and TDMA are found to be suitable for systems requiring high channel capacity but having few fluctuations in traffic, whereas PAMA and CDMA are used in systems with a large number of users having rapid changes in traffic requirements.

1.1.1 Frequency Division Multiple Access

FDMA is a well-known method of separating signals in radio-communications. It has been used successfully as the only multiple-access system in the INTELSAT network*. The main advantage of FDMA is that new or complex earth station equipment are not required. For analog FM message modulation, the existing hardware is adequate since only FM transmitters and receivers are required.

In FDMA, the satellite transponder bandwidth is divided into a number of non-overlapping frequency bands which constitute access channels [8]. Even though the assignment of different frequency bands as a means of separating radio-signals is a conventional communications technique, major problems arise in satellite communications. These problems are due to the nonlinear input-output characteristics of the travelling wave tube

* INTELSAT, the International Telecommunications Satellite Organization was formed in 1964 by 14 nations. In 1976, INTELSAT consists of 92 member nations.

amplifier (TWTA) in the satellite transponder. When several carrier signals are processed simultaneously by the transponder, they interact with each other, producing intermodulation noise and crosstalk. Moreover, if their input power levels are not the same, the signal with the nighest power tends to suppress the weaker ones. Linear applification can be approximately obtained by backing off the input signal level. Also, channelized systems may be used (e.g., SPADE, [9]) with adequate spacing so that the intermodulation noise will fall outside the signal band. In this case, however, much of the transponder bandwidth will be wasted and the capacity of the system reduced.

1.1.2 Time Division Multiple Access (TDMA)

Theoretically, all problems encountered in FDMA can be eliminated and a larger capacity can be obtained if at any instant there is only one carrier signal present at the satellite transponder. This can be achieved by using time division multiple access.

In TDMA, each carrier signal occupies the whole transponder bandwidth for a finite period of time called time slot. Thus many earth stations can transmit their signals which arrive at and pass through the satellite transponder in a sequential, non-overlapping mode [10]. Transmission occurs periodically at a definite rate called "frame repetition rate". The period of time between two successive transmissions is then called "frame length". For real-time voice transmissions, the frame length is equal to 125 μs, corresponding to the sampling rate of 8 KHz. For data transmissions, frame length may be longer (up to 750 μs) and a saving in the overall guard time will be obtained. Store-and-forward

operations could also be employed. With TDMA, transmission must be of digital form, thus analog messages, such as voice, must be digitized and transmitted in the form of pulses or bursts.

The major problem with TDMA is to maintain the non-overlapping, sequential processing of the signals at the transponder. To ensure that carrier signals will not overlap at the satellite input, synchronization between the satellite and the earth stations must be achieved, and guard times between adjacent time slots must be introduced.

1.1.3 Pulse Address Multiple Access (PAMA)

Pulse (or Packet) Address Multiple Access is a method in which pulse patterns are generated in the time-frequency plane and used as addresses. The frequency spectrum is divided into numbered bands, and pulses or packets of digits are transmitted in the various bands at preassigned times.

PAMA is suitable for computer-communication networks employing satellites [11]. Synchronization is not necessary for PAMA systems but network timing improves their performance (e.g., "pure" ALOHA [12] versus "slotted" ALOHA [13]).

1.1.4 Code Division Multiple Access (CDMA)

In CDMA, the carrier signals are frequency- or phase- modulated in such a way that their spectra occupy a common bandwidth. It is also possible that these signals overlap in time. Demultiplexing of the signals at the earth stations is achieved by correlation with some form of prearranged code which was impressed upon them.

Two types of CDMA may be considered [6]:

A. Constant-envelope, spread spectrum

In this type of CDMA, each carrier signal occupies the entire bandwidth of the satellite transponder. The multiple-access modulation has the form of a pseudorandom sequence of binary digits (PN sequence) which biphase modulates a constant amplitude carrier. The intended receiving earth station employs a copy of this pseudorandom sequence to separate the desired signal from the other carrier signals which were transmitted by the satellite.

B. Frequency-Hopping CDMA

In Frequency-Hopping CDMA, the multiple-access is accomplished by frequency hopping a pattern of pulses over the entire bandwidth. The hopping is controlled by a pseudorandom PN sequence [6].

CDMA is impervious to jamming signals, since the correlator tends to spread and weaken the jammer. Consequently, CDMA is well suitable for military applications.

1.1.5 Space Division Multiple Access (SDMA)

The multiple-access systems, discussed above, are based on modulation techniques. Separation of the carrier signals at the satellite can also be accomplished on the basis of geometry. This method, which utilizes the spot-beam zone technology, is called Space Division Multiple Access (SDMA).

The use of super high uplink and downlink frequencies (millimeter wavelengths) reduces the size of the microwave antennas, thus highly-

directive antennas can be employed, producing multiple spot-beam zones (Fig. 1.2). The use of spot-beam antennas provides two major advantages

1. increase in effective isotropic radiated power (e.i.r.p.), and
2. frequency reuse.

In Fig. 1.3.a the configuration of a conventional multitransponder satellite system using global-coverage antennas is shown [4].

For N transponders each one having bandwidth B, a total satellite bandwidth 2NB is required. Fig. 1.3.b shows the utilization of spot-beam antennas. The total satellite bandwidth now required is 2B. Thus, with SDMA an N-fold saving in spectrum is obtained.

It is possible to combine SDMA with a multiple-access modulation technique, such as FDMA or TDMA, so that a maximum efficiency and high satellite capacity would be achieved.

If FDMA is combined with SDMA, filters must be used on-board the satellite to separate the received signals and recombine them in different arrangements for each transmitting beam [2].

If TDMA is used along with SDMA, the satellite must be supplied with multiple microwave switch matrix (MSM) decks, each connecting a number of up-link beams to the corresponding down-link beams in a variety of configurations [5]. This is the so-called transponder-switched method. A second approach to accomplish interconnectivity among the earth stations of the same spot-beam zone and/or among earth stations in different spot-beam zones is to employ a variable pattern, single beam, spot-beam scanning antenna. A buffer memory is also required on-board the satellite to store the information until the scanning antenna illuminates the appropriate

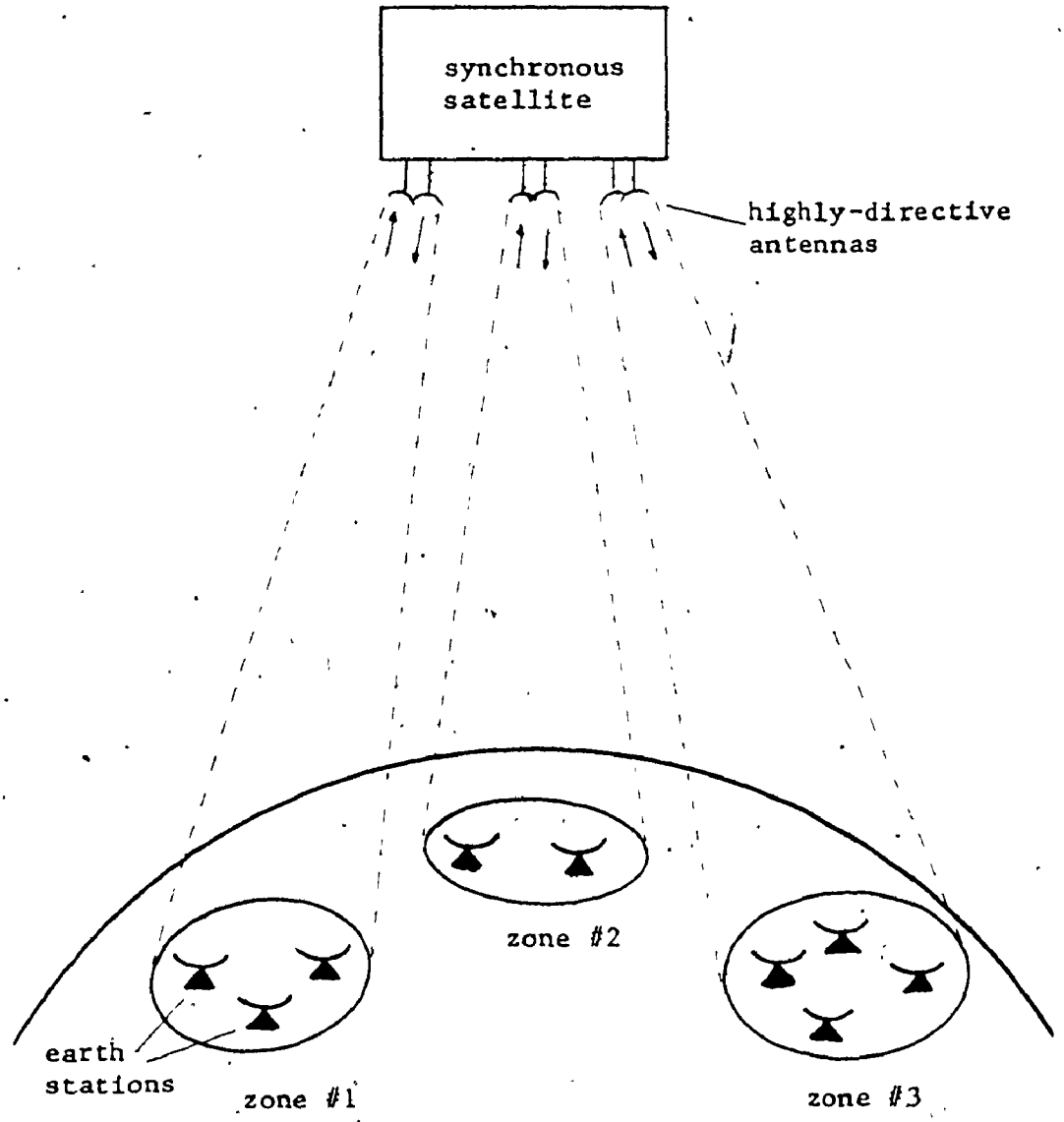

Fig. 1.2 SDMA satellite communication system

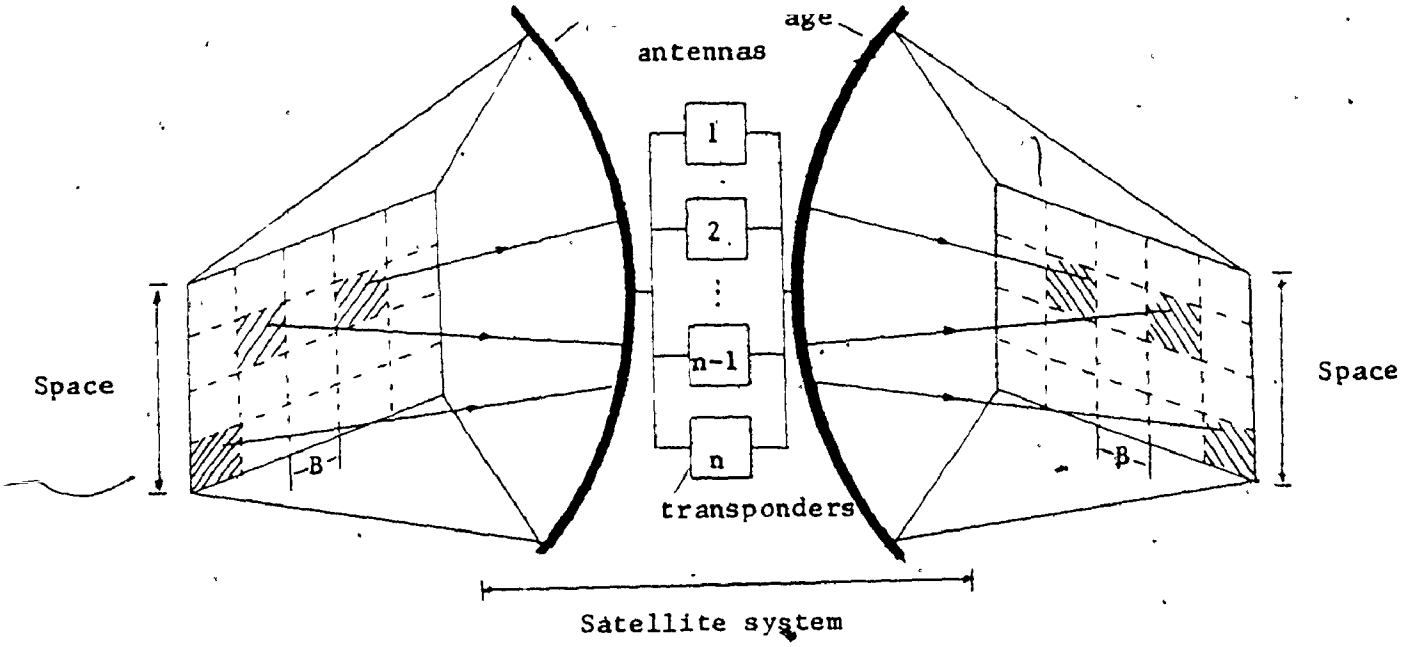

Fig. 1.3.a Use of frequency spectrum with global-coverage antennas

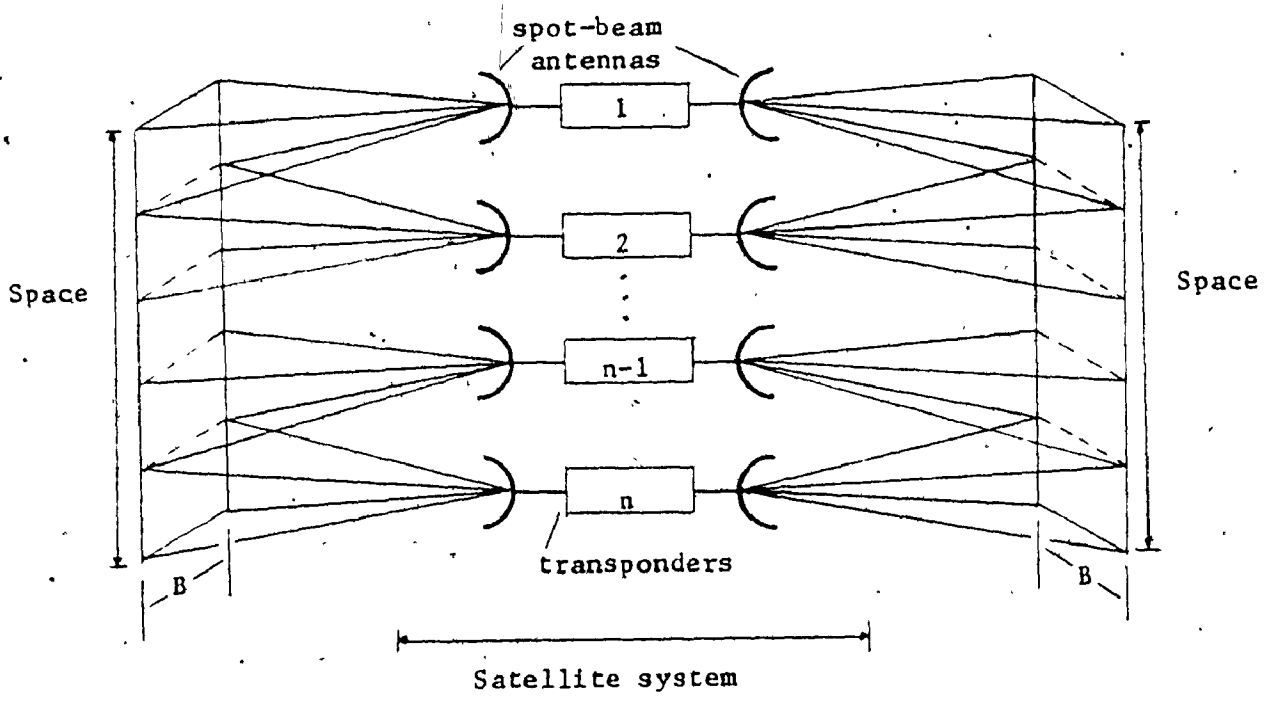

Fig. 1.3.b Frequency spectrum reuse with spot-beam antennas

earth station. This approach is called beam-switched method and can only be used by systems with light traffic [6].

It is strongly believed that SDMA will be used in the next generation of INTELSAT satellites.

It is also expected that SDMA will be combined with TDMA (SDMA/SS-TDMA: Space Division Multiple Access, Satellite-Switched (Transponder-Switched Method), Time Division Multiple Access, [14]), so that the desired increase in satellite capacity may be achieved, without increasing the spacecraft's weight and launching costs.

The SDMA/SS-TDMA system is shown in Fig. 1.4.

1.2 DESCRIPTION OF THE SWITCHING SATELLITE

A satellite operating in an SDMA/SS-TDMA system (Transponder-Switched method) must be supplied with two major configurations. A microwave switching matrix (MSM) and a distribution control unit (DCU). Memory, buffer/decoder, time base, and Telemetry & Command Units are also required [14]. An SDMA/SS-TDMA system is shown in Fig. 1.4.

The uplink and downlink beams are interconnected under the DCU's reprogrammable control. At the beginning of each frame length (see Section 1.1.2), a time interval (1-6 us) is reserved for the synchronization signal (sync burst). During this synchronization interval (called sync window), the MSM connects each spot-beam zone's uplink to its corresponding downlink. Thus all sync windows (one sync window for each spot-beam zone) occur simultaneously. This sync window configuration is used when each earth station obtains synchronization independently of all the others.
If three control stations are used for system synchronization

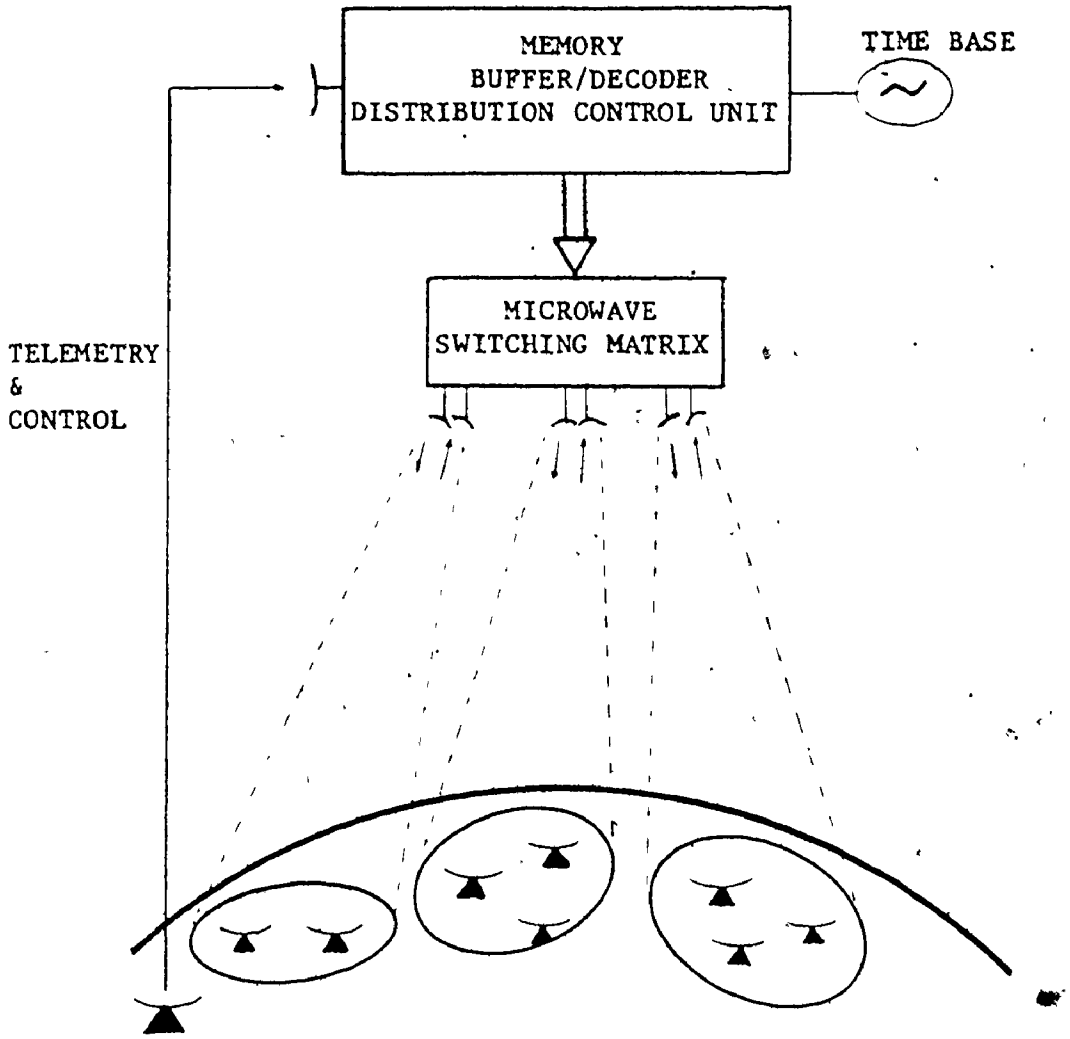

Fig. 1.4 SDMA/SS-TDMA satellite communication system

(see next Section), a modified sync window is required, i.e., during the synchronization interval all satellite receivers must be connected to all satellite transmitters. Sync window is a unique and important SDMA/SS-TDMA feature, quite necessary for the system synchronization.

A temperature-compensated crystal oscillator provides the satellite time base.

Telemetry Command is used to monitor the distribution control unit. Telemetry controls the memory performance and verifies the reception of new memory data before it is transferred to memory. The Command section generates control signals for memory content data transmission, new data load, data transfer to memory and direct switching matrix ground control.

Detailed description of an SDMA/SS-TDMA system developed by COMSAT Laboratories is given in [14].

1.3 PREVIOUS WORK RELATED TO SYNCHRONIZATION OF A SWITCHING SATELLITE

The use of Time Division Multiple Access and the synchronization problem associated with such an implementation have been studied since the early days of satellite communications [15],[16],[17],[18]. A particular synchronization technique is described in [15]. The satellite or a master station transmits a sync burst (unique word) which defines a particular point in time, i.e., the beginning of the frame period. This unique word is received by all the stations in the system which place their transmissions within their assigned time intervals (data windows). The major source of error in such a system is the error in predicted de-

lay (one way delay is the time required for a signal to travel to or from the satellite to the earth station = 135 ms) which does not exceed ± 100 ns.

G. Gabbard et al. (1968) designed and tested a burst synchronizer. Computer-predicted satellite range was used and the comparison of the master and the local stations' unique words provided a tracking facility to reduce delay uncertainties [16],[17],[18]. Results of the field test gave burst synchronization accuracies of ± 220 ns when the synchronizer was used with a synchronous satellite with eccentricity 0.0028 (INTELSAT I) and accuracies of better than ± 2 μs when used with a six-hour medium altitude satellite.

In an SDMA/SS-TDMA system, two kinds of synchronization functions must be considered [19],[20]. First, synchronization among spot-beam zones, i.e., between the earth stations and the distribution control unit (DCU) which drives the microwave switching matrix (MSM) on-board the satellite, and, second, synchronization among the stations in the same spot-beam zone. The first is a unique feature of a SDMA/SS-TDMA system, while the latter is simply the synchronization function used in the conventional TDMA systems which essentially utilizes the techniques discussed above.

Two methods have been suggested for achieving synchronization in an SDMA/SS-TDMA system. The first approach (proposed by Shimaski and Rapuano, COMSAT Laboratories [20]) is to require each earth station in the system to obtain synchronization independently of all the others. (Although, originally it was suggested that one earth station in each spot-beam zone should act as a reference station to achieve synchronization

among spot-beam zones, followed by synchronization among the earth stations of the same zone [19]. Using the sync window the concept of a reference station would be eliminated [20].)

In the second method three control stations are employed preferably located in different spot-beam zones [21]. This method requires that the sync window on-board the satellite must be modified so all satellite receivers are interconnected to all satellite transmitters for its duration.

(a) System with independently synchronized stations

Synchronization among spot-beam zones and among earth stations in the same zone can be obtained if each earth station in the system transmits its own signals and thus achieves synchronization independently of all the other stations.

The synchronization signals (sync bursts) have two distinctive features [20]. The first is a different code or different frequency and it is used to identify them with the transmitting station. The second is the time built-in reference which makes possible a timing comparison (i.e., define a timing error) between the satellite and earth station time bases.

The synchronization procedure can be divided into three modes of operation:

(a) the coarse search mode (initial synchronization),

(b) fine search mode (fine adjustments), and

(c) tracking mode.

Coarse search provides the earth station with an estimate of the satellite's

time base, i.e., the sync window's occurrence. Its function is to ensure that the sync bursts will pass through the sync window, at least partially. Once this is accomplished, the fine adjustments are initiated.

One-way-trip delay after its transmission, the sync burst reaches the satellite where it is pulse-time modulated by the sync window. Then, it is looped back to the same spot-beam zone where it is detected by the station which originally transmitted it. A measure of the timing error is now possible at the earth station and proper adjustments are made to shift the station's time base and reduce the timing error. When this process is completed, another sync burst (or set of sync bursts) is transmitted and the procedure is repeated until the timing error is minimized. Then the tracking network is activated, to further reduce the timing error eliminating the satellite's motion effects.

In such a system, where each station is required to achieve synchronization independently of all the others, using the technique described above, several problems arise [22]:

a. If more than one station of the same spot-beam zone perform synchronization procedures at the same time, there is a possibility that their sync bursts have to be processed by the same satellite transponder simultaneously. Although this is feasible, i.e., operating in an FDM configuration, intermodulation noise and crosstalk are created, due to the non-linearity of the TWT amplifier.

b. There exist as many synchronization signals as the earth stations in the same spot-beam zone. Thus, a restriction must be made upon the number of users (stations) in the given zone due to the transponder

bandwidth.

c. The guard time between data windows increases proportionately to the number of earth stations.

d. Interference in the data windows is produced first when a station initially attempts to obtain synchronization (coarse-search mode) and second when synchronization is lost and data bursts are transmitted in wrong data windows. This loss of synchronization cannot be detected before one round trip time (270 ms) due to the propagation delay of the signals.

(b) System using three control stations

It has been shown [21] that synchronization can be accomplished when three stations (control stations) are used. Thus, all the disadvantages (except (d) above) of the system described previously are eliminated. The tradeoffs are increased complexity in the synchronization equipment of the earth stations and a modified sync window onboard the satellite.

A modified sync window simply provides interconnection of all the satellite receivers to all satellite transmitters for the duration of the conventional sync window (i.e., beginning of each frame).

Any earth station in the system can achieve precise synchronization if two conditions are fulfilled:

a. The exact range from the earth station to the satellite (better still the one-way propagation delay) is known.

b. A reference signal passing through the modified sync window is available.

When an earth station requires synchronization, three signals giving the values of the one-way propagation delay between the satellite and each control station must be received. The propagation delay T_D between the station about to be synchronized and the satellite is then calculated [21], [22]. Finally, synchronization is obtained by advancing the station's time base by an amount equal to twice the propagation delay T_D relative to the reference signal.

Essentially, both of the techniques described above require that one station (either individual or control) achieves synchronization. Thus a synchronization loop, operating in a feedback control fashion, must be established. A configuration of a sync loop, proposed and designed by Rapuano and Shimasaki [20], was briefly discussed in Section 1.3(a). A detailed study of such an implementation was carried out by Carter [22]:

A new method for initial synchronization (coarse search) using coded search signals was introduced [23]. The behavior of the synchronization loop in the fine search mode employing coherent PSK and coherent FSK sync bursts was explored using the concept of error detection characteristics [24]. When the fine synchronization is completed, a tracking network can be matched to the timing circuits to eliminate timing errors caused by satellite motion [25]. A laboratory model was designed and constructed and experimental results were found to agree with the theoretical predictions [26].

CHAPTER 2

SYNCHRONIZATION LOOP FOR FINE ADJUSTMENTS USING NON-COHERENT FREQUENCY SHIFT KEYING (NCFSK)

An earth station-satellite-earth station loop, suitable for fine synchronization in a SDMA/SS-TDMA system, must include:

(a) sync burst generator and transmitter at the earth station,

(b) a sync window connection on-board the satellite,

(c) demodulator and detector at the earth station, and

(d) timing circuits to perform the proper adjustments to reduce the timing-error between the earth station and satellite time bases.

2.1 FREQUENCY SHIFT KEYING (FSK) IMPLEMENTATION

Many types of signals suitable for fine synchronization have been suggested [27]. Amongst them, phase shift keying (PSK) and frequency shift keying (FSK) signals are suitable for use as sync bursts: they are easy to generate and detect, and the transition between the two phase shifts or carrier frequencies constitutes an excellent time built-in reference. Moreover, the use of FSK pulses (instead of PSK) eliminates the problem of sync resolution due to carrier and bit recovery time. It also provides a possible frequency division multiplexing (FDM) of the sync bursts which originated from different stations at the same spot-beam zone, thus sharing the same sync window (see Section 1.3a). This can be accomplished by assigning a different pair of intermediate frequencies (consequently different RFs as well) to each station in the zone [19].

According to the detection schemes being used, two possible FSK implementations exist: noncoherent and coherent FSK. In a noncoherent detection, a pair of bandpass filters are used separately tuned to the two carrier frequencies. The filter outputs are envelope-detected and fed to a decision device. For a coherent (or synchronous) detection of an FSK signal, the i-f phase of each possible received signal must be precisely known. In every satellite system, frequency conversion (uplink to downlink) occurs on-board the satellite, where a possibly unreliable oscillator is being used. Moreover, transmission takes place over large distances and through fading media. Thus, phase coherence is difficult to maintain. Consequently, noncoherent detection is advantageous.

2.2 MODEL OF THE SYNCHRONIZATION LOOP

The complete synchronization loop is shown in Fig. 2.1. The FSK sync bursts, generated at the sync burst generator, consist of two parts corresponding to the two intermediate frequencies. A sync burst is generated at the beginning of each frame, its exact occurrence being controlled by the timing circuits to agree with the earth station time base. Then the sync burst is mixed with the uplink frequency, amplified at the output (uplink) amplifier and transmitted towards the satellite. The uplink path is assumed to produce only space delay (time delay) and space attenuation. On-board the satellite the signal is perturbed by the uplink noise at the satellite's input amplifier, and its carrier frequency is converted to the appropriate downlink. Then, it is time-

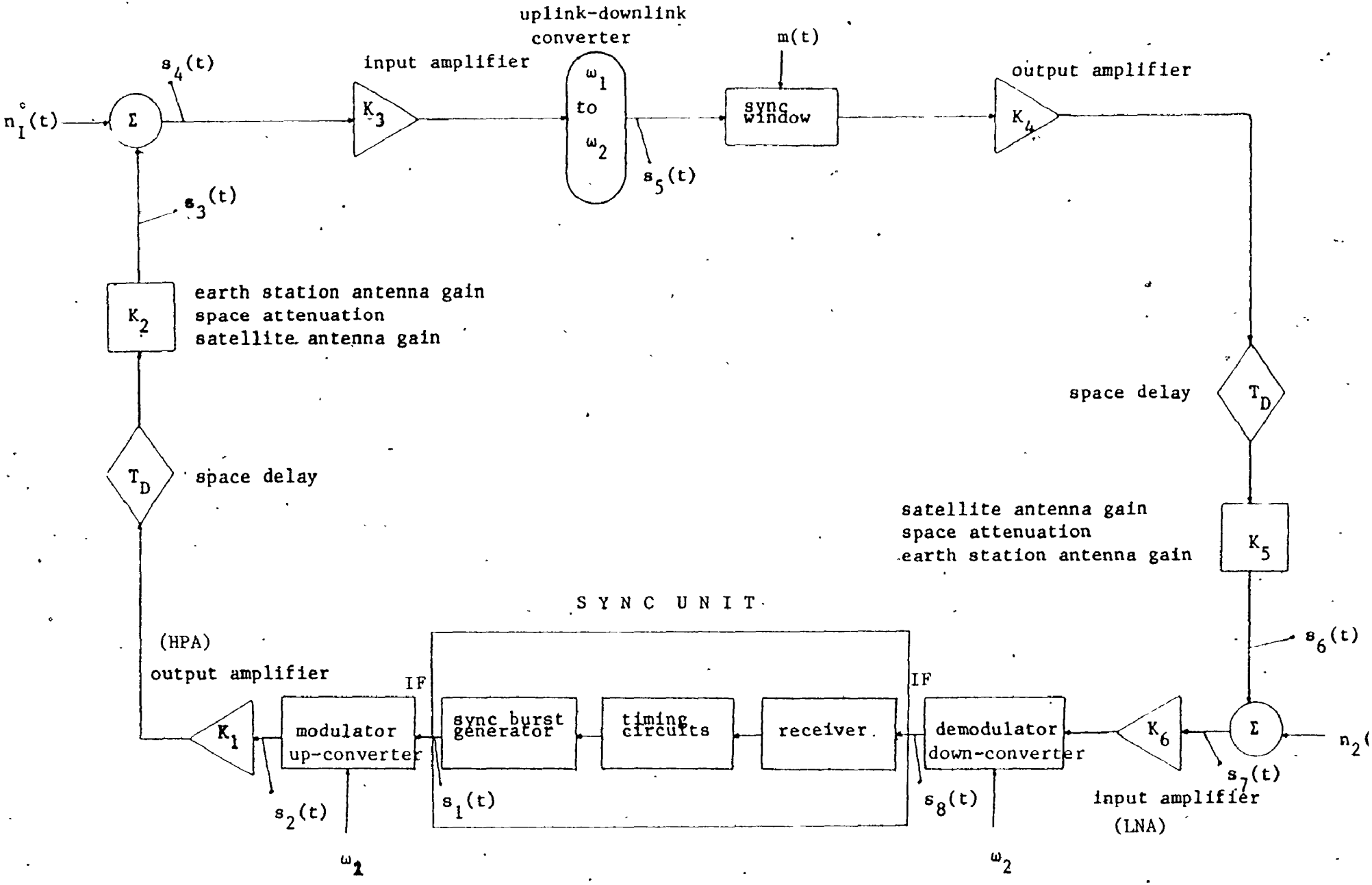

Fig. 2.1 Synchronization loop

pulse modulated by the sync window. Sync window modulation defines the timing error between the earth station and satellite time bases. The sync window modulated signal is amplified at the downlink amplifier and transmitted. Again the downlink path is assumed to produce only space delay and space attenuation. The signal received by the earth is perturbed by the downlink noise, amplified and demodulated. The IF signal is then processed at the receiver to yield the error voltage which is a measure of the timing error. This error voltage is used by the timing circuits to adjust the earth station's time base and reduce the timing error.

For a better system performance, instead of one sync burst, a train of L sync bursts may be used, having a repetition interval equal to the frame length (i.e., one sync burst at the beginning of each frame). The L noisy sync bursts are averaged in the video integrator (see Section 3.5, equation 3.29).

2.3 THE RECEIVER

The receiver portion of the earth station sync unit consists of

(a) the input gate,

(b) the noncoherent-dual filter FSK detector, and

(c) the video integrator (Fig. 2.2).

The input gate provides a train of pulses, being generated in the timing circuits and having a repetition interval equal to the frame length. The function of the input gate is to pass all of the sync window modulated signal and reject the noise, so that unnecessary processing

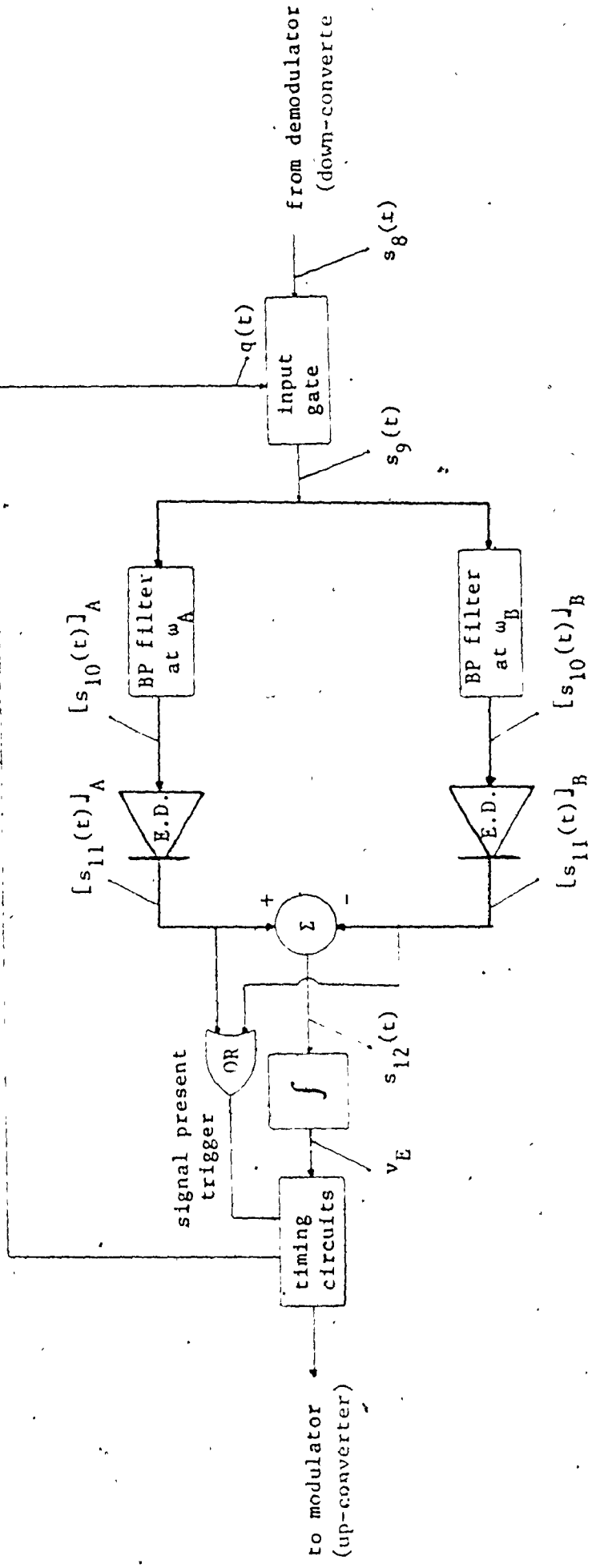

Fig. 2.2 Receiver

of noise (mostly downlink noise) is avoided. A way to define the input gate is to utilize the timing information obtained by previous received signals starting with the coarse search mode. Thus the input gate can generate one-way trip delay after the sync window occurrence has been established. Another technique is to ignore this timing information and generate the input gate a round-trip delay after the sync burst transmission. In this way, a larger input gate width is required to ensure that no useful signal will be rejected. In practice, the first technique is preferred since it provides minimum processing of noise.

The noncoherent FSK detector consists of a pair of bandpass filter-envelope detector branches and a summer [28].

The bandpass filters are tuned to the FSK intermediate frequencies. A nonlinear device (e.g., diode-resistor) followed by a low-pass filter can be used as envelope detector. The summer constitutes the binary-decision device where the two envelopes (signal plus noise envelope and envelope of noise) are subtracted. The video integrator is an important element of the synchronization loop. It eliminates the time dependence of the envelope pulses which were obtained from the detector and yields a voltage (called error voltage) which is related to the timing error.

2.4 TIMING ADJUSTMENTS

Every time a sync burst, or rather a train of sync bursts, makes a complete round trip and reaches the earth station it is bearing a new timing information, i.e., the timing error. As a measure of this timing

error, an error voltage can be provided by the receiver. It is the function of the timing circuits to utilize this error voltage and shift the earth station time base to reduce the timing error. The timing circuits are shown in Fig. 2.3.

After the video integrator processes L pulses, the error voltage, obtained at its output, is fed to the control terminal of the VCO (Voltage Controlled Oscillator) through the timing adjustment gate, for a duration T_G [24]. During this period, the frequency of the VCO changes by an amount proportional to the error voltage: If the error voltage is negative the output frequency of the VCO is less than its free running frequency and the counter reaches full count later than normal. Since the counter and the decoder trigger the sync burst generator, the sync bursts will be also generated later than normal and for an amount of time proportional to the error voltage. On the other hand, if the error voltage is positive, the sync bursts will be generated earlier than normal. The mode control logic provides the sync unit with the number of sync bursts to be transmitted, the input gate, and the timing adjustment gate. After the timing adjustment gate is over, the VCO returns to its normal stable frequency (free running frequency) and the shifted sync burst train is transmitted.

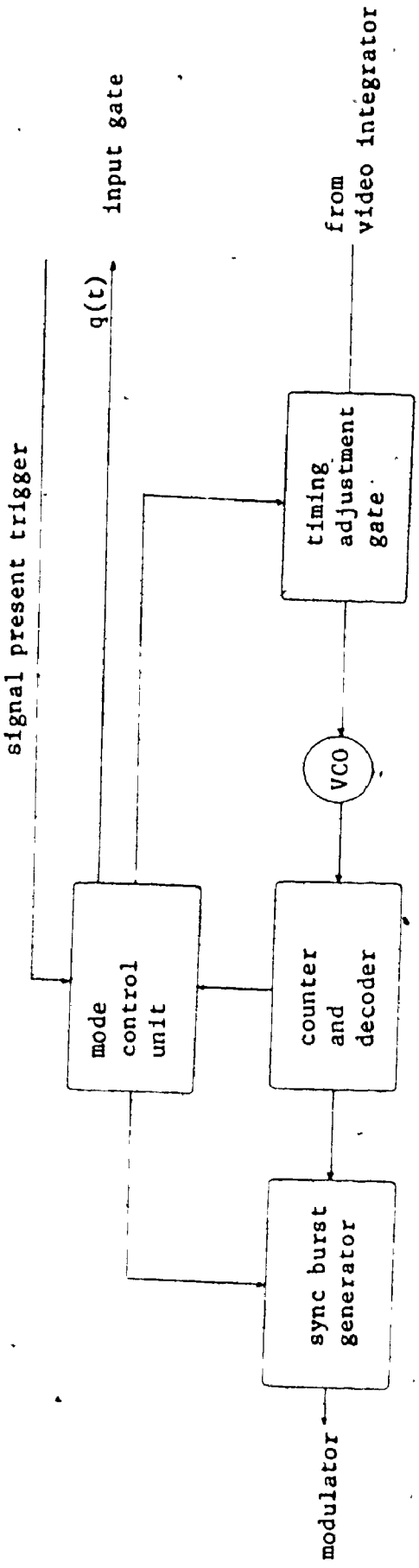

Fig. 2.3 Timing circuits

CHAPTER 3

ANALYSIS OF THE SYNCHRONIZATION LOOP

A detailed analysis of the synchronization loop (Fig. 2.1) is now presented. For the signal processing analysis, the complex notation for band-limited signals is used. All operations (signal generation, modulation-demodulation, amplification, filtering, etc.) are assumed to be ideal. The space delays, space losses (attenuation) and antenna gains are treated as lumped elements.

3.1 THE TRANSMITTED SIGNAL

The FSK sync burst is represented by the video signals $u_1(t)$ and $u_2(t)$ and by the intermediate frequencies IF $\omega_A/2\pi$ and $\omega_B/2\pi$. The intermediate frequencies usually differ from each other by an amount of 15-25 MHz.

For one sync burst the signal is given by: (assuming narrow-band representation) [29], [22].

$$s_1(t) = \mathrm{Re}\{u_1(t)\cdot e^{j\omega_A t} + u_2(t)\cdot e^{j\omega_B t}\} \tag{3.1}$$

where

$$u_1(t) = \begin{cases} A & -\frac{T_P}{2} \le t \le 0 \\ 0 & \text{elsewhere} \end{cases}$$

$$u_2(t) = \begin{cases} A & 0 \le t \le \frac{T_P}{2} \\ 0 & \text{elsewhere} \end{cases}$$

T_P: pulse duration (5-10 μsecs)

A: pulse amplitude

$|\omega_A - \omega_B|/2\pi$: 15-25 MHz

The sync burst signal is mixed in the modulator with a local oscillator at the uplink frequency ω_1 yielding:

$$s_2(t) = \mathrm{Re}\{u_1(t)e^{j(\omega_A+\omega_1)t} + u_2(t)e^{j(\omega_A+\omega_1)t}\} \tag{3.2}$$

The uplink frequencies are now located in the vicinity of 6 GHz. Future satellite systems will use higher frequencies [1],[2],[3], with uplink frequencies of 14 and 30 GHz. The corresponding downlink frequencies are 4, 12, and 20 GHz.

In the next stage the signal is amplified by K_1 at the output amplifier and transmitted.

The uplink is assumed to produce only a time delay (space delay) T_D (approximately 135 μsecs) and space attenuation. The uplink gain constant K_2 represents the earth station antenna gain, the space attenuation and the satellite antenna gain.

Thus,

$$s_3(t) = K_1 \cdot K_2 \cdot s_2(t-T_D) \tag{3.3}$$

$$= K_1 \cdot K_2 \cdot \mathrm{Re}\{u_1(t-T_D)e^{j(\omega_A+\omega_1)(t-T_D)} + u_2(t-T_D)e^{j(\omega_B+\omega_1)(t-T_D)}\}$$

The signal $s_3(t)$ is perturbed by the additive uplink noise $\eta_1(t)$ referred to the input amplifier.

Assuming narrow-band noise [29]

$$s_4(t) = s_3(t) + \eta_1(t) \tag{3.4}$$

where

$$\eta_1(t) = \mathrm{Re}\{z_1'(t)\cdot e^{j(\omega_A+\omega_1)t} + z_1''\cdot e^{j(\omega_B+\omega_1)t}\}$$

and

$$z_1'(t) = x_1'(t) + j\cdot y_1'(t)$$

$$z_1''(t) = x_1''(t) + j\cdot y_1''(t)$$

The signal is amplified by K_3 at the input amplifier and then converted to the downlink frequency ω_2, yielding

$$s_5(t) = K_3\cdot[K_1\cdot K_2\cdot \mathrm{Re}\{u_1(t-T_D)e^{j(\omega_A+\omega_2)(t-T_D)} + u_2(t-T_D)e^{j(\omega_B+\omega_2)(t-T_D)}\}$$

$$+ \mathrm{Re}\{z_1'(t)e^{j(\omega_A+\omega_2)t} + z_1''(t)e^{j(\omega_B+\omega_2)}\}] \qquad (3.5)$$

3.2 MODULATION OF THE TRANSMITTED SIGNAL BY THE SYNC WINDOW ON-BOARD THE SATELLITE

The signal $s_5(t)$ is pulse-time modulated by the sync window signal $m(t)$.

As far as synchronization is concerned, sync window modulation is the most important operation on-board the satellite. Essentially, it is a comparison between the earth station and satellite time bases. The time difference is detected and a timing error is defined which is simply the time difference between the center of the sync window and the time built-in reference (frequency transition) of the sync burst. The concept of the timing error provides the analytical expression for the sync window even if its exact occurrence is not known at the earth station.

If the synchronization is exact (zero timing error) the sync burst is centered in the sync window and the sync window modulated signal is symmetric. On the other hand, if the sync window modulated signal is not symmetric, its asymmetry is detected by the receiver to yield a measure of the error voltage (see Section 3.5). (It should be recalled that this is the fine search mode of operation and it is assumed that the sync burst passes through the sync window at least partially.)

Signal $s_5(t)$, after being pulse-time modulated by the sync window signal $m(t)$, is amplified at the output amplifier by K_4. Similarly the downlink is assumed to produce only space delay T_D and space attenuation. The downlink constant K_5 represents the satellite antenna gain, space attenuation, and earth station antenna gain.

Thus the signal in the input amplifier is

$$s_6(t) = K_4 \cdot K_5 \cdot s_5(t-T_D) \cdot m(t-T_D)$$

$$= K_3 \cdot K_4 \cdot K_5 [K_1 \cdot K_2 \cdot \mathrm{Re}\{u_1(t-2T_D) \cdot e^{j(\omega_A+\omega_2)(t-2T_D)} + u_2(t-2T_D) \cdot e^{j(\omega_B+\omega_2)(t-2T_D)}\}$$

$$+ \mathrm{Re}\{z_1'(t-T_D) \cdot e^{j(\omega_A+\omega_2)(t-T_D)} + z_1''(t-T_D) \cdot e^{j(\omega_B+\omega_2)(t-T_D)}\}] \cdot m(t-T_D) \qquad (3.6)$$

where

$$m(t-T_D) = \begin{cases} 1 & 2T_D - t_E - \frac{1}{2}T_W \le t \le 2T_D - t_E + \frac{1}{2}T_W \\ 0 & \text{elsewhere} \end{cases} \qquad (3.7)$$

T_W: window duration (1-6 μsecs)

t_E: timing error (Figs. 3.1, 3.2)

The signal $s_6(t)$ is perturbed by the additive downlink noise $n_2(t)$ referred to the input earth station amplifier:

$$s_7(t) = s_6(t) + n_2(t)$$

where

$$n_2(t) = \mathrm{Re}\{z_2'(t)\cdot e^{j(\omega_A+\omega_2)t} + z_2''(t)\cdot e^{j(\omega_B+\omega_2)t}\}$$

and

$$z_2'(t) = x_2'(t) + j\cdot y_2'(t)$$

$$z_2''(t) = x_2''(t) + j\cdot y_2''(t) \quad \text{(narrow-band representation)}$$

The narrow-band representation of the uplink and downlink noise is valid since the signal is filtered in the sync unit of the earth station.

3.3 THE RECEIVED SIGNAL AND ITS PROCESSING

The signal $s_7(t)$ is amplified at the input amplifier by K_6 and demodulated to yield the IF signal $s_8(t)$:

$$s_8(t) = K_3\cdot K_4\cdot K_5\cdot K_6\cdot [K_1\cdot K_2\cdot \mathrm{Re}\{u_1(t-2T_D)\cdot e^{j\omega_A(t-2T_D)} + u_2(t-2T_D)\cdot e^{j\omega_B(t-2T_D)}\}$$

$$+ \mathrm{Re}\{z_1'(t-T_D)\cdot e^{j\omega_A(t-T_D)} + z_1''(t-T_D)\cdot e^{j\omega_B(t-T_D)}\}]\cdot m(t-T_D)$$

$$+ K_6\cdot \mathrm{Re}\{z_2'(t)\cdot e^{j\omega_A t} + z_2''(t)\cdot e^{j\omega_B t}\} \qquad (3.8)$$

The receiver portion of the earth station sync unit (described in Section 2.3) consists of

(a) the input gate,

(b) the dual filter-one output, incoherent detector and

(c) the video integrator.

The input gate provides a train of pulses having a repetition interval equal to the frame length. The pulses are generated in the timing circuits by previously received signals starting with the coarse mode.

The function of the input gate is to pass all of the sync window modulated signal and therefore all the sync window modulated uplink noise but only the gate width of the downlink.

For one pulse, the input gate signal q(t) is given by:

$$q(t) = \begin{cases} 1 & 2T_D - t_E - \frac{1}{2}T_Q \leq t \leq 2T_D - t_E + \frac{1}{2}T_Q \\ 0 & \text{elsewhere} \end{cases} \qquad (3.9)$$

where $T_Q > T_W$

Thus, the signal $s_9(t)$ prior to detection is

$$s_9(t) = s_8(t) \cdot q(t)$$

The incoherent detector (Fig. 2.2) consists of two band-pass filters tuned to ω_A and ω_B, each one being followed by an envelope detector. The two detected signals (signal plus noise and noise alone) are subtracted and their difference is fed to the video integrator to yield the error voltage.

The analytical expression of each signal is now derived in detail.

Signal $[s_{10}(t)]_A$ at the output of the ideal bandpass filter tuned at ω_A is given by:

$$[s_{10}(t)]_A = q(t)\cdot[K_3\cdot K_4\cdot K_5\cdot K_6\cdot[K_1\cdot K_2\cdot \mathrm{Re}\{u_1(t-2T_D)\cdot e^{j\omega_A(t-2T_D)}\}$$

$$+ \mathrm{Re}\{z_1'(t-T_D)\cdot e^{j\omega_A(t-T_D)}\}]\cdot m(t-T_D) + K_6\cdot \mathrm{Re}\{z_2'(t)\cdot e^{j\omega_A t}\}] \qquad (3.10)$$

Likewise

$$[s_{10}(t)]_B = q(t)\cdot[K_3\cdot K_4\cdot K_5\cdot K_6\cdot[K_1\cdot K_2\cdot \mathrm{Re}\{u_2(t-2T_D)\cdot e^{j\omega_B(t-2T_D)}\}$$

$$+ \mathrm{Re}\{z_1''(t-T_D)\cdot e^{j\omega_B(t-T_D)}\}]\cdot m(t-T_D) + K_6\cdot \mathrm{Re}\{z_2''(t)\cdot e^{j\omega_B t}\}] \qquad (3.11)$$

Signals $[s_{10}(t)]_A$, $[s_{10}(t)]_B$ can be written in a more explicit and convenient form:

$$[s_{10}(t)]_A = q(t)\cdot \mathrm{Re}\{v_A(t)\cdot e^{j\omega_A(t-2T_D)}\} \qquad (3.12)$$

where

$$v_A(t) = [C_1\cdot u_1(t-2T_D) + C_2\cdot z_1'(t-T_D)\cdot e^{j\omega_A T_D}] + K_6\cdot z_2'(t)\cdot e^{2j\omega_A T_D}$$

and

$$C_1 = K_1\cdot K_2\cdot K_3\cdot K_4\cdot K_5\cdot K_6$$

$$C_2 = K_3\cdot K_4\cdot K_5\cdot K_6$$

Assuming stationary noise, phase and time delays can be eliminated and the noise signals may be written as

$$z_1'(t-T_D)\cdot e^{j\omega_A T_D} = z_1'(t) = x_1'(t) + j\cdot y_1'(t)$$

$$z_2'(t)\cdot e^{2j\omega_A T_D} = z_2'(t) = x_2'(t) + j\cdot y_2'(t)$$

The complex signal (pre-envelope) $v_A(t)$ may also be expressed as:

$$v_A(t) = \alpha_A(t) + j\cdot\beta_A(t) \tag{3.13}$$

where

$$\alpha_A(t) = C_1\cdot m(t-T_D)\cdot u_1(t-2T_D) + C_2\cdot m(t-T_D)\cdot x_1'(t) + K_6\cdot x_2'(t)$$

$$\beta_A(t) = C_2\cdot y_1'(t)\cdot m(t-T_D) + K_6\cdot y_2'(t)$$

Similarly the signal $[s_{10}(t)]_B$ is given by:

$$[s_{10}(t)]_B = q(t)\cdot Re\{v_B(t)\cdot e^{j\omega_B(t-2T_D)}\} \tag{3.14}$$

where

$$v_B(t) = \alpha_B(t) + j\cdot\beta_B(t)$$

and

$$\alpha_B(t) = C_1\cdot m(t-T_D)\cdot u_2(t-2T_D) + C_2\cdot m(t-T_D)\cdot x_1''(t) + K_6\cdot x_2''(t)$$

$$\beta_B(t) = C_2\cdot y_1''(t)\cdot m(t-T_D) + K_6\cdot y_2''(t)$$

The bandpass signals $[s_{10}(t)]_A$ and $[s_{10}(t)]_B$ are now processed by the envelope detectors to yield $[s_{11}(t)]_A$ and $[s_{11}(t)]_B$ [30].

$$[s_{11}(t)]_A = q(t)\cdot\sqrt{\alpha_A^2(t) + \beta_A^2(t)} \tag{3.15}$$

The sum of the squares: $\alpha_A^2(t) + \beta_A^2(t)$ is given by:

$$\alpha_A^2(t) + \beta_A^2(t) = [C_1 \cdot m(t-T_D) \cdot u_1(t-2T_D)]^2$$

$$+ [C_2 \cdot m(t-T_D)]^2 [x_1'^2(t) + y_1'^2(t)] + K_6^2 [x_2'^2(t) + y_2'^2(t)]$$

$$+ 2C_1 \cdot C_2 [m(t-T_D)]^2 \cdot u_1(t-2T_D) \cdot x_1'(t) + 2K_6 \cdot C_1 \cdot m(t-T_D) \cdot u_1(t-2T_D) \cdot x_2'(t)$$

$$+ 2K_6 \cdot C_2 \cdot m(t-T_D) \cdot x_1'(t) \cdot x_2'(t) + 2K_6 \cdot C_2 \cdot m(t-T_D) \cdot y_1'(t) \cdot y_2'(t) \qquad (3.16)$$

or

$$\alpha_A^2(t) + \beta_A^2(t) = [C_1 \cdot m(t-T_D) \cdot u_1(t-2T_D)]^2 + [C_2 \cdot m(t-T_D) \cdot z_1'(t)]^2 + [K_6 \cdot z_1'(t)]^2$$

$$+ 2C_1 \cdot m(t-T_D) \cdot u_1(t-2T_D) [C_2 \cdot m(t-T_D) \cdot x_1'(t) + K_6 \cdot x_2(t)]$$

$$+ 2K_6 \cdot C_2 \cdot m(t-T_D) \cdot [x_1'(t) \cdot x_2'(t) + y_1'(t) \cdot y_2'(t)]$$

Likewise,

$$[s_{11}(t)]_B = q(t) \cdot \sqrt{\alpha_B^2(t) + \beta_B^2(t)} \qquad (3.17)$$

where

$$\alpha_B^2(t) + \beta_B^2(t) = [C_1 \cdot m(t-T_D) \cdot u_2(t-2T_D)]^2 + [C_2 \cdot m(t-T_D) \cdot z_1''(t)]^2 + [K_6 \cdot z_2''(t)]^2$$

$$+ 2C_1 \cdot m(t-T_D) \cdot u_2(t-2T_D) [C_2 \cdot m(t-T_D) \cdot x_1''(t) + K_6 \cdot x_2''(t)]$$

$$+ 2K_6 \cdot C_2 \cdot m(t-T_D) [x_1''(t) \cdot x_2''(t) + y_1''(t) \cdot y_2''(t)]$$

The signals $[s_{11}(t)]_A$ and $[s_{11}(t)]_B$ are subtracted to yield $s_{12}(t)$.

$$s_{12}(t) = q(t) \cdot \left[\sqrt{\{[C_1 \cdot m(t-T_D) \cdot u_1(t-2T_D)]^2 + [C_2 \cdot m(t-T_D) \cdot z_1'(t)]^2 + [K_6 \cdot z_2'(t)]^2 \right.$$

$$\left. + 2C_1 \cdot m(t-T_D) \cdot u_1(t-2T_D) [C_2 \cdot m(t-T_D) \cdot x_1'(t) + K_6 \cdot x_2'(t)]} \right.$$

$$+ 2K_6 \cdot C_2 \cdot m(t-T_D)[x_1'(t) \cdot x_2'(t) + y_1'(t) \cdot y_2'(t)]\}$$

$$- \sqrt{\{[C_1 \cdot m(t-T_D) \cdot u_2(t-2T_D)]^2 + [C_2 \cdot m(t-T_D) \cdot z_1''(t)]^2 + [K_6 \cdot z_2''(t)]^2}$$

$$+ 2C_1 \cdot m(t-T_D) \cdot u_2(t-2T_D)[C_2 \cdot m(t-T_D) \cdot x_1''(t) + K_6 \cdot x_2''(t)]$$

$$+ 2K_6 \cdot C_2 \cdot m(t-T_D)[x_1''(t) \cdot x_2''(t) + y_1''(t) \cdot y_2''(t)]\}\Big] \qquad (3.18)$$

3.4 CHARACTERIZATION OF THE PROCESSED SIGNAL PRIOR TO INTEGRATION

Equation (3.18) is the general analytical expression for the signal $s_{12}(t)$ at the output of the summer and prior to integration. Before the mathematical manipulations of the integration are carried out, it is necessary to characterize the signal $s_{12}(t)$. The following characterization will also be very useful for the computer simulation (Chapter 5)

Two cases are considered:

I. $2T_W < T_P$ and II. $T_W < T_P < 2T_W$

[Note: A third case, $T_P \leq T_W$ is not considered here, since it gives no timing information for timing errors [21]:

$$|t_E| \leq \frac{1}{2}(T_W - T_P)$$

I. $2T_W < T_P$

Depending on the timing error between the sync burst and the sync window (Figs. 3.1a and 3.1b), $s_{12}(t)$ can be

1. For

$$-\frac{1}{2}(T_P + T_W) < t_E < -\frac{1}{2}(T_P - T_W) \qquad \text{(Fig. 3.1a)}$$

a. For

$$2T_D - t_E - \tfrac{1}{2}T_Q < t < 2T_D - t_E - \tfrac{1}{2}T_W$$

$u_1(t-2T_D) = 0$ (see equation (3.1))

$u_2(t-2T_D) = 0$ (see equation (3.1))

$m(t-T_D) = 0$ (see equation (3.7))

$q(t) = 1$ (see equation (3.9))

thus,

$$s_{12}(t) = K_6 \cdot \sqrt{z_2'^2(t)} - K_6 \cdot \sqrt{z_2''^2(t)}$$

$$= K_6(|z_2'(t)| - |z_2''(t)|) \qquad (3.19a)$$

b. For

$$2T_D - t_E - \tfrac{1}{2}T_W < t < 2T_D + \tfrac{1}{2}T_P$$

$u_1(t-2T_D) = 0$ (see equation (3.1))

$u_2(t-2T_D) = A$ (see equation (3.1))

$m(t-T_D) = 1$ (see equation (3.7))

$q(t) = 1$ (see equation (3.9))

thus,

$$s_{12}(t) = \sqrt{\{C_2^2 \cdot z_1'^2(t) + K_6^2 \cdot z_2'^2(t) + 2K_6 \cdot C_2 \cdot x_1'(t) \cdot x_2'(t) + 2K_6 \cdot C_2 \cdot y_1'(t) \cdot y_2'(t)\}}$$

$$\sqrt{\{C_1^2 \cdot A^2 + C_2^2 \cdot z_1''^2(t) + K_6^2 z_2''^2(t) + 2C_1 \cdot C_2 \cdot A[x_1''(t) + x_2''(t)] + 2K_6 \cdot C_2[x_1''(t) \cdot x_2''(t) + y_1''(t) \cdot y_2''(t)]\}}$$

$$= |C_2 \cdot z_1'(t) + K_6 \cdot z_2'(t)| - |[C_1 A + C_2 \cdot x_1''(t) + K_6 \cdot x_2''(t)) + j(C_2 \cdot y_1''(t) + K_6 \cdot y_2''(t))| \quad (3.19b)$$

c. For

$$2T_D + \tfrac{1}{2}T_P < t < 2T_D - t_E + \tfrac{1}{2}T_W$$

$$u_1(t-2T_D) = 0$$

$$u_1(t-2T_D) = 0$$

$$m(t-T_D) = 1$$

$$q(t) = 1$$

thus,

$$s_{12}(t) = \sqrt{\{C_2^2 \cdot z_1'^2(t) + K_6^2 \cdot z_2'^2(t) + 2K_6 \cdot C_2(x_1'(t) \cdot x_2'(t) + y_1'(t) \cdot y_2'(t))\}}$$

$$- \sqrt{\{C_2^2 \cdot z_1''^2(t) + K_6^2 \cdot z_1''^2(t) + 2K_6 \cdot C_2(x_1''(t) \cdot x_2''(t) + y_1''(t) \cdot y_2''(t))\}}$$

$$= |C_2 \cdot z_1'(t) + K_6 \cdot z_2'(t)| - |C_2 \cdot z_1''(t) + K_6 \cdot z_2''(t)| \quad (3.19c)$$

d. For

$$2T_D - t_E + \tfrac{1}{2}T_W < t < 2T_D - t_E + \tfrac{1}{2}T_Q$$

$$m(t-T_D) = 0$$

$$u_1(t-2T_D) = 0$$

$$u_2(t-2T_D) = 0$$

$$q(t) = 1$$

thus,

$$s_{12}(t) = K_6(|z_2'(t)| - |z_2''(t)|) \quad (3.19d)$$

e. For

$$t < 2T_D - t_E - \tfrac{1}{2}T_Q \qquad \text{and} \qquad t > 2T_D - t_E + \tfrac{1}{2}T_Q$$

$$q(t) = 0$$

thus,

$$s_{12}(t) = 0 \tag{3.19e}$$

In the same way $s_{12}(t)$ is characterized as follows.

2. For

$$-\tfrac{1}{2}(T_P - T_W) < t_E < -\tfrac{1}{2}T_W \qquad \text{(Fig. 3.1b)}$$

$$s_{12}(t) = \begin{cases} K_6(\,z_2'(t) - z_2''(t)\,) & 2T_D - t_E - \frac{1}{2}T_Q < t < 2T_D - t_E - \frac{1}{2}T_W \\ |C_2 \cdot z_1'(t)| - |(C_1 \cdot A + C_2 \cdot x_1''(t) + K_6 \cdot x_2''(t)) + j(C_2 \cdot y_1''(t) + K_6 \cdot y_2''(t))| & \\ & 2T_D - t_E - \frac{1}{2}T_W < t < 2T_D - t_E + \frac{1}{2}T_W \\ K_6(|z_2'(t)| - |z_2''(t)|) & 2T_D - t_E + \frac{1}{2}T_W < t < 2T_D - t_E + \frac{1}{2}T_D \\ 0 & \text{elsewhere} \end{cases} \tag{3.20}$$

3. For

$$-\tfrac{1}{2}T_W < t_E < \tfrac{1}{2}T_W \qquad \text{(Fig. 3.1c)}$$

$$s_{12}(t) = \begin{cases} K_6(|z_2'(t)| - |z_2''(t)|) & 2T_D - t_E - \frac{1}{2}T_Q < t < 2T_D - t_E - \frac{1}{2}T_W \\ |(C_1 \cdot A + C_2 \cdot x_1'(t) + K_6 \cdot x_2'(t)) + j(C_2 \cdot y_1'(t) + K_6 \cdot y_2'(t)| - |C_2 \cdot z_1''(t) + K_6 \cdot z_2''(t)| & \\ & 2T_D - t_E - \frac{1}{2}T_W < t < 2T_D \\ |C_2 \cdot z_1'(t) + K_6 \cdot z_2'(t)| - |(C_1 \cdot A + C_2 \cdot x_1''(t) + K_6 \cdot x_2''(t)) + j(C_2 \cdot y_1''(t) + K_6 \cdot y_2''(t))| & \\ & 2T_D < t < 2T_D - t_E + \frac{1}{2}T_W \\ K_6(|z_2'(t)| - |z_2''(t)|) & 2T_D - t_E + \frac{1}{2}T_W < t < 2T_D - t_E + \frac{1}{2}T_Q \\ 0 & \text{elsewhere} \end{cases} \tag{3.21}$$

4. For

$$\frac{1}{2}T_W < t_E \leq \frac{1}{2}(T_P - T_W) \qquad \text{(Fig. 3.1d)}$$

$$s_{12}(t) = \begin{cases} K_6(|z_2'(t)| - |z_2''(t)|) & 2T_D - t_E - \frac{1}{2}T_Q < t < 2T_D - t_E - \frac{1}{2}T_W \\ |(C_1 \cdot A + C_2 \cdot x_1'(t) + K_6 \cdot x_2''(t)) + j(C_2 \cdot y_1'(t) + K_6 \cdot y_2'(t))| - |C_2 \cdot z_1''(t) + K_6 \cdot z_2''(t)| & \\ & 2T_D - t_E - \frac{1}{2}T_W < t < 2T_D - t_E + \frac{1}{2}T_W \\ K_6(|z_2'(t)| - |z_2''(t)|) & 2T_D - t_E + \frac{1}{2}T_W < t < 2T_D - t_E + \frac{1}{2}T_Q \\ 0 & \text{elsewhere} \end{cases} \qquad (3.22)$$

5. For

$$\frac{1}{2}(T_P - T_W) < t_E < \frac{1}{2}(T_P + T_W) \qquad \text{(Fig. 3.1e)}$$

$$s_{12}(t) = \begin{cases} K_6(z_2'(t) - z_2''(t)) & 2T_D - t_E - \frac{1}{2}T_Q < t < 2T_D - t_E - \frac{1}{2}T_W \\ |C_2 \cdot z_1'(t) + K_6 \cdot z_2'(t)| - |C_2 \cdot z_1''(t) + K_6 \cdot z_2''(t)| & \\ & 2T_D - t_E - \frac{1}{2}T_W < t < 2T_D - \frac{1}{2}T_P \\ |(C_1 \cdot A + C_2 \cdot x_1'(t) + K_6 \cdot x_2'(t)) + j(C_2 \cdot y_1'(t) + K_6 \cdot y_2'(t))| - |C_2 \cdot z_1''(t) + K_6 \cdot z_2''(t)| & \\ & 2T_D - \frac{1}{2}T_D < t < 2T_D - t_E + \frac{1}{2}T_W \\ K_6(|z_2'(t)| - |z_2''(t)|) & 2T_D - t_E + \frac{1}{2}T_W < t < 2T - t_E + \frac{1}{2}T_Q \\ 0 & \text{elsewhere} \end{cases} \qquad (3.23)$$

II. $T_W < T_P < 2T_W$

1. For

$$-\frac{1}{2}(T_P + T_W) < t_E < -\frac{1}{2}T_W \qquad \text{(Fig. 3.2a)}$$

$$s_{12}(t) = \begin{cases} K_6(|z_2'(t)| - |z_2''(t)|) & 2T_D - t_E - \frac{1}{2}T_Q < t < 2T_D - t_E - \frac{1}{2}T_W \\ |C_2 \cdot z_1'(t) + K_6 \cdot z_2'(t)| - |(C_1 \cdot A + C_2 \cdot x_1''(t) + K_6 \cdot x_2''(t)) + j(C_2 \cdot y_1''(t) + K_6 \cdot y_2''(t))| & \\ & 2T_D - t_E - \frac{1}{2}T_W < t < 2T_D + \frac{1}{2}T_D \\ |C_2 \cdot z_1'(t) + K_6 \cdot z_2'(t)| - |C_2 \cdot z_1''(t) + K_6 \cdot z_2''(t)| & \\ & 2T_D + \frac{1}{2}T_P < t < 2T_D - t_E + \frac{1}{2}T_W \\ K_6(|z_2'(t)| - |z_2''(t)| & 2T_D - t_E + \frac{1}{2}T_W < t < 2T_D - t_E + \frac{1}{2}T_Q \\ 0 & \text{elsewhere} \end{cases} \tag{3.24}$$

2. For

$$-\frac{1}{2}T_W < t_E < -\frac{1}{2}(T_P - T_W) \qquad \text{(Fig. 3.2b)}$$

$$s_{12}(t) = \begin{cases} K_6(|z_2'(t)| - |z_2''(t)|) & 2T_D - t_E - \frac{1}{2}T_Q < t < 2T_D - t_E - \frac{1}{2}T_W \\ |(C_1 \cdot A + C_2 \cdot x_1'(t) + K_6 \cdot x_2''(t)) + j(C_2 \cdot y_1'(t) + K_6 \cdot y_2'(t))| - |C_2 \cdot z_1''(t) + K_6 \cdot z_2''(t)| & \\ & 2T_D - t_E - \frac{1}{2}T_W < t < 2T_D \\ |C_2 \cdot z_1'(t) + K_6 \cdot z_2'(t)| - |(C_1 \cdot A + C_2 \cdot x_1''(t) + K_6 \cdot x_2''(t)) + j(C_2 \cdot y_1''(t) + K_6 \cdot y_2''(t))| & \\ & 2T_D < t < 2T_D + \frac{1}{2}T_P \\ |C_2 \cdot z_1'(t) + K_6 \cdot z_2'(t)| - |C_2 \cdot z_1''(t) + K_6 \cdot z_2''(t)| & \\ & 2T_D + \frac{1}{2}T_P < t < 2T_D - t_E + \frac{1}{2}T_W \\ K_6(|z_2'(t)| - |z_2''(t)|) & 2T_D - t_E + \frac{1}{2}T_W < t < 2T_D - t_E + \frac{1}{2}T_Q \\ 0 & \text{elsewhere} \end{cases} \tag{3.25}$$

3. For

$$-\frac{1}{2}(T_P - T_W) < t_E < \frac{1}{2}(T_P - T_W) \qquad \text{(Fig. 3.2c)}$$

$$s_{12}(t) = \begin{cases} K_6(|z_2'(t)| - |z_2''(t)|) & 2T_D - t_E - \frac{1}{2}T_Q < t < 2T_D - t_E - \frac{1}{2}T_W \\ |(C_1 \cdot A + C_2 \cdot x_1'(t) + K_6 \cdot x_2'(t)) + j(C_2 \cdot y_1'(t) + K_6 \cdot y_2'(t))| - |C_1 \cdot z_1''(t) + K_6 \cdot z_2''(t)| & \\ & 2T_D - t_E - \frac{1}{2}T_W < t < 2T_D \\ |C_2 \cdot z_1'(t) + K_6 \cdot z_2'(t)| - |(C_1 \cdot A + C_2 \cdot x_1''(t) + K_6 \cdot x_2''(t)) + j(C_2 \cdot y_1''(t) + K_6 \cdot y_2''(t))| & \\ & 2T_D < t < 2T_D - t_E + \frac{1}{2}T_W \\ K_6(|z_2'(t)| - |z_2''(t)|) & 2T_D - t_E + \frac{1}{2}T_W < t < 2T_D - t_E + \frac{1}{2}T_Q \\ 0 & \text{elsewhere} \end{cases} \tag{3.26}$$

4. For

$$\frac{1}{2}(T_P - T_W) < t_E < \frac{1}{2}T_W) \qquad \text{(Fig. 3.2d)}$$

$$s_{12}(t) = \begin{cases} K_6(|z_2'(t)| - |z_2''(t)|) & 2T_D - t_E - \frac{1}{2}T_Q < t < 2T_D - t_E - \frac{1}{2}T_W \\ |C_2 \cdot z_1'(t) + K_6 \cdot z_2'(t)| - |C_2 \cdot z_1''(t) + K_6 \cdot z_2''(t)| & \\ & 2T_D - t_E - \frac{1}{2}T_W < t < 2T_D - \frac{1}{2}T_P \\ |(C_1 \cdot A + C_2 \cdot x_1'(t) + K_6 \cdot x_2'(t)) + j(C_2 \cdot y_1'(t) + K_6 \cdot y_2'(t)| - |C_2 \cdot z_1''(t) + K_6 \cdot z_2''(t)| & \\ & 2T_D - \frac{1}{2}T_P < t < 2T_D \\ |C_2 \cdot z_1'(t) + K_6 \cdot z_2'(t)| - |(C_1 \cdot A + C_2 \cdot x_1''(t) + K_6 \cdot x_2''(t)) + j(C_2 \cdot y_1''(t) + K_6 \cdot y_2''(t))| & \\ & 2T_D < t < 2T_D - t_E + \frac{1}{2}T_W \\ K_6(|z_2'(t)| - |z_2''(t)|) & 2T_D - t_E + \frac{1}{2}T_W < t < 2T_D - t_E + \frac{1}{2}T_Q \\ 0 & \text{elsewhere} \end{cases} \tag{3.27}$$

5. For

$$\frac{1}{2}T_W < t_E < \frac{1}{2}(T_P + T_W) \qquad \text{(Fig. 3.2e)}$$

$$s_{12}(t)=\begin{cases} K_6(|z_2'(t)| - |z_2''(t)|) & 2T_D - t_E - \frac{1}{2}T_Q < t < 2T_D - t_E - \frac{1}{2}T_W \\ |C_2\cdot z_1'(t)+K_6\cdot z_2'(t)| - |C_2\cdot z_1''(t)+K_6\cdot z_2''(t)| & \\ & 2T_D - t_E - \frac{1}{2}T_W < t < 2T_D - \frac{1}{2}T_P \\ |(C_1\cdot A+C_2\cdot x_1'(t)+K_6\cdot x_2'(t)) + j(C_2\cdot y_1'(t)+K_6\cdot y_2'(t))| - |C_2\cdot z_1''(t)+K_6\cdot z_2''(t)| & \\ & 2T_D - \frac{1}{2}T_P < t < 2T_D - t_E + \frac{1}{2}T_W \\ K_6(|z_2'(t)| - |z_2''(t)|) & 2T_D - t_E + \frac{1}{2}T_W < t < 2T_D - t_E + \frac{1}{2}T_Q \\ 0 & \text{elsewhere} \end{cases} \tag{3.28}$$

(Note: All the above analysis were referred to one sync burst.)

3.5 POST DETECTION INTEGRATION

When synchronization is not exact, signal $s_{12}(t)$ is not symmetric, i.e., the time duration of its positive portion is not equal to the duration of its negative one. By video integration, the time dependence is eliminated and this asymmetry is converted to a voltage (i.e., error voltage) which clearly is a function of the timing error. Integration is an important operation in the receiver since it recovers the synchronization information, i.e., the timing error. Also by integrating the L pulses of the detected signal, random noise effects are reduced and a better system performance is obtained. The error voltage at the output of the integrator is given by

$$v_E = \frac{1}{T_I} \int_{L \text{ pulses}} s_{12}(t)\cdot dt \tag{3.29}$$

T_I = integrator time constant

L = number of pulses to be processed.

[Note: in the next chapter, $s_{12}(t)$ will be considered to consist of L pulses identically modulated by the sync window on-board the satellite.]

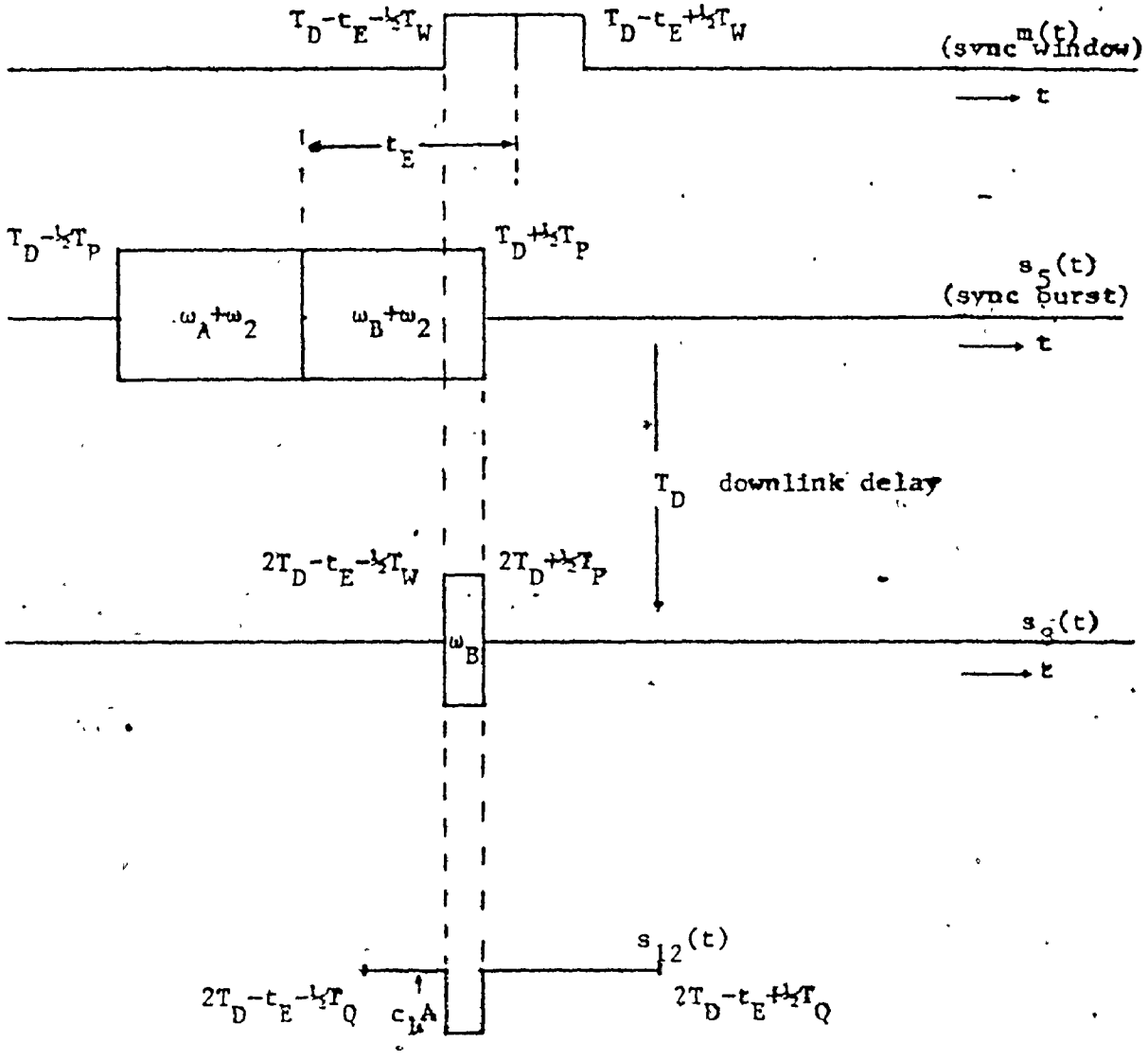

Fig. 3.1.a Sync window/modulation on-board the satellite and detection at the earth station.

(case I. Reg. E: $-\frac{1}{2}(T_P+T_W) < t_E < -\frac{1}{2}(T_P-T_W)$)

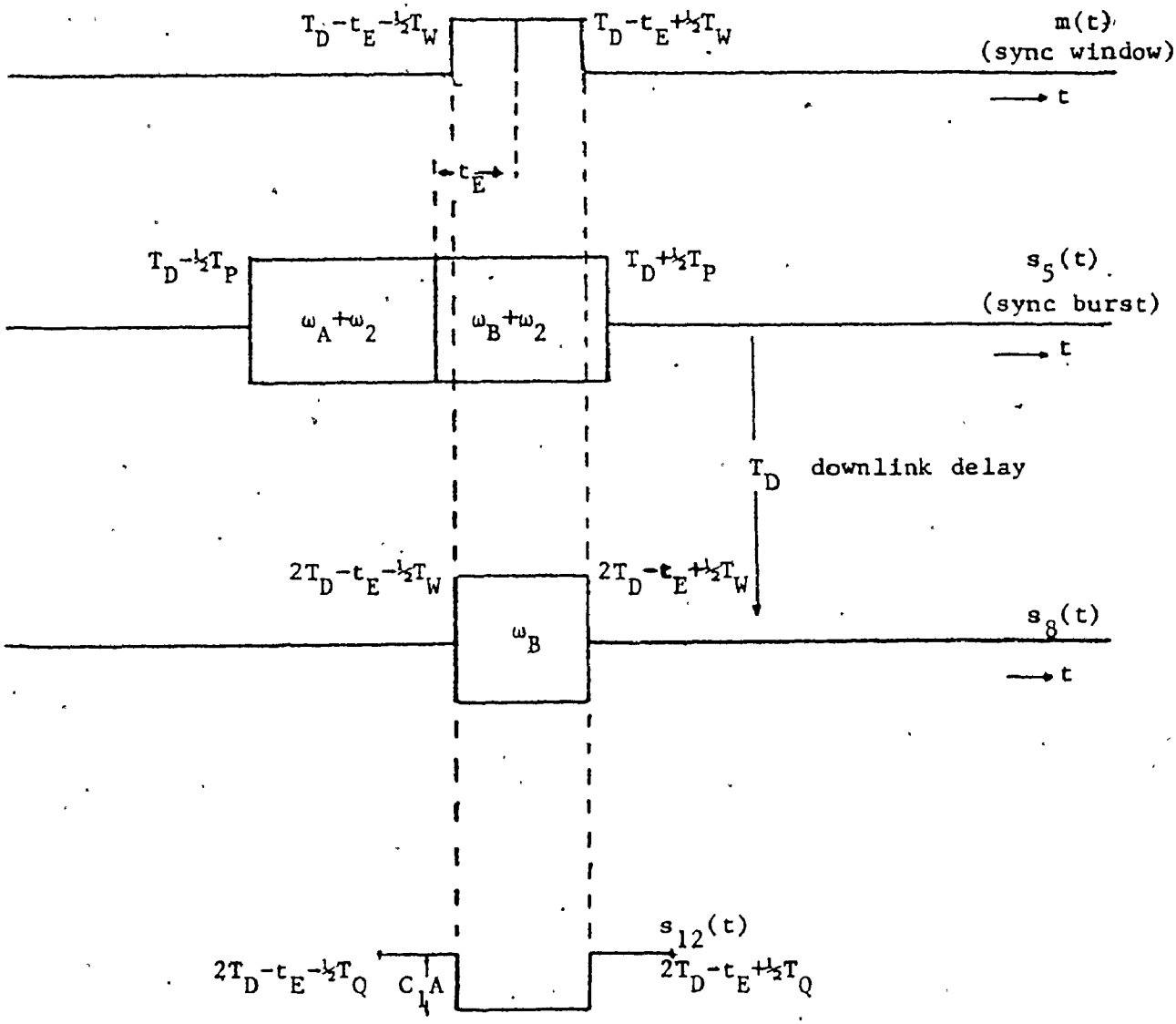

Fig. 3.1.b Sync window modulation on-board the satellite and detection at the earth station.

(case I. Reg. D: $-\frac{1}{2}(T_P - T_W) < t_E < -\frac{1}{2}T_W$)

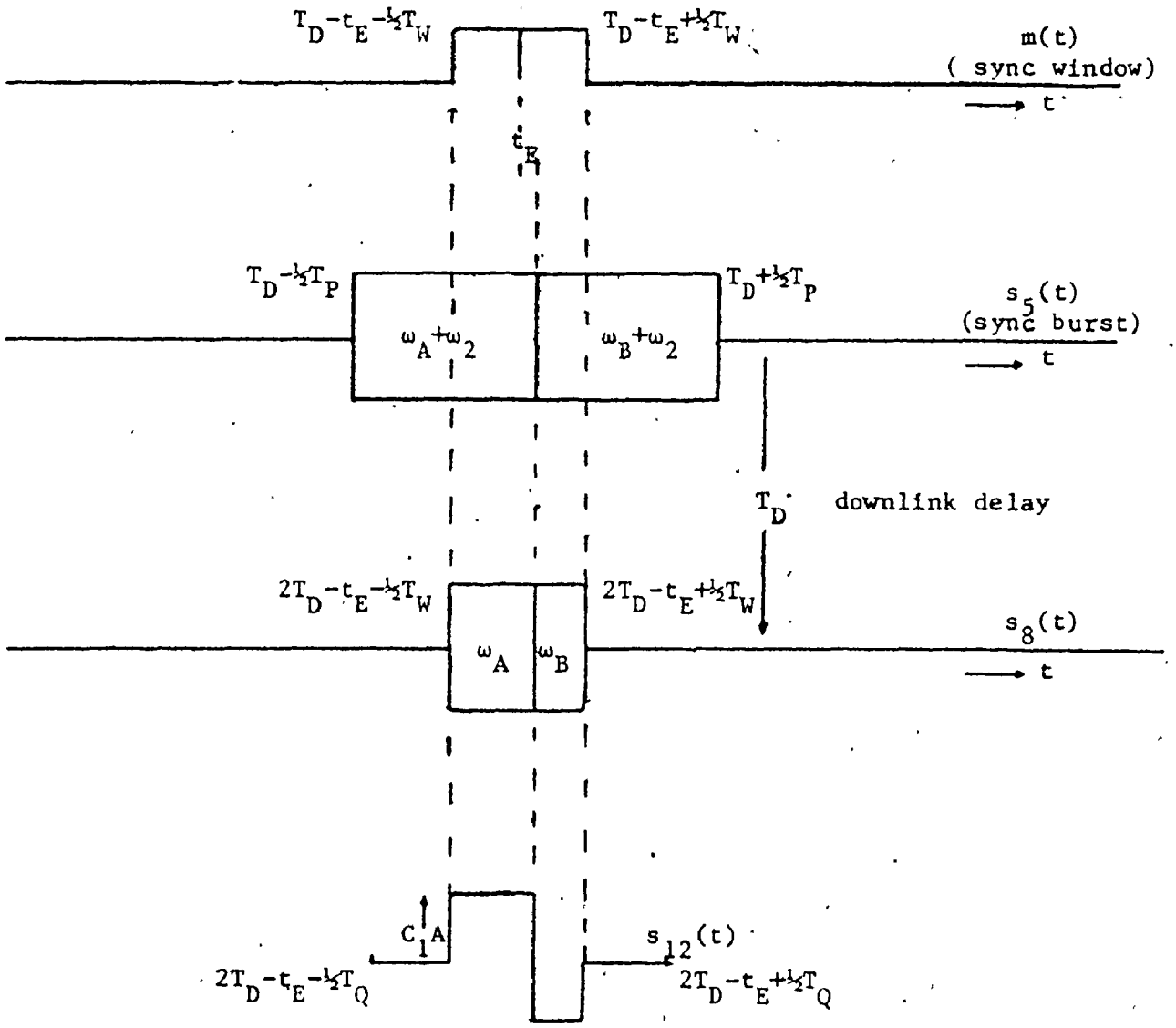

Fig. 3.1.c Sync window modulation on-board the satellite and detection at the earth station.

(case I. Reg. C: $\frac{1}{2}T_W < t_E < \frac{1}{2}T_W$)

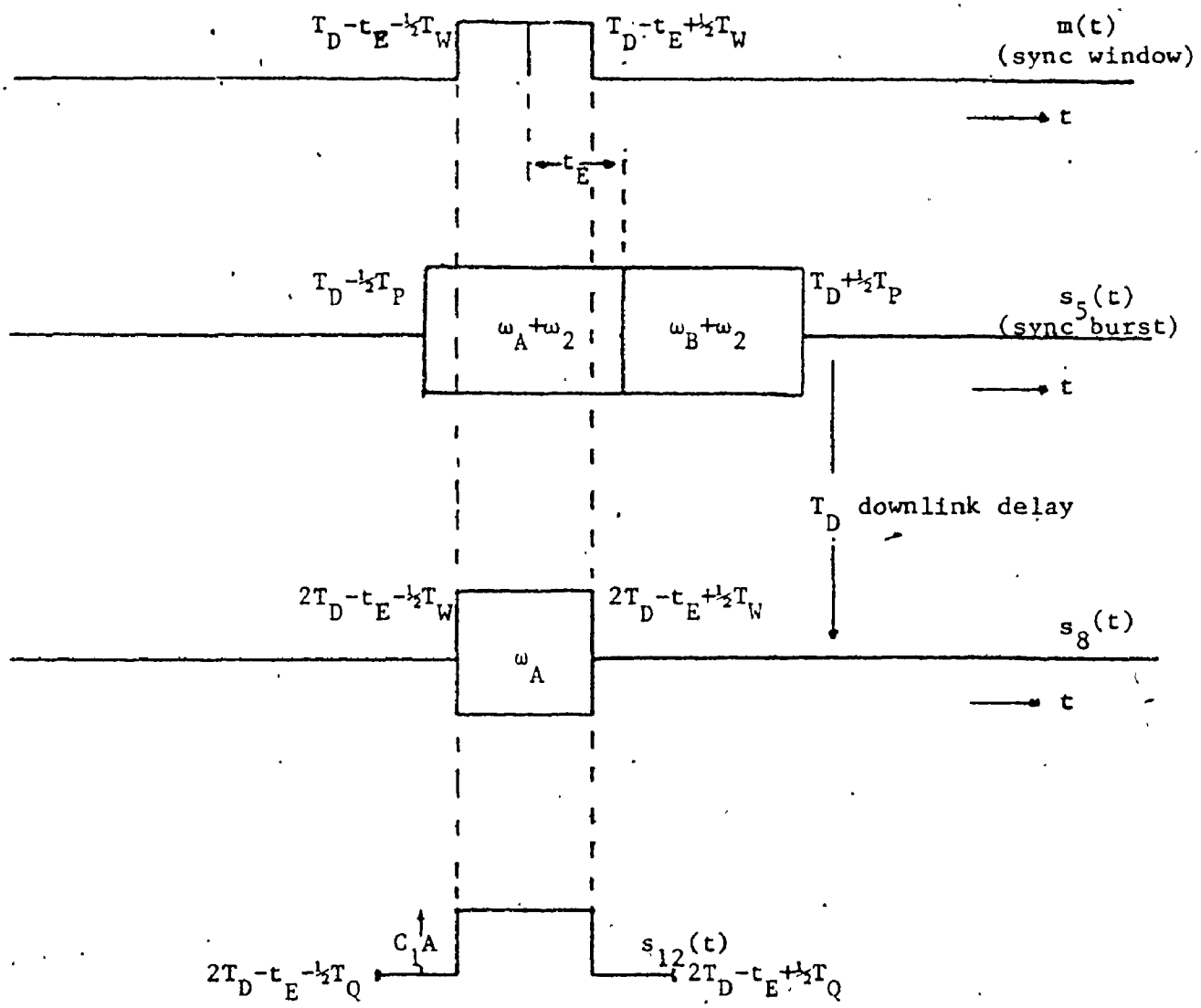

Fig. 3.1.d Sync window modulation on-board the satellite and detection at the earth station.

(case I. Reg. B: $\frac{1}{2}T_W < t_E < \frac{1}{2}(T_P - T_W)$)

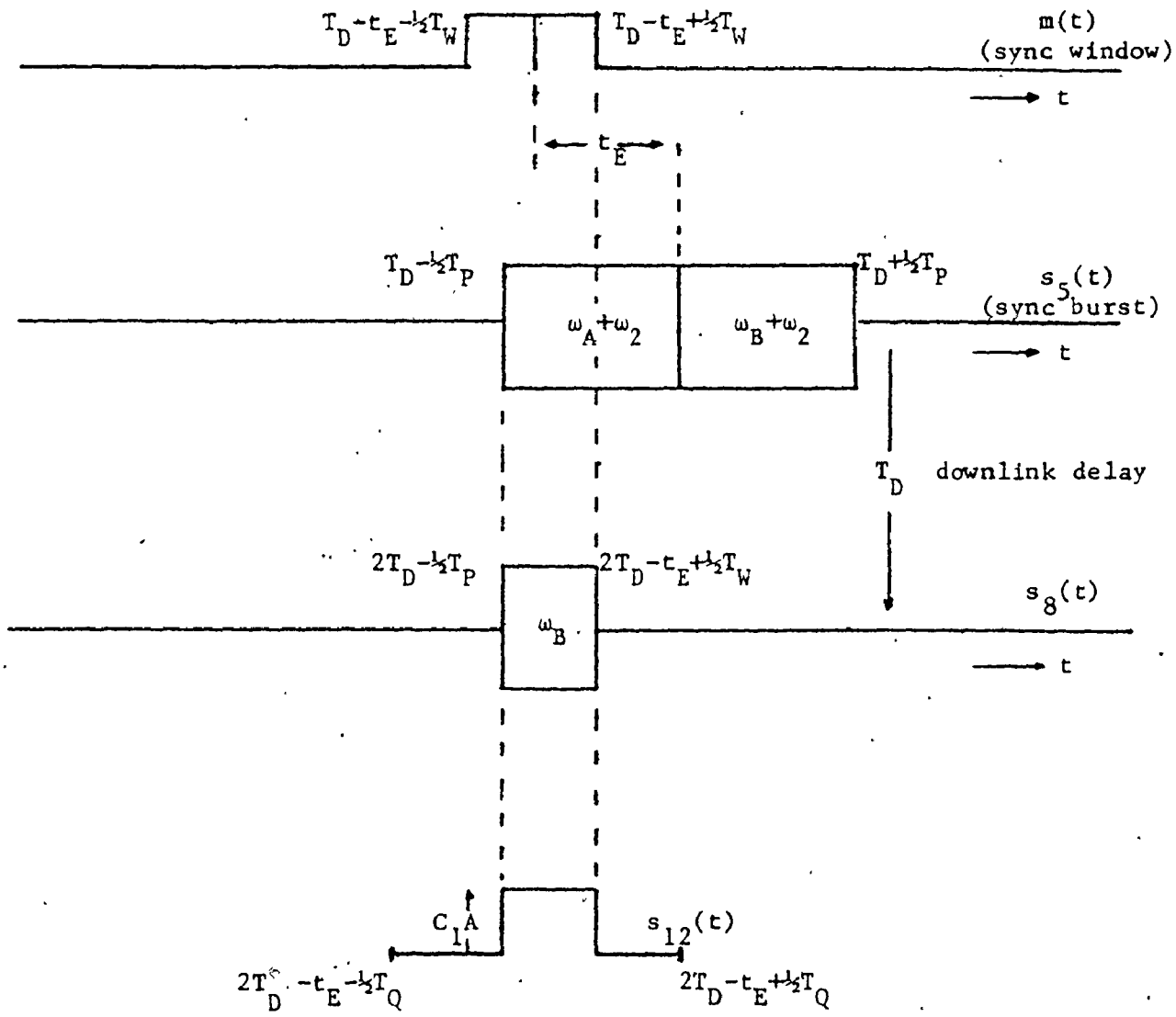

Fig. 3.1.e Sync window modulation on-board the satellite and detection at the earth station.

(case I. Reg. A: $\frac{1}{2}(T_P-T_W)<t_E<\frac{1}{2}(T_P+T_W)$)

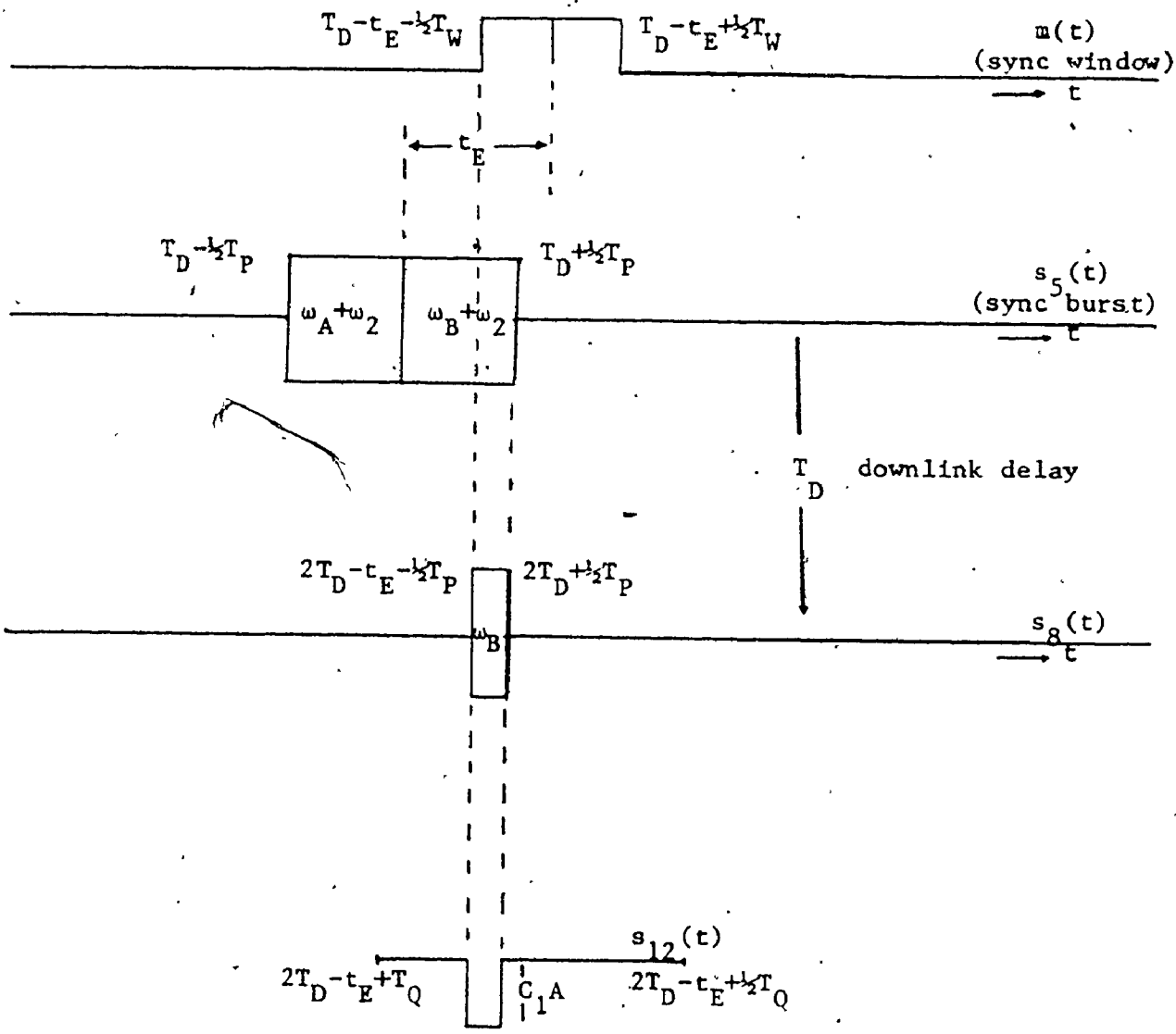

Fig. 3.2.a Sync window modulation on-board the satellite and detection at the earth station.

(case II. Reg. E: $-\frac{1}{2}(T_P+T_W) < t_E < -\frac{1}{2}T_W$)

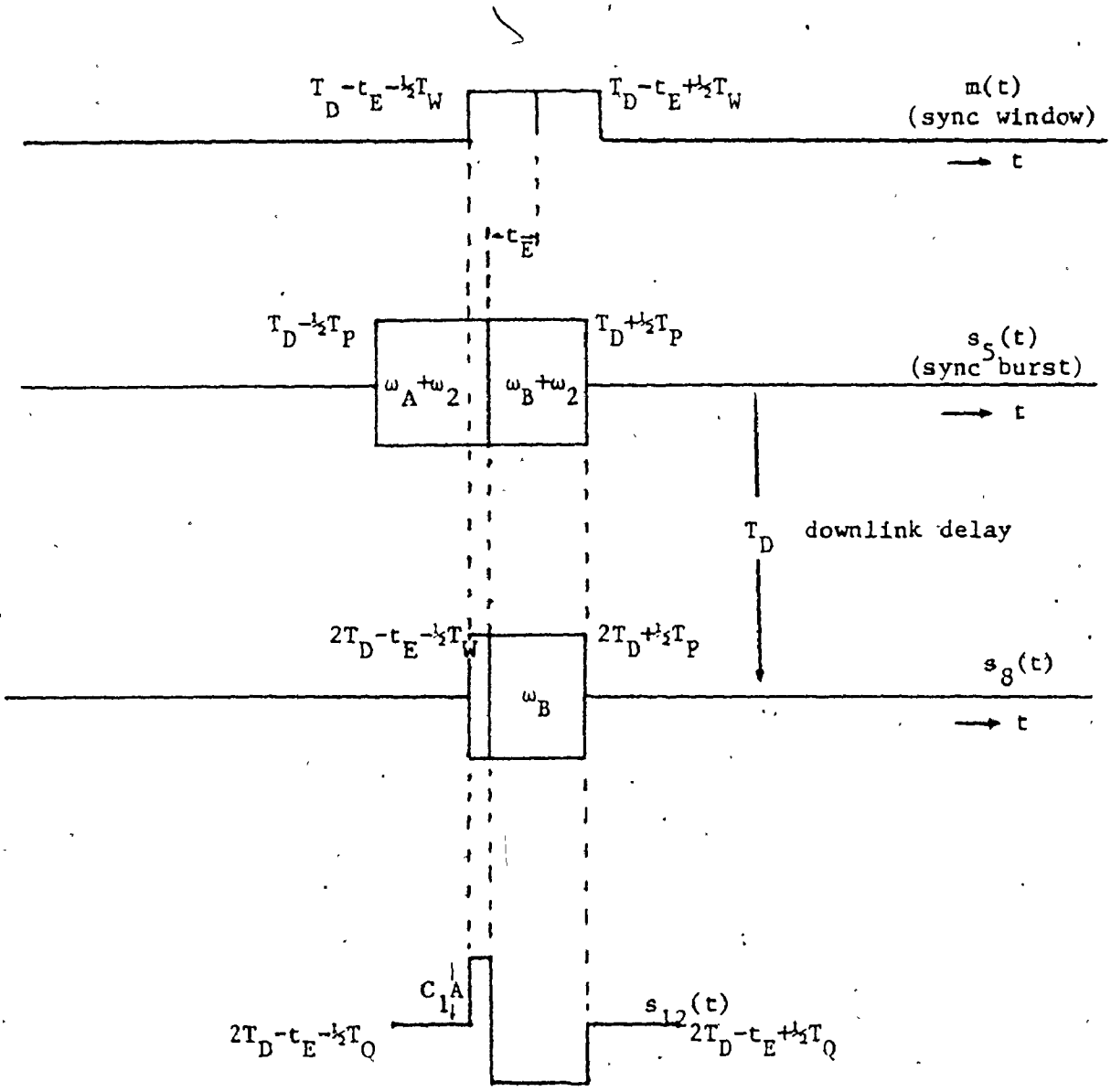

Fig. 3.2.b Sync window modulation on-board the satellite and detection at the earth station.

(case II. Reg. D: $-\frac{1}{2}T_W < t_E < -\frac{1}{2}(T_P - T_W)$)

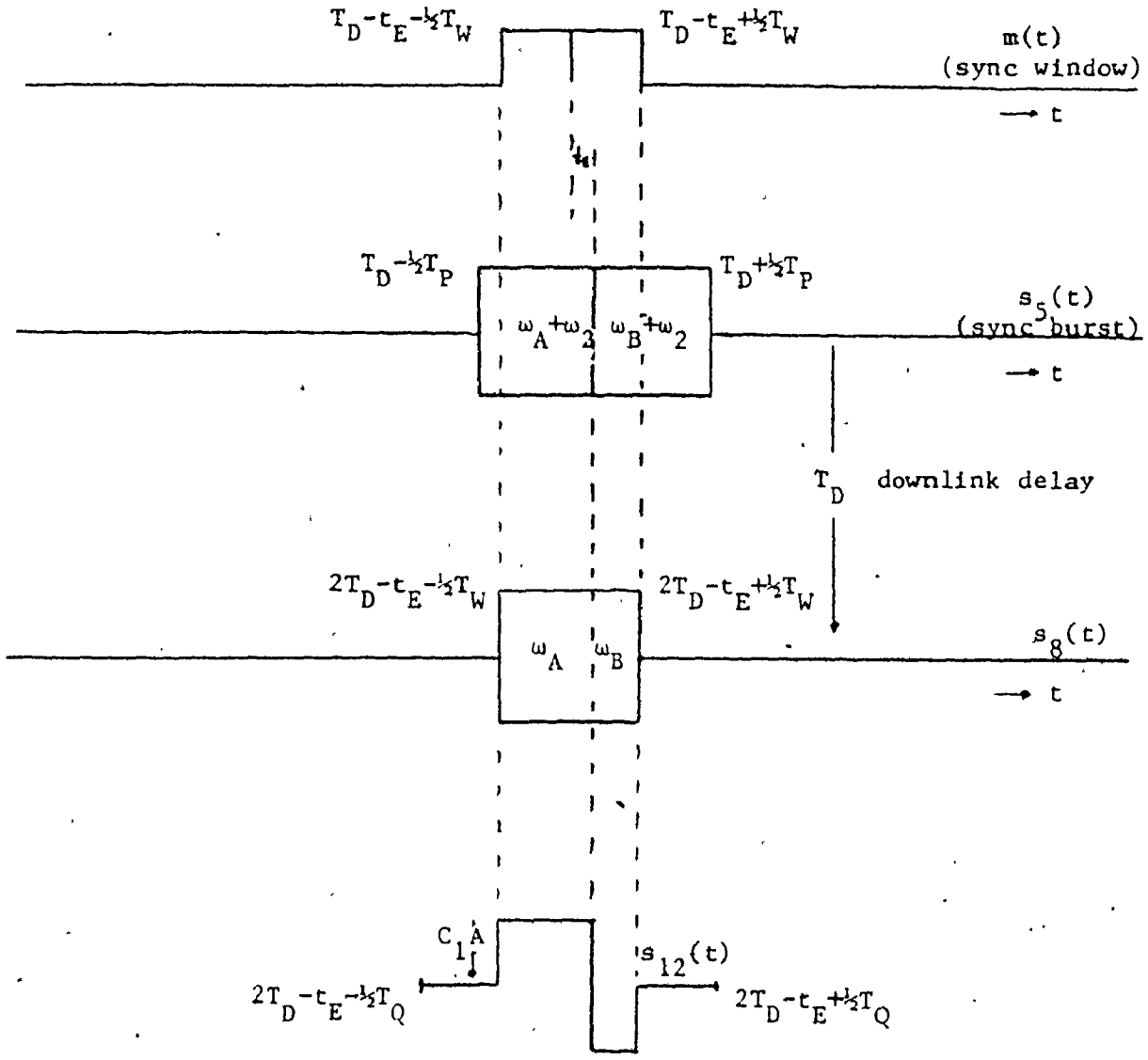

Fig. 3.2.c Sync window modulation on-board the satellite and detection at the earth station.

(case II. Reg. C: $-\frac{1}{2}(T_P - T_W) < t_E < \frac{1}{2}(T_P - T_W)$)

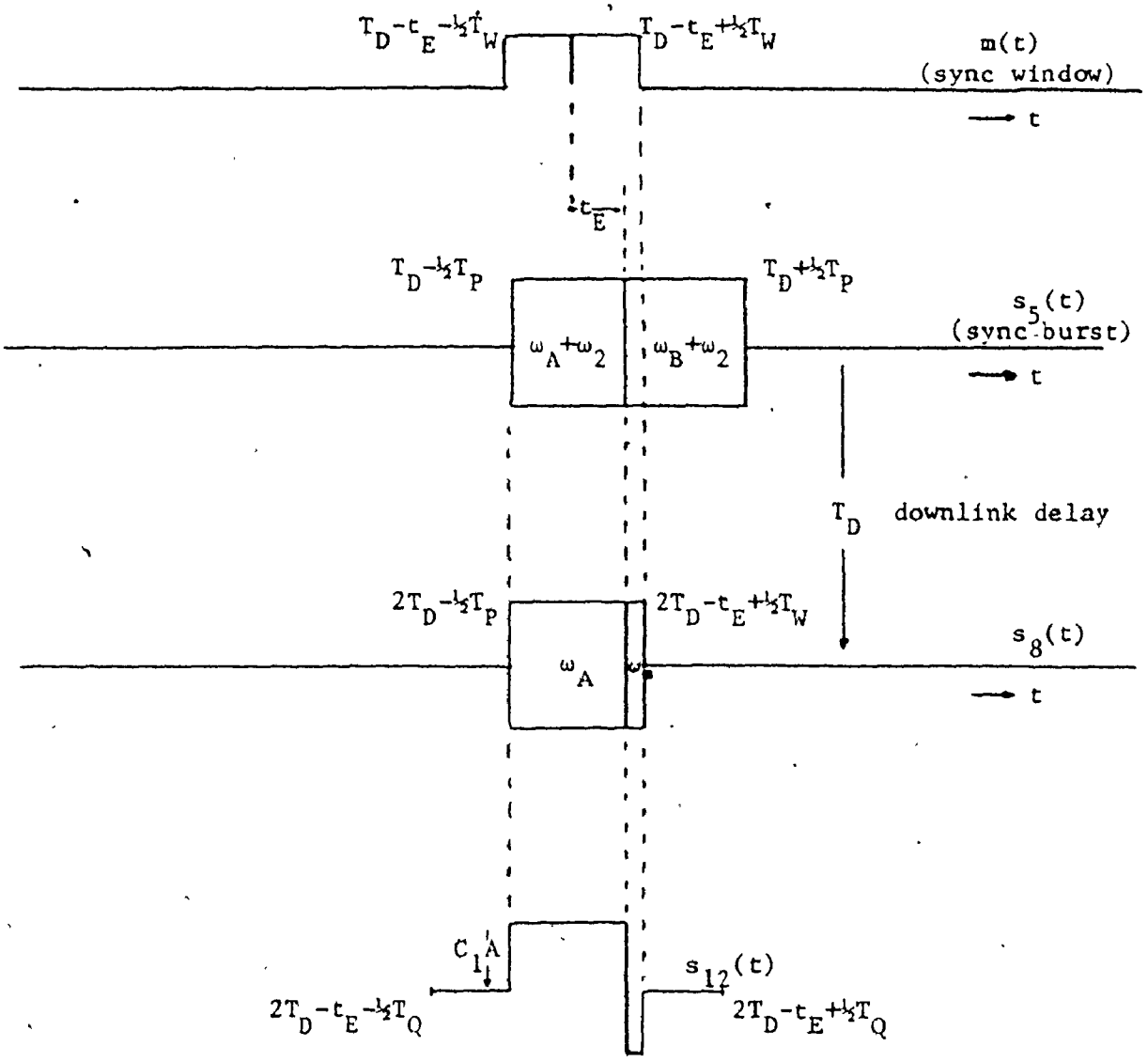

Fig. 3.2.d Sync window modulation on-board the satellite and detection at the earth station.

(case II. Reg. B: $\frac{1}{2}(T_P - T_W) < t_E < \frac{1}{2}T_W$)

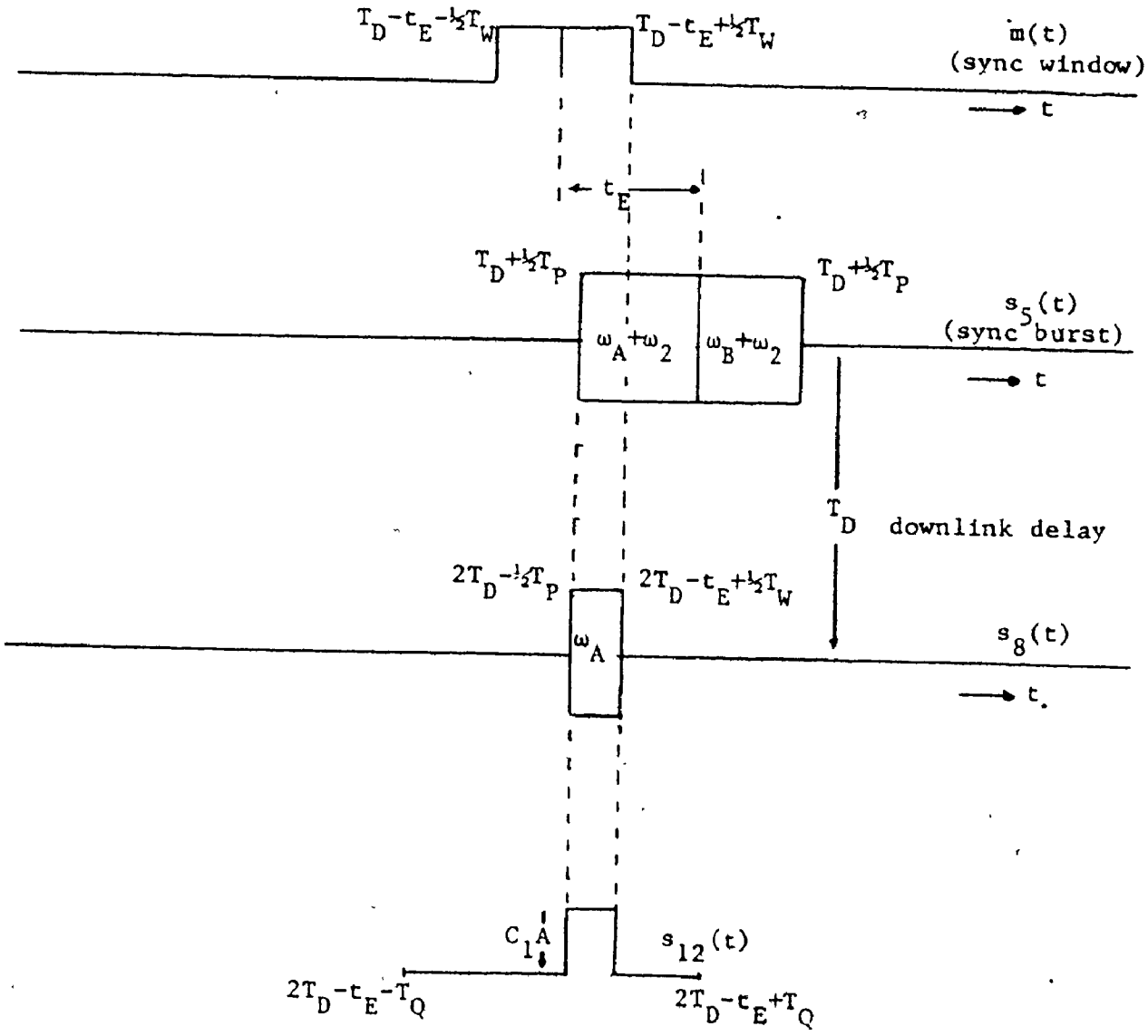

Fig. 3.2.e Sync window modulation on-board the satellite and detection at the earth station.

(case II. Reg. A: $\frac{1}{2}T_W < t_E < \frac{1}{2}(T_P + T_W)$)

CHAPTER 4

ERROR DETECTION CHARACTERISTICS

By integrating the incoherently detected signal (signal $s_{12}(t)$), the time dependence disappears and the error voltage is simply a function of the timing error and noise. The relation between the error voltage and the timing error (i.e., the error detection characteristic) is very important for the timing error analysis.

Two cases are studied again.

I. $2T_W < T_P$

II. $T_W < T_P < 2T_W$

In both cases, the error detection characteristic has an odd symmetry and consists of five regions. The transition from one region to the other is studied in the timing error analysis.

Error detection characteristics are given for both the signal portion of the error voltage (noise-free signal) and its expected value in a noisy environment. Uplink and downlink carrier-to-noise ratios are defined. Then the ratio of the expected value of the error voltage to its noise-free value is studied as a function of the CNR_U (uplink carrier-to-noise ratio) and the CNR_D (downlink carrier-to-noise ratio). (Note: Although high CNR is a valid assumption for this system, the following analysis is valid for any value of the carrier-to-noise ratio.)

In the timing error analysis, the expected value of the timing error after r iterations (transmissions of a sync burst train) is evaluated.

as well as the number of iterations needed for transition from one region to the other.

4.1 THE ERROR DETECTION CHARACTERISTICS IN A NOISE-FREE ENVIRONMENT

Assuming that no noise source exists in the system, signal $s_{12}(t)$ can be easily integrated to yield the noise-free error voltage as a function of only the timing error.

The sync window on-board the satellite modulates uniformly all L sync bursts of the same train of pulses. Moreover, since noise-free (n-f) signals are assumed, all L pulses of signal $[s_{12}(t)]_{n-f}$ are identical. Hence,

$$[v_E]_{n-f} = \frac{1}{T_I} \int_{L \text{ pulses}} [s_{12}(t)]_{n-f} dt = \frac{L}{T_I} \int_{1 \text{ pulse}} [s_{12}(t)]_{n-f} dt$$

$$= \frac{L}{T_I} \int_{2T_D - t_E - \frac{1}{2}T_Q}^{2T_D - t_E + \frac{1}{2}T_Q} [s_{12}(t)]_{n-f} dt \qquad (4.1)$$

$[s_{12}(t)]_{n-f}$ can be extracted from equations (3.19) to (3.28). As an example, the error voltage in a noise-free environment for $-\frac{1}{2}(T_P+T_W) < t_E < -\frac{1}{2}(T_P-T_W)$. (case I. $2T_W < T_P$) is calculated as follows:

$$[s_{12}(t)]_{n-f} = \begin{cases} -C_1 A, & 2T_D - t_E - \frac{1}{2}T_W < t < 2T_D + \frac{1}{2}T_P \\ 0, & \text{elsewhere} \end{cases}$$

and

$$[v_E]_{n-f} = \frac{L}{T_I} \int_{2T_D - t_E - \frac{1}{2}T_W}^{2T_D + \frac{1}{2}T_P} -C_1 A dt = -\frac{L}{T_I} C_1 A \cdot [t_E + \frac{1}{2}(T_P+T_W)] \qquad (4.2)$$

Similarly the error detection characteristics in a noise-free environment are calculated as follows:

ERROR DETECTION CHARACTERISTIC I. $2T_W < T_P$

$$[v_E]_{n-f} = \begin{cases} -C_1'A[t_E + \frac{1}{2}(T_P+T_W)], & -\frac{1}{2}(T_P+T_W) < t_E < -\frac{1}{2}(T_P-T_W) & \text{(reg. E)} \\ -C_1'A\cdot T_W, & -\frac{1}{2}(T_P-T_W) < t_E < -\frac{1}{2}T_W & \text{(reg. D)} \\ 2C_1'A\cdot t_E, & -\frac{1}{2}T_W < t_E < \frac{1}{2}T_W & \text{(reg. C)} \\ C_1'A\cdot T_W, & \frac{1}{2}T_W < t_E < \frac{1}{2}(T_P-T_W) & \text{(reg. B)} \\ -C_1'A[t_E - \frac{1}{2}(T_P+T_W)], & \frac{1}{2}(T_P-T_W) < t_E < \frac{1}{2}(T_P+T_W) & \text{(reg. A)} \end{cases} \quad (4.3)$$

ERROR DETECTION CHARACTERISTIC II. $T_W < T_P < 2T_W$

$$[v_E]_{n-f} = \begin{cases} -C_1'A[t_E + \frac{1}{2}(T_P+T_W), & -\frac{1}{2}(T_P+T_W) < t_E < -\frac{1}{2}T_W & \text{(reg. E)} \\ C_1'A[t_E - \frac{1}{2}(T_P-T_W), & -\frac{1}{2}T_W < t_E < -\frac{1}{2}(T_P-T_W) & \text{(reg. D)} \\ 2C_1'A\cdot t_E, & -\frac{1}{2}(T_P-T_W) < t_E < \frac{1}{2}(T_P-T_W) & \text{(reg. C)} \\ C_1'A[t_E + \frac{1}{2}(T_P-T_W), & \frac{1}{2}(T_P-T_W) < t_E < \frac{1}{2}T_W & \text{(reg. B)} \\ -C_1'A[t_E - \frac{1}{2}(T_P+T_W), & \frac{1}{2}T_W < t_E < \frac{1}{2}(T_P+T_W) & \text{(reg. A)} \end{cases} \quad (4.4)$$

where $$C_1' = \frac{L}{T_I}\cdot C_1$$

The error detection characteristics are plotted in Figs. 4.1 and 4.2.

4.2 EXPECTED VALUE OF THE ERROR VOLTAGE IN A NOISY ENVIRONMENT

The error voltage (v_E) is a function of the timing error

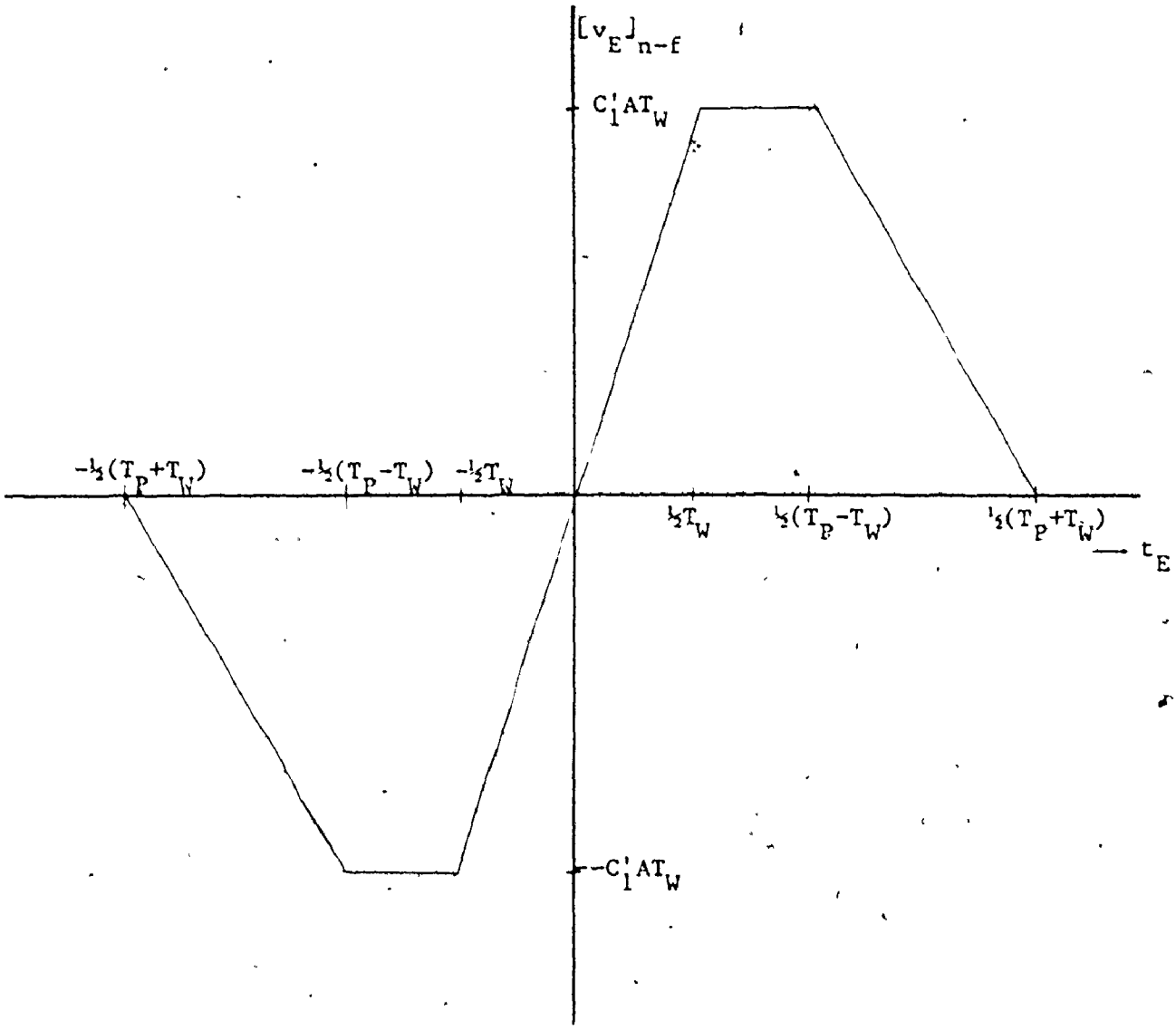

Fig. 4.1 Error detection characteristic, case I. $2T_W<T_P$

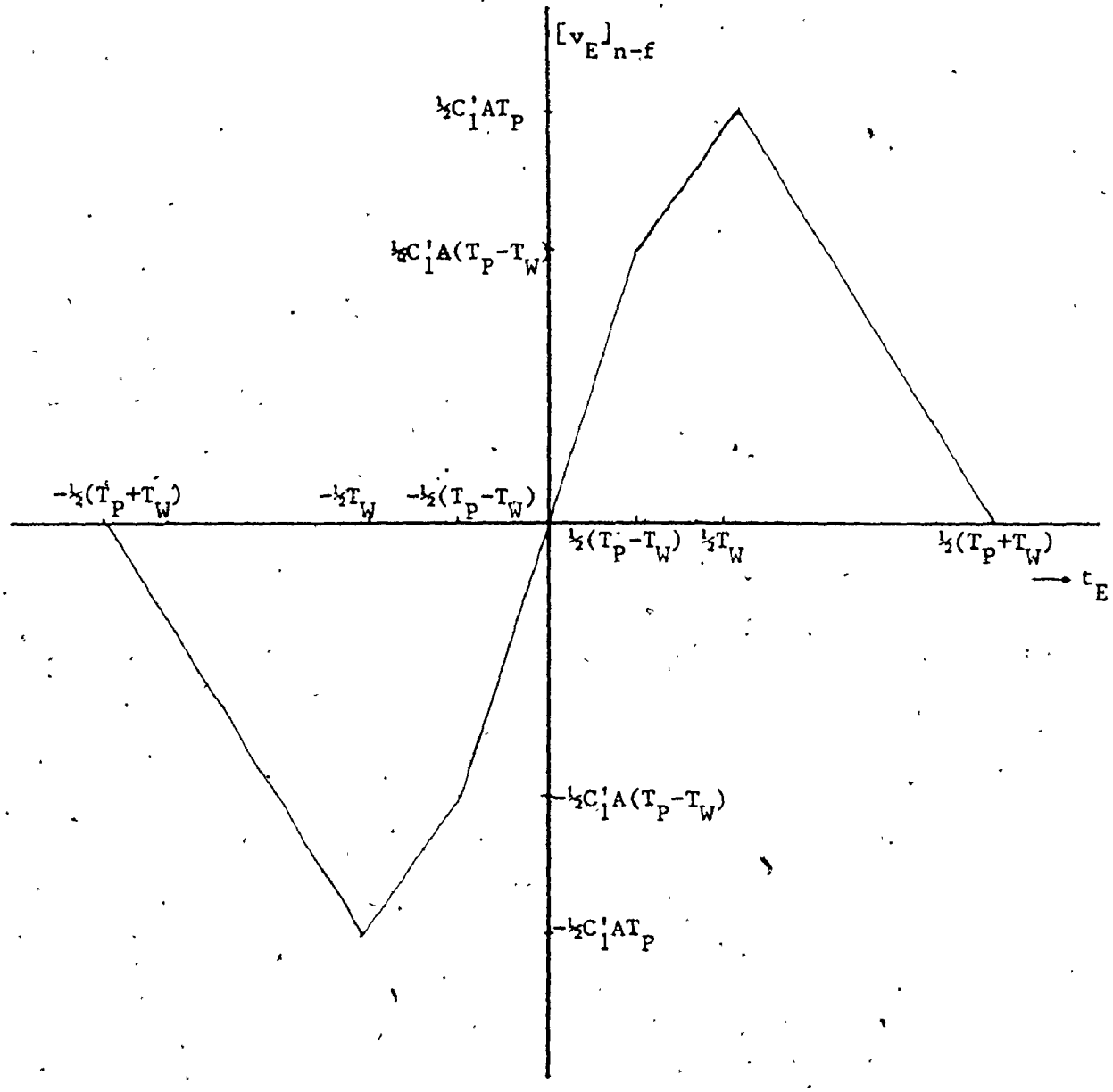

Fig. 4.2 Error detection characteristic, case II. $T_W<T_P<2T_W$

and the noise.

It is possible to average this error voltage over the noise and obtain its expected value.

The expected value of the error voltage (equation (3.29)) is given by:

$$E[v_E] = E\left(\frac{1}{T_I} \int_{L \text{ pulses}} s_{12}(t)dt\right) \tag{4.5}$$

Since stationary noise is assumed and all L sync bursts of the same train are identically modulated by the sync window, equation (4.5) may be written as:

$$E[v_E] = \frac{L}{T_I} \cdot E\left(\int_{2T_D - t_E - \frac{1}{2}T_Q}^{2T_D - t_E + \frac{1}{2}T_Q} s_{12}(t)dt \right) \tag{4.6}$$

In Appendix A the expected values of three representative integrals of noise (A-1,A-2) and signal plus noise (A-3) are calculated. With the aid of A-1, A-2 and A-3, the error detection characteristics for the expected value of the error voltage in a noisy environment are derived as follows:

Case I. $2T_W < T_P$

$$E[v_E] = \begin{cases} -C[t_E + \frac{1}{2}(T_P+T_W)], & -\frac{1}{2}(T_P+T_W) < t_E < -\frac{1}{2}(T_P-T_W) \quad \text{(reg. E)} \\ -C \cdot T_W, & -\frac{1}{2}(T_P-T_W) < t_E < -\frac{1}{2}T_W \quad \text{(reg. D)} \\ 2C \cdot t_E, & -\frac{1}{2}T_W < t_E < \frac{1}{2}T_W \quad \text{(reg. C)} \\ C \cdot T_W, & \frac{1}{2}T_W < t_E < \frac{1}{2}(T_P-T_W) \quad \text{(reg. B)} \\ -C[t_E - \frac{1}{2}(T_P+T_W)], & \frac{1}{2}(T_P-T_W) < t_E < \frac{1}{2}(T_P+T_W) \quad \text{(reg. A)} \end{cases} \tag{4.7}$$

Case II. $T_W < T_P < 2T_W$

$$E[v_E] = \begin{cases} -C[t_E + \frac{1}{2}(T_P+T_W)], & -\frac{1}{2}(T_P+T_W) < t_E < -\frac{1}{2}T_W \quad \text{(Reg. E)} \\ C[t_E - \frac{1}{2}(T_P-T_W)], & -\frac{1}{2}T_W < t_E < -\frac{1}{2}(T_P-T_W) \quad \text{(Reg. D)} \\ 2C \cdot t_E, & -\frac{1}{2}(T_P-T_W) < t_E < \frac{1}{2}(T_P-T_W) \quad \text{(Reg. C)} \\ C[t_E + \frac{1}{2}(T_P-T_W)], & \frac{1}{2}(T_P-T_W) < t_E < \frac{1}{2}T_W \quad \text{(Reg. B)} \\ -C[t_E - \frac{1}{2}(T_P+T_W)], & \frac{1}{2}T_W < t_E < \frac{1}{2}(T_P+T_W) \quad \text{(Reg. A)} \end{cases} \tag{4.8}$$

where $C = \frac{L}{T_I} \cdot (K - \sqrt{\frac{\pi}{2}} \cdot \sigma)$

$$= \frac{L}{T_I} C_1 \cdot A \cdot \frac{\sqrt{\pi}}{2} \cdot \frac{1}{\sqrt{\frac{C_1^2 A^2}{2\sigma^2}}} \left[\exp\left[-\frac{C_1^2 A^2}{2\sigma^2}\right] \cdot {}_1F_1\left(\frac{3}{2};1;\frac{C_1^2 A^2}{2\sigma^2}\right) - 1\right]$$

$$= C_1' \cdot A \cdot \frac{\sqrt{\pi}}{2} \cdot \frac{1}{\sqrt{\frac{C_1^2 A^2}{2\sigma^2}}} \left[\exp\left[-\frac{C_1^2 A^2}{2\sigma^2}\right] \cdot {}_1F_1\left(\frac{3}{2};1;\frac{C_1^2 A^2}{2\sigma^2}\right) - 1\right] \tag{4.9}$$

${}_1F_1(\frac{3}{2};1;x)$: Confluent Hypergeometric Function

4.3 UPLINK AND DOWNLINK CARRIER-TO-NOISE RATIOS

In this system both uplink carrier-to-noise ratio (CNR_U) and downlink carrier-to-noise ratio (CNR_D) are quite high. Moreover, now that new uplink and downlink frequencies are going to be used, taken from the "empty" microwave bands of the 11/14 GHz and 20/30 GHz, the transmitted power and therefore the carrier-to-noise ratios can be high.

Uplink C/N can vary from 20 to 40 db and downlink C/N from 5 to 30 db.

Uplink C/N is always greater than the downlink. The satellite antenna gain is also small and the efficiency of the TWTs does not exceed 50%.

The carrier-to-noise ratio is defined as

$$CNR = \frac{E}{N} \qquad \text{(N mean noise power)}$$

For narrow-band noise, it can be expressed as:

$$CNR = \frac{E}{n_o B} \tag{4.10}$$

where E: energy of the carrier signal measured at the amplifier's input, normalized over 1 ohm resistor

$n_o/2$: double-sided noise spectrum density

B: bandwidth of the noise.

The uplink carrier-to-noise ratio CNR_U calculated at the satellite's input amplifier is given by:

$$CNR_U = \frac{E_U}{n_o B} = \frac{\left[\frac{K_1 K_2 A}{\sqrt{2}}\right]^2}{n_o B} = \frac{(C_1/C_2)^2 A^2}{2n_o B} \tag{4.11}$$

The downlink carrier-to-noise ratio CNR_D calculated at the earth station's input amplifier is given by:

$$CNR_D = \frac{E_D}{n_o B} = \frac{\left[\frac{K_1 K_2 K_3 K_4 K_5 A}{\sqrt{2}}\right]^2}{n_o B} = \frac{(C_1/K_6)^2 A^2}{2n_o B} \tag{4.12}$$

Now the ratio $\frac{C_1^2 A^2}{2\sigma^2}$ which appears in equation (4.9) can be expressed in terms of the CNR_U, CNR_D:

$$\frac{C_1^2 A^2}{2\sigma^2} = \frac{C_1^2 A^2}{2(C_2^2+K_6^2) n_o B} = \frac{1}{\frac{2n_o B}{(C_1/C_2)^2 A^2} + \frac{2n_o B}{(C_1/K_6)^2 A^2}}$$

or

$$\frac{C_1^2 A^2}{2\sigma^2} = \frac{1}{\frac{1}{CNR_U} + \frac{1}{CNR_D}} \tag{4.13}$$

For convenience the ratio $\frac{C_1^2 A^2}{2\sigma^2}$ will be called normalized carrier-to-noise ratio CNR_N and it represents the overall CNR of the system.

$$CNR_N = \frac{1}{\frac{1}{CNR_U} + \frac{1}{CNR_D}} \tag{4.14}$$

For $CNR_U >> CNR_D$ (say $CNR_U > CNR_D + 20$ db)

$$CNR_N \simeq CNR_D \tag{4.14a}$$

Equations (4.14) and (4.14a) show that the system performance depends mostly on the downlink carrier-to-noise ratio.

4.4 THE RATIO OF THE EXPECTED VALUE OF THE ERROR VOLTAGE TO ITS NOISE-FREE VALUE

In the error detection characteristics (equations (4.3) and (4.4)) the noise-free error voltage $[v_E]_{n-f}$ is given in terms of $C_1'A$, t_E and T_W, T_P. Thus it can be written as:

$$[v_E]_{n-f} = C_1 A \cdot f(t_E, T_W, T_P) \tag{4.15}$$

where $f(t_E, T_W, T_P)$ is generally a simple, linear function of the timing error, and T_P, T_W. Clearly the function $f(t_E, T_W, T_P)$ has different form for the various regions of the characteristics.

The expected value of the error voltage (equations (4.8), (4.9))

can be also expressed as:

$$E[v_E] = C \cdot f(t_E, T_W, T_P) \tag{4.16}$$

where $f(t_E, T_W, T_P)$ is the same function as in equation (4.15) for any given value of t_E.

Therefore, the ratio of the expected value of the error voltage to its noise-free value can be expressed in terms of the CNR_N, namely in terms of uplink and downlink carrier-to-noise ratio (equation (4.14)). Thus:

$$\frac{E[v_E]}{[v_E]_{n-f}} = \frac{C}{C_1 A} = \frac{\sqrt{\pi}}{2} \cdot \frac{1}{\sqrt{CNR_N}} \cdot [\exp(-CNR_N) \cdot {}_1F_1(\tfrac{3}{2};1;CNR_N) - 1] \tag{4.17}$$

The confluent hypergeometric function ${}_1F_1(a;b;z)$ was calculated by Kummer's function [31]

$${}_1F_1(a;b;z) = 1 + \frac{az}{b} + \frac{(a)_2 z^2}{(b)_2 2!} + \ldots + \frac{(a)_n z^n}{(b)_n n!} + \ldots \tag{4.18}$$

where

$$(a)_n = a(a+1) \ldots (a+n-1) \quad \text{and} \quad a_o = 0$$

The number of terms required so that this series converges was found to be greater than the argument z, i.e., $n > z$.

For large value of CNR_N, $\exp(-CNR_N)$ becomes too small and ${}_1F_1(\frac{3}{2};1;CNR_N)$ too large to be calculated by the computer. Consequently, the product $\exp(-CNR_N) \cdot {}_1F_1(\frac{3}{2};1;CNR_N)$ has to be calculated by the following formula [31]:

$${}_1F_1(a;b;z) = \frac{\Gamma(b)}{\Gamma(a)} \cdot e^z \cdot z^{a-b} \cdot (1+0(|z|^{-1})), \qquad \text{Re}\, z > 0$$

for z very large $\qquad 0(|z|^{-1}) \to 0$

So

$$e^{-z} \cdot {}_1F_1(a;b;z) \approx \frac{\Gamma(b)}{\Gamma(a)} z^{a-b} \qquad (4.19)$$

Thus

$$\frac{E[v_E]}{[v_E]_{n-f}} = \begin{cases} \frac{\sqrt{\pi}}{2} \cdot \frac{1}{\sqrt{CNR_N}} \cdot [\exp(-CNR_N) \cdot {}_1F_1(\frac{3}{2};1;CNR) - 1] \\ \\ 1 - \frac{\sqrt{\pi}}{2} \cdot \frac{1}{\sqrt{CNR_N}} \cdot \end{cases} \quad \text{for } CNR_N > 28 \text{ db or } 650 \qquad (4.20)$$

In Table 1 the above functions are calculated for $CNR_N = 650$ to 674. It is seen that equation (4.19) is a good approximation, and even for $CNR_N = 650$ (28.1 db) the approximation error does not exceed 0.04%. From equation (4.20) it is verified that for $CNR_N \to \infty$

$$\therefore \quad \frac{E[v_E]}{[v_E]_{n-f}} \to 1 \qquad \text{i.e.} \qquad E[v_E] \to [v_E]_{n-f}$$

In Fig. 4.3 the ratio $\frac{E[v_E]}{[v_E]_{n-f}}$ is plotted versus CNR_U and CNR_D.

In Fig. 4.4 the ratio $\frac{E[v_E]}{[v_E]_{n-f}}$ is plotted versus CNR_N (see equations (4.14) and (4.14a)).

4.5 TIMING ERROR ANALYSIS

The timing circuits (Fig. 2.3) and their operations are described in detail in Section 2.4. The voltage error is fed to the control terminal of the VCO through the timing adjustment gate T_G.

The VCO output frequency is given as:

$$f = f_o + Sv_E \qquad (4.21)$$

T A B L E I

CNR_N	CNR_N in db	Y_1	Y_2	approximation error %
650.	28.129	.96562	.95524	.0398
651.	28.136	.96565	.95527	.0398
652.	28.142	.96568	.95529	.0397
653.	28.149	.96570	.95532	.0397
654.	28.156	.96573	.95535	.0396
655.	28.162	.96575	.95537	.0395
656.	28.169	.96578	.95540	.0395
657.	28.176	.96581	.95542	.0394
658.	28.182	.96583	.95545	.0393
659.	28.189	.96586	.95548	.0393
660.	28.195	.96588	.95550	.0392
661.	28.202	.96591	.95553	.0392
662.	28.209	.96593	.95556	.0391
663.	28.215	.96596	.95558	.0390
664.	28.222	.96598	.95561	.0390
665.	28.229	.96601	.95563	.0389
666.	28.235	.96603	.95566	.0389
667.	28.241	.96606	.95569	.0388
668.	28.248	.96609	.95571	.0387
669.	28.254	.96611	.95574	.0387
670.	28.261	.96614	.95576	.0386
671.	28.267	.96616	.95579	.0386
672.	28.274	.96619	.95581	.0385
673.	28.280	.96621	.95584	.0385
674.	28.287	.96623	.95586	.0384

$$Y_1 = \frac{\sqrt{\pi}}{2} \cdot \frac{1}{\sqrt{CNR_N}} \cdot \left[\exp(-CNR_N) \cdot {}_1F_1\left(\frac{3}{2}; 1; CNR_N\right) - 1\right]$$

$$Y_2 = 1 - \frac{\sqrt{\pi}}{2} \cdot \frac{1}{\sqrt{CNR_N}}$$

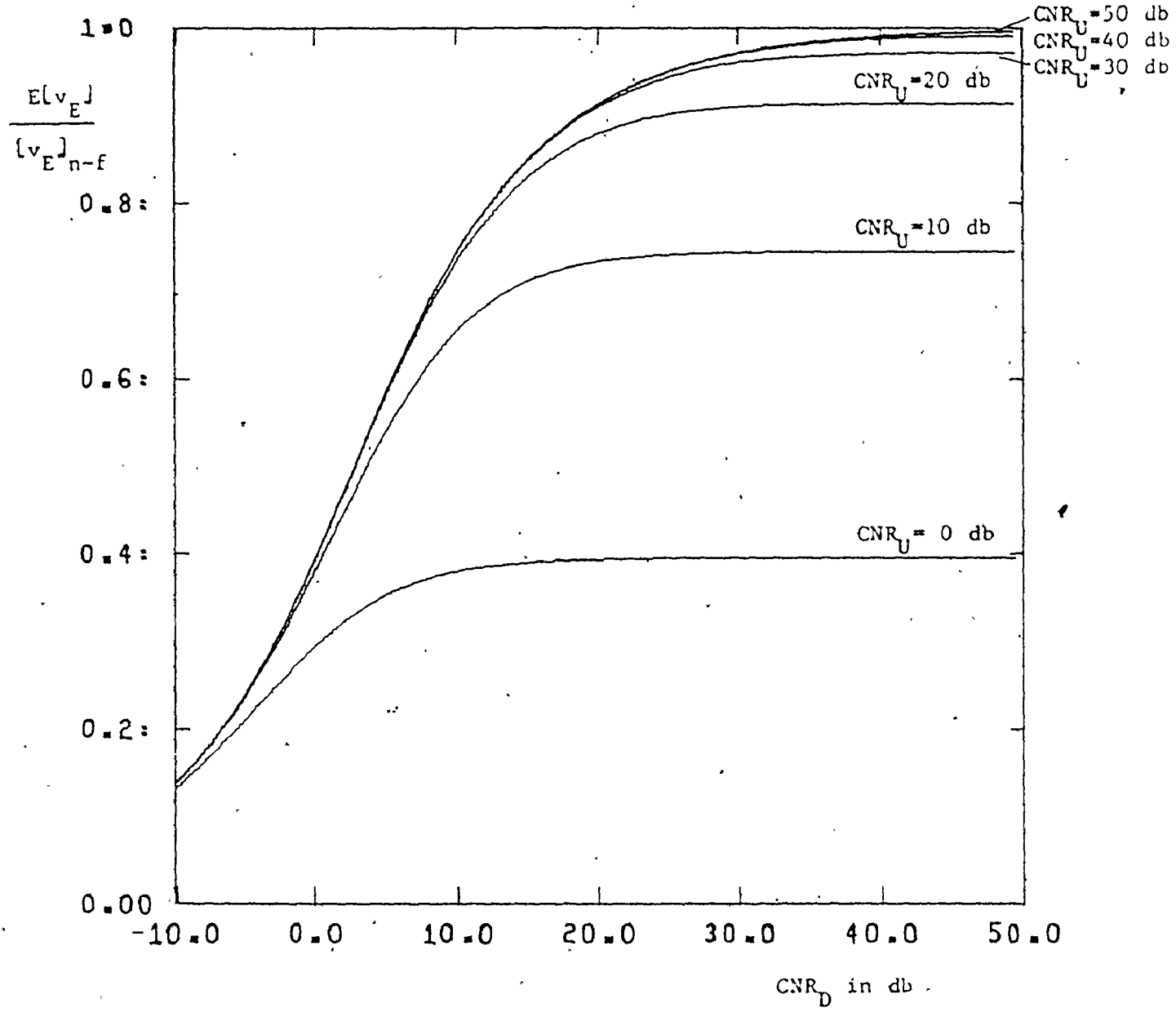

Fig. 4.3 The ratio of the expected value of the error voltage to its noise-free value vs the uplink and downlink carrier-to-noise ratio

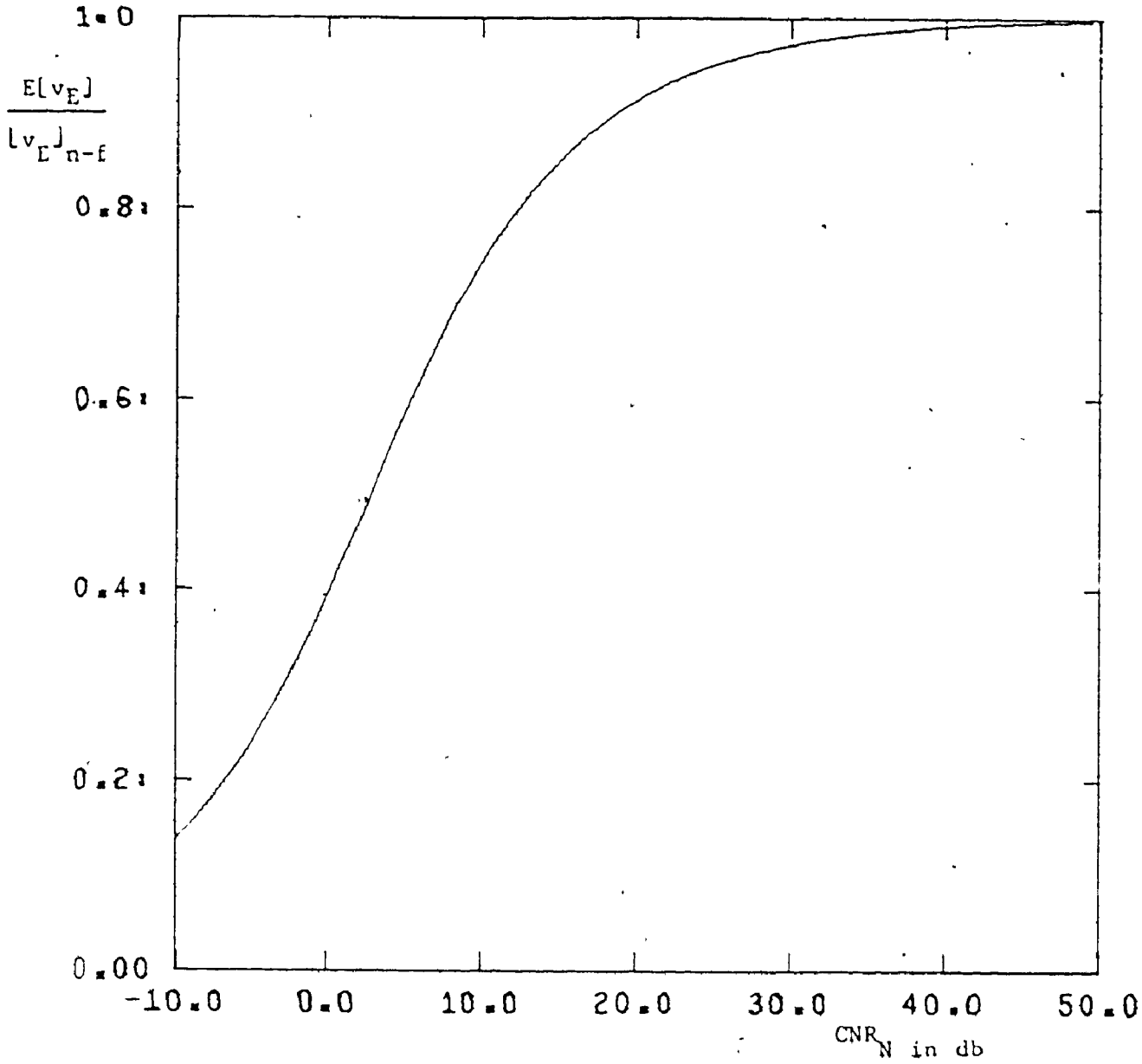

Fig. 4.4 The ratio of the expected value of the error voltage to its noise-free value vs the normalized carrier-to-noise ratio

where f_o: free-running VCO frequency (31.992 MHz [20])

S: sensitivity of the VCO in Hz/V.

The interpulse spacing of the pulses produced by the counter and decoder is

$$T = \frac{K_C}{f} \tag{4.22}$$

where K_C: constant of the counter and

f: VCO output frequency.

From equations (4.21) and (4.22)

$$T = \frac{K_C}{f_o + Sv_E} \approx \frac{K_C}{f_o}\left(1 - \frac{Sv_E}{f_o}\right)$$

$$= T_o\left(1 - \frac{Sv_E}{f_o}\right) \tag{4.23}$$

where T_o: interpulse spacing of the counter pulses with $v_E = 0$ [24]. For an interval T_o the timing shift is $-\frac{ST_o}{f_o} v_E$. Thus for a gate length of T_G the total timing shift is

$$t_S = -\frac{ST_G}{f_o} v_E$$

$$= -bv_E \tag{4.24}$$

Let $t_E(0)$ be the initial timing error obtained from the coarse search mode and $v_E(0)$ its corresponding error voltage measured at the integrator output, then the first timing shift is:

$$t_S(1) = -bv_E(0) \tag{4.25}$$

Consequently the first timing error of the fine search mode is given by:

$$t_E(1) = t_E(0) + t_S(1) + t_M$$

$$= t_E(0) - bv_E(0) + t_M \qquad (4.26)$$

t_M is the change in path delay between two successive transmissions due to the satellite motion [33],[34].

Assuming constant velocity satellite motion, t_M is given as

$$t_M = \frac{V_X}{C}(2T_D + T_{EP}) \approx \frac{V_X}{C} \cdot 2T_D$$

where V_X: radial velocity

C: velocity of light

$2T_D$: round trip time delay

T_{EP}: time required by the earth station to process the L received sync bursts ($T_{EP} \approx LT_o << 2T_D$)

The change in path delay t_M has been estimated to be of the order of 18 ns [20].

Equations (4.25) and (4.26) can be generalized as follows:

$$t_S(n+1) = -b \cdot v_E(n) \qquad (4.27)$$

$$t_E(n+1) = t_E(n) - bv_E(n) + t_M \qquad (4.28)$$

From the error detection characteristics (equations (4.3), (4.4) and (4.7), (4.8)) it is seen that for a positive timing error, the corresponding error voltage is also positive so that the timing shift (4.27) is negative.

Assuming small path delay due to satellite motion: $t_M < t_E(n) - bv_E(n)$

$$\therefore \quad t_E(n+1) < t_E(n)$$

or

$$|t_E(n+1)| < |t_E(n)| \qquad (4.29)$$

Similarly, when the timing error is negative, the error voltage is also negative and the corresponding timing shift positive. Then,

$$t_E(n+1) > t_E(n)$$

or

$$|t_E(n+1)| < |t_E(n)| \qquad (4.30)$$

Equations (4.29) and (4.30) verify that the timing circuits always provide an absolute reduction in the timing error.

[Note: The case where the timing error of two successive iterations are of opposite sign (region C) is not considered since it is shown in equations (4.43) and (4.49) that under the restriction $0 < 2bC < 2$ and after a large number of iterations, the timing error converges to zero or, if we consider satellite motion, to $\frac{t_M}{2bC}$ (order of ns).]

The detailed analysis of timing error reduction in the Regions A, B, C is described next. Due to odd symmetry of the error detection characteristics, timing error analysis for the regions D and E can be obtained from the corresponding analysis of Regions B and A.

4.5.1 Case I. $2T_W < T_P$

a. Analysis for Region A $\quad \frac{1}{2}(T_P - T_W) < t_E < \frac{1}{2}(T_P + T_W)$

In Region A the expected value of the error voltage (equation (4.7)) is given as:

$$E[v_{EA}(n)] = -C[t_{EA}(n) - \tfrac{1}{2}(T_P + T_W)] \qquad (4.31)$$

After the first iteration, the timing error is (equation (4.8))

$$t_{EA}(1) = t_{EA}(0) - bv_E(0) + t_M \qquad (4.32)$$

$t_{EA}(0)$ is the initial timing error obtained from the coarse

search mode and must be less than $\frac{1}{2}(T_P+T_W)$. The expected value of $t_{EA}(1)$ is calculated as

$$E[t_{EA}(1)] = t_{EA}(0) - b\cdot E[v_{EA}(0)] + t_M$$

$$= t_{EA}(0) + bCt_{EA}(0) - \frac{bC}{2}(T_P+T_W) + t_M \qquad (4.33)$$

After the second iteration the timing error becomes:

$$t_{EA}(2) = t_{EA}(1) - bv_{EA}(1) + t_M$$

and its expected value is (see Appendix B)

$$E[t_{EA}(2)] = E[E[t_{EA}(1)] + bCt_{EA}(1) - \frac{bC}{2}(T_P+T_W) + t_M]$$

$$= E[E[t_{EA}(1)] + bCt_{EA}(1) - \frac{bC}{2}(T_P+T_W) + t_M]$$

$$= (1+bC)\cdot E[t_{EA}(1)] - \frac{bC}{2}(T_P+T_W) + t_M$$

Substituting $E[t_{EA}(1)]$ from equation (4.33), $E[t_{EA}(2)]$ becomes

$$E[t_{EA}(2)] = (1+bC)^2 t_{EA}(0) - [\frac{bC}{2}(T_P+T_W) - t_M][1 + (1+bC)] \qquad (4.34)$$

Similarly, the expected value of the timing error after r iterations is given as:

$$E[t_{EA}(r)] = (1+bC)^r\cdot t_{EA}(0) - [\frac{bC}{2}(T_P+T_W) - t_M]\cdot \sum_{n=1}^{r} (1+bC)^{r-1}$$

$$= (1+bC)^r\cdot t_{EA}(0) - [\frac{bC}{2}(T_P+T_W) - t_M]\cdot \frac{(1+bC)^r - 1}{(1+bC) - 1}$$

$$= (1+bC)^r\cdot [t_{EA}(0) - \frac{1}{2}(T_P+T_W) + \frac{t_M}{bC}] + \frac{1}{2}(T_P+T_W) - \frac{t_M}{bC}$$

$$= (1+bC)^r\cdot t_{EA}(0) - [1 + (1+bC)^r][\frac{1}{2}(T_P+T_W) - \frac{t_M}{bC}] \qquad (4.35)$$

For high carrier-to-noise ratio $bC \to bC_1 A$ and the expected value of the timing error after r iterations in the case of noncoherent FSK sync bursts reduces to the corresponding value for the case of coherent FSK sync bursts [22].

The number of iterations r_A required for transition from region A to region B is now calculated. First, the real number r, such that: $E[t_{EA}(r)] = \frac{1}{2}(T_P - T_W)$, is calculated. $\frac{1}{2}(T_P - T_W)$ is the boundary between Region A and Region B.

$$(1+bC)^r \left[t_{EA}(0) - \frac{1}{2}(T_P+T_W) + \frac{t_M}{bC}\right] + \frac{1}{2}(T_P+T_W) - \frac{t_M}{bC} = \frac{1}{2}(T_P-T_W)$$

or

$$(1+bC)^r = \frac{T_W - \frac{t_M}{bC}}{\frac{1}{2}(T_P+T_W) - \frac{t_M}{bC} - t_{EA}(0)}$$

Thus,

$$r = \frac{\ln\left(T_W - \frac{t_M}{bC}\right) - \ln\left[\frac{1}{2}(T_P+T_W) - \frac{t_M}{bC} - t_{EA}(0)\right]}{\ln(1+bC)}$$

Then the required number of iterations r_A for transition from Region A to Region B is the smallest integer such that:

$$(r_A)_{\substack{\text{smallest}\\ \text{integer}}} > \frac{\ln\left(T_W - \frac{t_M}{bC}\right) - \ln\left[\frac{1}{2}(T_P+T_W) - \frac{t_M}{bC} - t_{EA}(0)\right]}{\ln(1+bC)} \qquad (4.36)$$

To achieve convergence with satellite motion, bC must be large enough so $E[t_{EA}(r)] < E[t_{EA}(r-1)]$ [22]. Assuming positive t_M, this requirement yields:

$$bC > \frac{t_M}{\frac{1}{2}(T_P+T_W) - t_{EA}(0)} \qquad (4.36a)$$

b. Analysis for Region B $\frac{1}{2}T_W < t_E < \frac{1}{2}(T_P - T_W)$

In Region B, the expected value of the error voltage (equation (4.7)) is given by

$$E[v_{EB}(n)] = CT_W \tag{4.37}$$

After the first iteration, the timing error is

$$t_{EB}(1) = t_{EB}(0) - bv_E(0) + t_M \tag{4.38}$$

where $t_{EB}(0)$ is defined by the transition from the Region A to Region B as:

$$t_{EB}(0) = E[t_{EA}(r_A)] \quad \text{and} \quad r_A \text{ is defined in (4.36)}$$

The expected value of the first timing error is then,

$$E[t_{EB}(1)] = t_{EB}(0) - bCT_W + t_M$$

The expected value of the timing error after r iterations is then given as:

$$E[t_{EB}(r)] = t_{EB}(0) - r\cdot[bCT_W - t_M] \tag{4.39}$$

The number of iterations r_B required for transition from Region B to Region C is calculated as:

$$(r_B)_{\substack{\text{smallest}\\ \text{integer}}} > \frac{t_{EB}(0) - \frac{1}{2}T_W}{bCT_W - t_M} \tag{4.40}$$

To achieve convergence with satellite motion bC must be [22]:

$$bC > \frac{t_M}{T_W} \tag{4.40a}$$

c. Analysis for Region C $-\frac{1}{2}T_W < t_E < \frac{1}{2}T_W$

In Region C the expected value of the error voltage (equation 4.7) is given as:

$$E[v_{EC}(n)] = 2Ct_{EC}(n) \tag{4.41}$$

As in Region A (section 4.5.1a) the expected value of the timing error after r iterations is:

$$E[t_{EC}(r)] = (1-2bC)^r \cdot [t_{EC}(0) - \frac{t_M}{2bC}] + \frac{t_M}{2bC} \tag{4.42}$$

Again $t_{EC}(0)$ is the initial timing error in Region C and is defined as

$$t_{EC}(0) = E[t_{EB}(r_B)]$$

where r_B is given in equation (4.40).

In order that the timing error converges, a restriction must be imposed upon the carrier-to-noise dependent factor 2bC:

$$|1 - 2bC| < 1$$

or

$$0 < 2bC < 2 \tag{4.43}$$

[Note: 2bC depends on the synchronization loop parameters such as:

S: sensitivity of the VCO,

T_G: timing adjustment gate,

f_o: VCO free running frequency,

C_1: the total loop gain,

A: signal amplitude

and the uplink and downlink carrier-to-noise ratio (see equations (4.9), (4.13), (4.24).]

Thus, the steady state error due to satellite motion and noise is

$$\frac{t_M}{2bC}$$

4.5.2 Case II. $T_W < T_P < 2T_W$

The analysis for Case II is essentially the same as in Section 4.5.1, thus only the results will be presented:

a. Analysis for Region A $\frac{1}{2}T_W < t_E < \frac{1}{2}(T_P+T_W)$

$$E[v_{EA}(n)] = -C[t_{EA}(n) - \tfrac{1}{2}(T_P+T_W)]$$

$$E[t_{EA}(r)] = (1+bC)^r \cdot t_{EA}(0) - [1 + (1+bC)^r] \cdot [\tfrac{1}{2}(T_P+T_W) - \frac{t_M}{bC}]$$

$$= (1+bC)^r \cdot [t_{EA}(0) - \tfrac{1}{2}(T_P+T_W) + \frac{t_M}{bC}] + \tfrac{1}{2}(T_P+T_W) - \frac{t_M}{bC} \qquad (4.44)$$

The number of iterations r_A required for transition from Region A to Region B is

$$(r_A)_{\substack{\text{smallest}\\ \text{integer}}} > \frac{\ln(\frac{1}{2}T_P - \frac{t_M}{bC}) - \ln[\frac{1}{2}(T_P+T_W) - \frac{t_M}{bC} - t_{EA}(0)]}{\ln(1+bC)} \qquad (4.45)$$

Convergence with satellite motion is as in equation (4.36a).

b. Analysis for Region B $\frac{1}{2}(T_P-T_W) < t_E < \frac{1}{2}T_W$

$$E[v_{EB}(n)] = C[t_{EB}(n) + \tfrac{1}{2}(T_P-T_W)]$$

$$E[t_{EB}(r)] = (1-bC)^r \cdot t_{EB}(0) - [1 - (1-bC)^r] \cdot [\tfrac{1}{2}(T_P-T_W) - \frac{t_M}{bC}]$$

$$= (1-bC)^r [t_{EB}(0) + \tfrac{1}{2}(T_P-T_W) - \frac{t_M}{bC}] - [\tfrac{1}{2}(T_P-T_W) - \frac{t_M}{bC}] \qquad (4.46)$$

The number of iterations r_B required to reach Region C is

$$(r_B)_{\substack{\text{smallest}\\\text{integer}}} > \frac{\ell n[(T_P-T_W) - \frac{t_M}{bC}] - \ell n[t_{EB}(0) + \frac{1}{2}(T_P-T_W) - \frac{t_M}{bC}]}{\ell n(1-bC)} \qquad (4.47)$$

Convergence with satellite motion

$$bC > \frac{t_M}{\frac{1}{2}(T_P-T_W) + t_{EB}(0)}$$

c. Analysis for Region C $\quad -\frac{1}{2}(T_P-T_W) < t_E < \frac{1}{2}(T_P-T_W)$

$$E[v_{EC}(n)] = 2Ct_E(n)$$

$$E[t_{EC}(r)] = (1-2bC)^r \cdot [t_{EC}(0) - \frac{t_M}{2bC}] + \frac{t_M}{2bC} \qquad (4.48)$$

Again, $$|1 - 2bC| < 1 \qquad (4.49)$$

or $$0 < 2bC < 2$$

The steady state error due to noise and satellite motion is again $\frac{t_M}{2bC}$.

APPENDIX A

INTEGRATED ENVELOPES OF GAUSSIAN NOISE AND SIGNAL PLUS NOISE AND THEIR FIRST-ORDER STATISTICS

The expected values of three representative integrals, averaged over the noise are evaluated.

1. $$\int_{t_1}^{t_2} |z(t)| \cdot dt$$

Since noise z(t) is a stationary process, its envelope $|z(t)|$ is also stationary and its expected value $E[|z(t)|]$ will be a constant independent of time [37]. Thus the expected value of the above integral may be written as:

$$E\left(\int_{t_1}^{t_2} |z(t)| \cdot dt\right) = (t_2 - t_1) \cdot E(|z(t)|)$$

For a Gaussian narrow-band noise with zero mean value and standard deviation $\sqrt{n_o B}$ [38] the probability distribution of its instantaneous value $z(t_o)$ is given by [39]:

$$p(z) = \frac{1}{\sqrt{2\pi n_o B}} \exp\left(-\frac{z^2}{2n_o B}\right)$$

where $n_o/2$: double-sided noise spectral density

B: bandwidth of the noise.

Then its envelope $|z(t)|$ is Rayleigh-distributed [40] with the expected value [41]:

$$E(|z(t)|) = \sqrt{\frac{\pi}{2} n_o B}$$

Therefore:

$$E\left(\int_{t_1}^{t_2} |z(t)| \cdot dt\right) = \int_{t_1}^{t_2} E(|z(t)|) \cdot dt = (t_2 - t_1) \sqrt{\frac{\pi}{2} n_o B} \qquad \text{(A-1)}$$

2. $$\int_{t_1}^{t_2} |C_2 z_1(t) + K_6 z_2(t)| \cdot dt$$

The stochastic processes $C_2 z_1(t)$ (uplink noise) and $C_2 z_2(t)$ (downlink noise) are Gaussian-distributed with zero mean and standard deviation $\sqrt{C_2^2 n_o B}$ and $\sqrt{K_6^2 n_o B}$, respectively [35]. Consequently, the process $(C_2 z_1(t) + K_6 z_2(t))$ is also Gaussian with zero mean value and standard deviation $\sigma = \sqrt{(C_2^2 + K_6^2) n_o B}$ [36].

Therefore, $|C_2 z_1(t) + K_6 z_2(t)|$ is a Rayleigh-distributed process with expected value [41]

$$E(|C_2 z_1(t) + K_6 z_2(t)|) = \sqrt{\frac{\pi}{2}}\,\sigma = \sqrt{\frac{\pi}{2}(C_2^2 + K_6^2) n_o B}$$

Thus,

$$E\left(\int_{t_1}^{t_2} |C_2 z_1(t) + K_6 z_2(t)| \cdot dt\right) = (t_2 - t_1) \cdot \sqrt{\frac{\pi}{2}(C_2^2 + K_6^2) n_o B} \qquad \text{(A-2)}$$

3. $$\int_{t_1}^{t_2} |(C_1 \cdot A + C_2 \cdot x_1(t) + K_6 \cdot x_2(t)) + j(C_2 \cdot y_1(t) + K_6 \cdot y_2(t))| \cdot dt$$

Put $$\alpha(t) = C_1 \cdot A + C_2 \cdot x_1(t) + K_6 \cdot x_2(t)$$

$$\beta(t) = C_2 \cdot y_1(t) + K_6 \cdot y_2(t)$$

Process $\alpha(t)$ is Gaussian-distributed with mean value $C_1 \cdot A$ and standard

deviation $\sigma = \sqrt{(C_2^2+K_6^2)n_oB}$ Process $\beta(t)$ is also Gaussian with zero mean and the same standard deviation [35],[36],

i.e.,

$$p(\alpha) = \frac{1}{\sigma\sqrt{2\pi}} \exp[-\frac{(\alpha-C_1A)^2}{2\sigma^2}] = \frac{1}{\sqrt{2\pi(C_2^2+K_6^2)n_oB}} \exp[-\frac{(\alpha-C_1A)^2}{2(C_2^2+K_6^2)n_oB}]$$

$$p(\beta) = \frac{1}{\sigma\sqrt{2\pi}} \exp[-\frac{\beta^2}{2\sigma^2}] = \frac{1}{\sqrt{2\pi(C_2^2+K_6^2)n_oB}} \exp[-\frac{\beta^2}{2(C_2^2+K_6^2)n_oB}]$$

put

$$\alpha(t) = r(t)\cdot\cos\theta(t)$$

$$\beta(t) = r(t)\cdot\cos\theta(t)$$

$$\therefore \quad r^2(t) = \alpha^2(t) + \beta^2(t)$$

then

$$p(r,\theta) = r\cdot p(\alpha)p(\beta) \qquad [42]$$

and

$$p(r) = \int_0^{2\pi} p(r,\theta)\cdot d\theta$$

$$p(r,\theta) = \frac{r}{2\pi\sigma^2} \cdot \exp -\frac{C_1^2A^2 - 2\alpha C_1A + \alpha^2 + \beta^2}{2\sigma^2}$$

$$= \frac{r}{2\pi\sigma^2} \cdot \exp -\frac{C_1^2A^2 - 2rC_1A\cos\theta + r^2}{2\sigma^2}$$

$$= \frac{r}{\sigma^2} \cdot \exp[-\frac{C_1^2A^2 + r^2}{2\sigma^2}] \cdot \frac{1}{2\pi} \exp\frac{rC_1A\cos\theta}{\sigma^2}$$

So,

$$p(r) = \frac{r}{\sigma^2} \cdot \exp[-\frac{C_1^2A^2 + r^2}{2\sigma^2}] \cdot \frac{1}{2\pi} \int_0^{2\pi} \exp\frac{rC_1A\cos\theta}{\sigma^2} \cdot d\theta$$

$$= \frac{r}{\sigma^2} \cdot \exp[-\frac{C_1^2A^2 + r^2}{2\sigma^2}] \cdot I_o(\frac{rC_1A}{\sigma^2})$$

where $I_o(x)$ is the modified Bessel function of the first kind and zeroth order [41].

The above distribution is called the Rician distribution [43]. The expected value of the process:

$$\int_{t_1}^{t_2} \left|(C_1 \cdot A + C_2 \cdot x_1(t) + K_6 \cdot x_2(t)) + j(C_2 \cdot y_2(t) + K_6 \cdot y_2(t))\right| dt$$

$$= \int_{t_1}^{t_2} \sqrt{\alpha^2(t) + \beta^2(t)}\ dt$$

$$= \int_{t_1}^{t_2} r(t)dt$$

is now calculated.

$$E\left(\int_{t_1}^{t_2} r(t)dt\right) = \int_{t_1}^{t_2} E[r(t)]dt = (t_2 - t_1)E[r(t)]$$

where

$$E[r(t)] = \int_o^\infty rp(r)dr$$

$$= \frac{\exp[-\frac{C_1^2 A^2}{2\sigma^2}]}{\sigma^2} \cdot \int_o^\infty r^2 \cdot \exp[-\frac{r^2}{2\sigma^2}] \cdot I_o(\frac{rC_1 A}{\sigma^2})\, dr$$

In [44] the definite integral

$$\int_o^\infty x^\mu \cdot \exp(-ax^2) \cdot J_\nu(\beta x)dx$$

is given as

$$\int_o^\infty x^\mu \cdot \exp(-ax^2) \cdot J_\nu(\beta x)\, dx = \frac{(\frac{\mu+\nu+1}{2})}{2^{\nu+1}\, a^{\frac{1}{2}(\mu+\nu+1)} \cdot \Gamma(\nu+1)} \cdot {}_1F_1(\frac{\nu+\mu+1}{2}; \nu+1; \frac{-\beta^2}{4a})$$

where $J_\nu(x)$: Bessel function of the first kind and νth order, and

${}_1F_1(a;b;x)$: Confluent Hypergeometric function.

Using the relation [45]:

$$J_\nu(\beta x) = j^\nu \cdot I_\nu(-j\beta x)$$

the above integral becomes

$$\int_0^\infty x^\mu \cdot \exp(-ax^2) I_\nu(-j\beta x)\,dx = \frac{\beta^\nu \cdot \Gamma(\frac{\mu+\nu+1}{2})}{j^\nu \cdot 2^{\nu+1} \cdot a^{\frac{1}{2}(\mu+\nu+1)} \cdot \Gamma(\nu+1)} \cdot {}_1F_1(\frac{\nu+\mu+1}{2};\nu+1;\frac{-\beta^2}{4a^2})$$

and for $b = -j\beta$ $\quad(\beta = jb)$

$$\int_0^\infty x^\mu \cdot \exp(-ax^2) I_\nu(bx)\,dx = \frac{b^\nu \cdot \Gamma(\frac{\mu+\nu+1}{2})}{2^{\nu+1} \cdot a^{\frac{1}{2}(\mu+\nu+1)} \cdot \Gamma(\nu+1)} \cdot {}_1F_1(\frac{\nu+\mu+1}{2};\nu+1;\frac{b^2}{4a^2})$$

For $\mu = 2$, $\nu = 0$, $a = \frac{1}{2\sigma^2}$, and $b = \frac{C_1 A}{\sigma^2}$

$$E[r(t)] = \sqrt{2} \cdot \Gamma(\tfrac{3}{2}) \cdot \sigma \cdot \exp[-\frac{C_1^2 A^2}{2\sigma^2}] \cdot {}_1F_1(\tfrac{3}{2};1;\frac{C_1^2 A^2}{2\sigma^2})$$

So

$$E\left(\int_{t_1}^{t_2} \left|(C_1 \cdot A + C_2 \cdot x_1(t) + K_6 \cdot x_2(t)) + j(C_2 \cdot y_1(t) + K_6 \cdot y_2(t)\right| dt\right)$$

$$= (t_2 - t_1)\sqrt{\frac{\pi}{2}} \cdot \sigma \cdot \exp[-\frac{C_1^2 A^2}{2\sigma^2}] \cdot {}_1F_1(\tfrac{3}{2};1;\frac{C_1^2 A^2}{2\sigma^2}) \qquad (A\text{-}3)$$

$$= K(t_2 - t_1)$$

where

$$K = \sqrt{\frac{\pi}{2}} \cdot \sigma \cdot \exp\left[-\frac{C_1^2 A^2}{2\sigma^2}\right] \cdot {}_1F_1\left(\frac{3}{2}; 1; \frac{C_1^2 A^2}{2\sigma^2}\right)$$

and

$$\sigma = \sqrt{\frac{\sigma_{ps}}{(C_2^2 + K_6^2) n_o B}}$$

APPENDIX B

THE EXPECTED VALUE OF A FUNCTION OF TWO DEPENDENT RANDOM VARIABLES

Let $z = g(x,y)$ be a function of the random variables x,y. Then its total expected value if given by [46]:

$$E_z(z) = E\{g(x,y)\} = E_x\{E\{g(x,y)/x\}\} \tag{B-1}$$

where $E_x\{\cdot\}$ denotes the expected value over the random variable x and $E\{g(x,y)/x\}$ the conditional expected value [47] which is clearly a function of the r.v. x.

Let now $z = g(x,y)$ be of the special form

$$g(x,y) = x + y \tag{B-2}$$

Then [46]

$$E\{g(x,y)/x\} = E\{x/x\} + E\{y/x\} \tag{B-3}$$

Clearly, $E\{x/x\} = \hat{x}$

Let, finally, $E\{y/x\}$ be equal to $ax + b$, i.e.,

$$E\{y/x\} = ax + b \tag{B-4}$$

where a, b are constants.

Substituting equation (B-4) into equation (B-3) and then in (B-1), the total expected value of $z = g(x+y)$ becomes

$$E_z(z) = \hat{x} + a\hat{x} + b = (1 + a)\hat{x} + b \tag{B-5}$$

Equation (B-5) is used in Section 4.5, where $z = g(x,y)$ is the timing

error after n iterations ($t_E(n)$), x is the timing error after n-1 iterations ($t_E(n-1)$) and y is the time shift $t_{sh}(n) = -bV_E(n-1)$.

Thus for Case I, $2T_W < T_P$ and for Region A

$$E\{t_{sh}/t_E(n-1)\} = bCt_E(n-1) - \frac{bC}{2}(T_P+T_W)$$

and

$$E\{t_E(n)\} = (1+bC)\cdot E\{t_E(n-1)\} - \frac{bC}{2}(T_P+T_W)$$

CHAPTER 5

COMPUTER SIMULATION

A computer program was developed to simulate the processed signal $s_{12}(t)$ (signal plus noise) prior to integration. Integration of signal $s_{12}(t)$ yields the error voltage. The expected value of the error voltage over the noise, is simply derived by simulating and integrating signal $s_{12}(t)$ for different sets of noise samples, and averaging the so-obtained values of the error voltage. The mean square value of the error voltage is derived in a similar way.

Clearly, the error voltage is a function of the timing error. Thus by repeating the above procedure for different values of the timing error, the first- and second-order error detection characteristics can be obtained, i.e., the expected and mean square values of the error voltage as functions of the timing error. The first-order error detection characteristic is compared with the theoretical one (Chapter 4).

The second-order error detection characteristics can be approximated (fitted) with smooth curves (linear, quadrature and parabola). Following this, the mean square value of the timing error as a function of the number of iterations can be calculated.

5.1 SIMULATION OF THE PROCESSED SIGNAL PRIOR TO INTEGRATION

It is possible that the signal $s_{12}(t)$ can be simulated by a digital computer in the form of a sampled signal.

The signal $s_{12}(t)$ exists between $2T_D - t_E + \frac{1}{2} T_Q$ and $2T_D - t_E + \frac{1}{2}T_Q$. The round trip space delay $2T_D$ is assumed constant and is not considered

any further. Thus, the duration of signal $s_{12}(t)$ is equal to the input gate T_Q. This duration is divided into the desired number of samples which form the signal $s_{12}(t)$. Let the number of samples be N, then the stepsize H between two successive samples is $H = T_Q/N$.

Each of the N points on the time axes is supplied with eight (8) noise samples. These eight (8) sets of N bandlimited Gaussian noise samples represent:

XI1, $(x_1'(t))$: represents the in-phase component of the uplink noise with respect to the frequency ω_A of the FSK sync burst

XII1, $(x_1''(t))$: represents the in-phase component of the uplink noise with respect to the frequency ω_B of the FSK sync burst

XI2, $(x_2'(t))$: represents the in-phase component of the downlink noise with respect to the frequency ω_A of the FSK sync burst

XII2, $(x_2''(t))$: represents the in-phase component of the downlink noise with respect to the frequency ω_B of the FSK sync burst

YI1, $(y_1'(t))$: represents the quadrature component of the uplink noise with respect to the frequency ω_A of the FSK sync burst

YII1, $(y_1''(t))$: represents the quadrature component of the uplink noise with respect to the frequency ω_B of the FSK sync burst

YI2, $(y_2'(t))$: represents the quadrature component of the downlink noise with respect to the frequency ω_A of the FSK sync burst

YII2, $(y_2''(t))$: represents the quadrature component of the downlink noise with respect to the frequency ω_B of the FSK sync burst

These noise samples were taken from a Gaussian noise generator and recorded on magnetic tape.

The analytical expression for signal $s_{12}(t)$ is given in Section 3.4.

It is seen that for a given value of the timing error (i.e., in a certain Region) $s_{12}(t)$ consists of different functions of noise and functions of signal plus noise.

The time limits NT1, NT2 of each of the above functions are derived, starting with $(NT1)_{1st} = 1$ and $(NT2)_{1st}$ = (duration of the first function)/H, for the first function (Fig. 5.1). Then, the values of each sample from $(NT1)_{1st}$ to $(NT2)_{1st}$ are calculated and stored in an array X( ). The time limits of the second function are derived as:

$$(NT1)_{2nd} = (NT2)_{1st} + 1$$
$$(NT2)_{2nd} = (\Delta t_{1st} + \Delta t_{2nd})/H \qquad (5.1)$$

where Δt_{1st} = duration of the first function

Δt_{2nd} = duration of the second function

Again the values of the $(NT1)_{2nd}$th to $(NT2)_{2nd}$th samples of the signal $s_{12}(t)$ are calculated and stored successively in the array X( ).

Finally, the time limits of the last function are derived as:

$$(NT1)_{last} = (NT2)_{previous} + 1$$
$$(NT2)_{last} = T_Q/H = N \qquad (5.2)$$

After the calculation and storing of the samples referred to the last function, the array X( ) contains the N samples which form the processed signal prior to integration (signal $s_{12}(t)$).

The computer program which was used to simulate signal $s_{12}(t)$ is listed at the end of this chapter. Simulation was performed for a system with the following parameters:

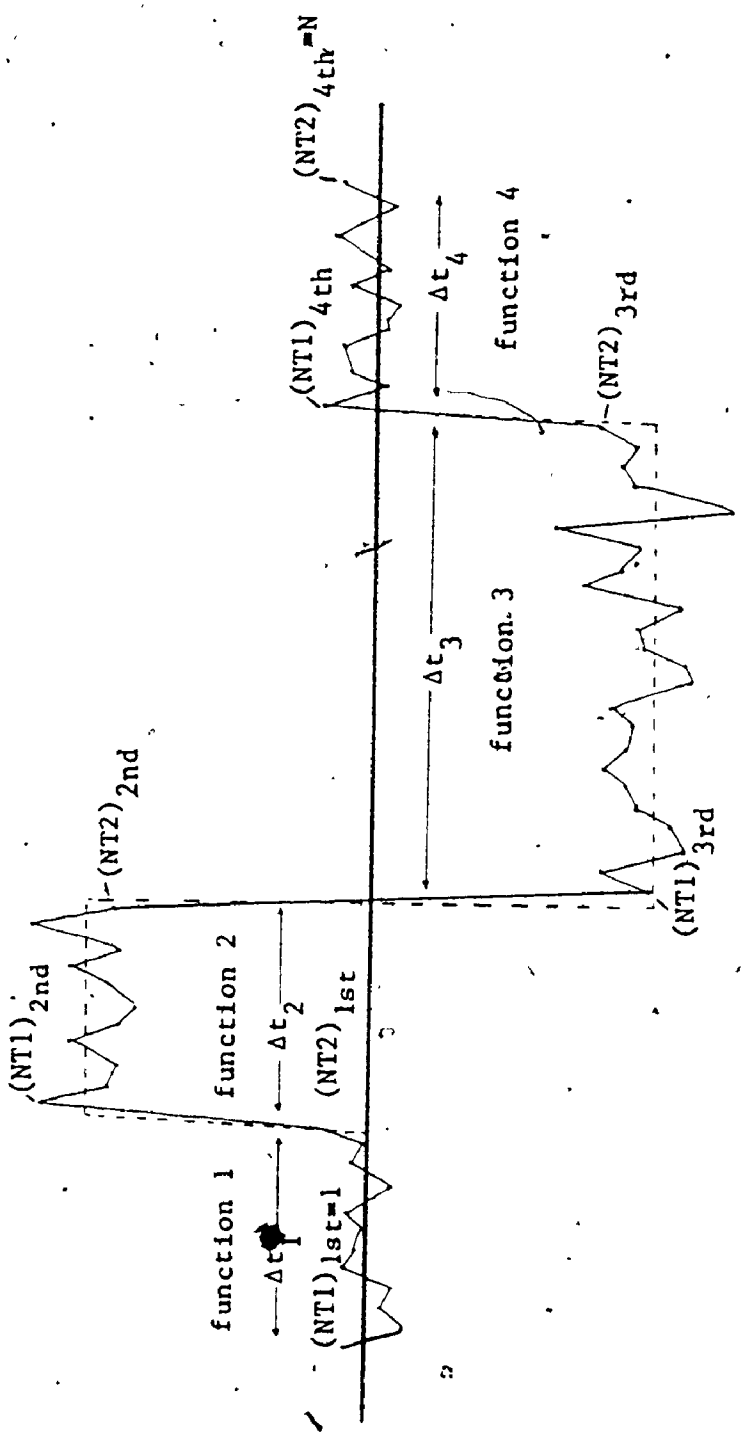

Fig. 5.1 Formation of the computer simulated signal $s_{12}(t)$' (signal prior to integration)

Voltage level of the transmitted signal	A = 1 Volt
Total gain of the synchronization loop	$C_1 = 1$
Gain of the downlink	$C_2 = 1$
Gain of the input amplifier (earth station)	$K_6 = 1$
Input gate duration	$T_Q = 4$ μs
Sync window duration	$T_W = 2$ μs
FSK sync burst duration	$T_p = 6$ μs (case I) or $T_p = 3$ μs (case II)

The noise power ($n_o B$) was varied to yield appropriate values of the uplink/downlink carrier-to-noise ratio:

$n_o B$ (in Watts)	yields	CNR_U/CNR_D in db
$10^{-3}/2$ (.0005)		50/30 (practically noise-free)
$10^{-2}/2$ (.005)		40/20
$10^{-1}/2$ (.05)		30/10

A few samples of the simulated signal for different values of the timing error are shown in Figures 5.2, 5.3 and 5.4 (computer plottings).

5.2 THE FIRST-ORDER ERROR DETECTION CHARACTERISTIC OF THE SIMULATED ERROR VOLTAGE AND ITS COMPARISON WITH THE THEORY

The error voltage is obtained by integrating signal $s_{12}(t)$ (see Section 3.5). Computer integration of the simulated signal $s_{12}(t)$ was performed by means of the trapezoidal rule [48]:

$$z = \int_{x_1}^{x_n+(N-1)h} y(x)dx = \frac{h}{2}(y_1 + 2y_2 + \ldots + 2y_{N-1} + y_N)$$

$$= \frac{h}{2}(y_1 + y_N) + h \sum_{i=2}^{N-1} y_i \qquad (5.3)$$

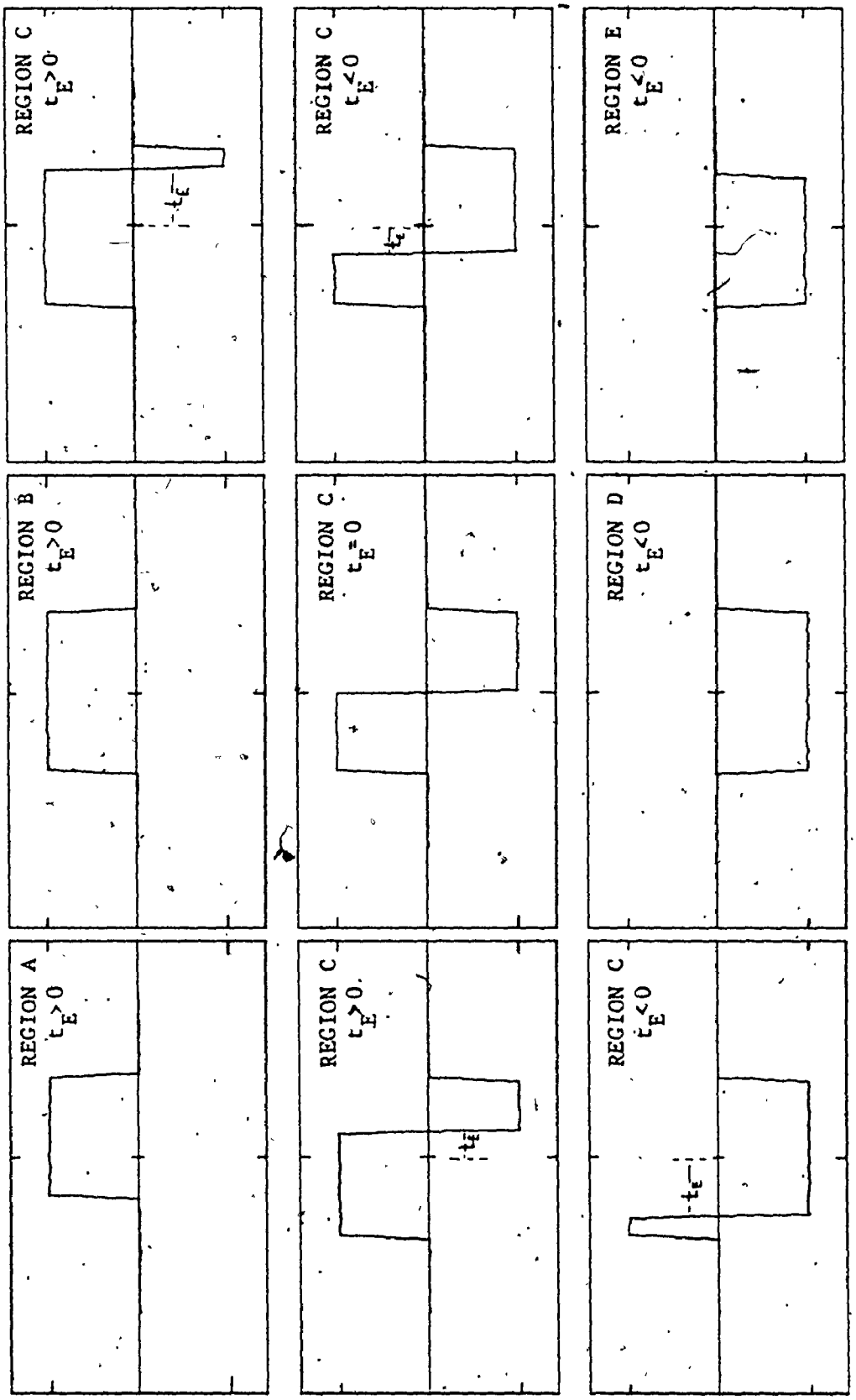

Fig. 5.2 Examples of the computer-simulated signal $s_{12}(t)$ (signal prior to integration) for $CNR_U/CNR_D = 50/30$ db. (computer plottings)

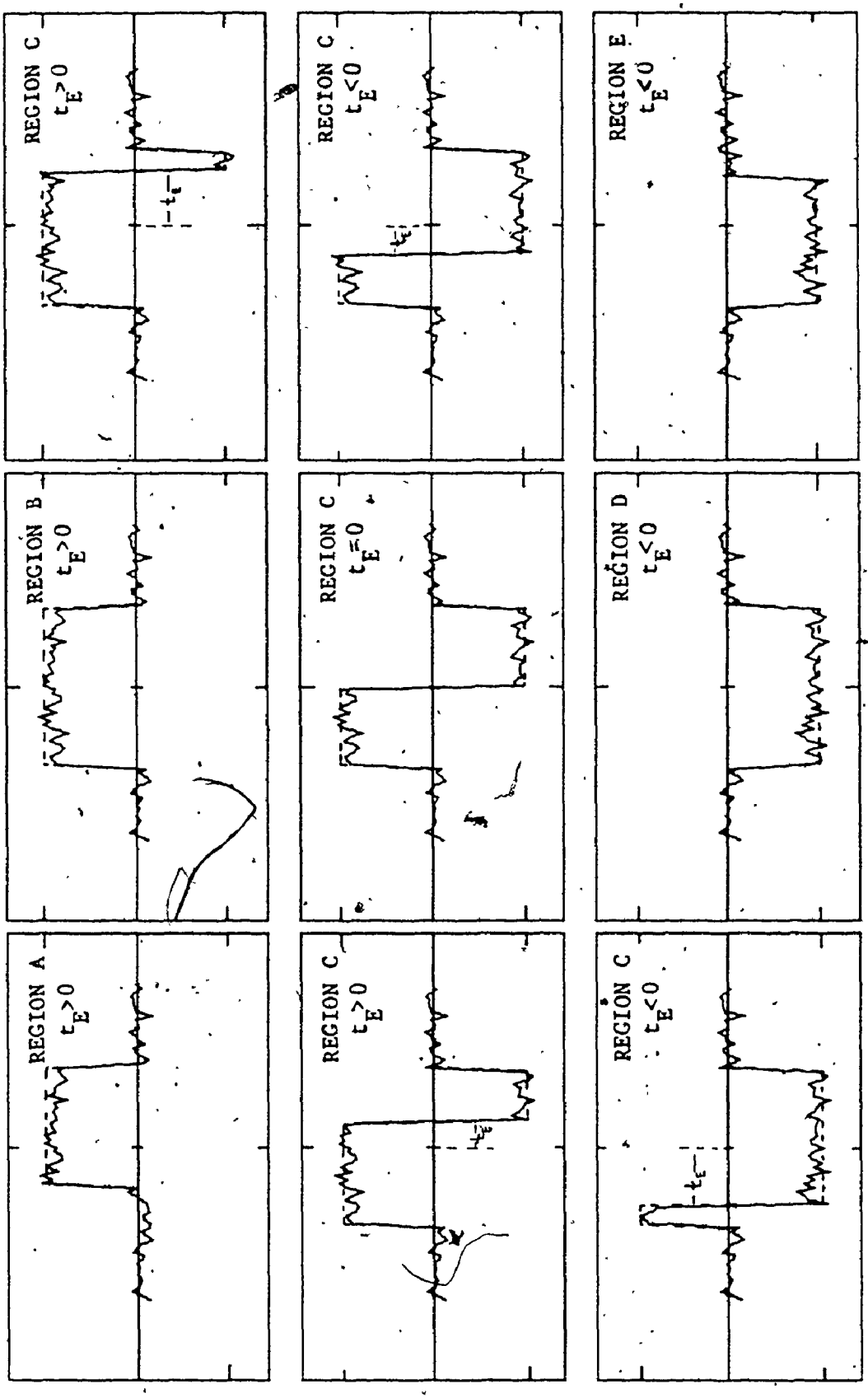

Fig. 5.3 Examples of the computer-simulated signal $s_{12}(t)$ (signal prior to intgration) for CNR_U/CNR_D = 40/20 db (computer plottings)

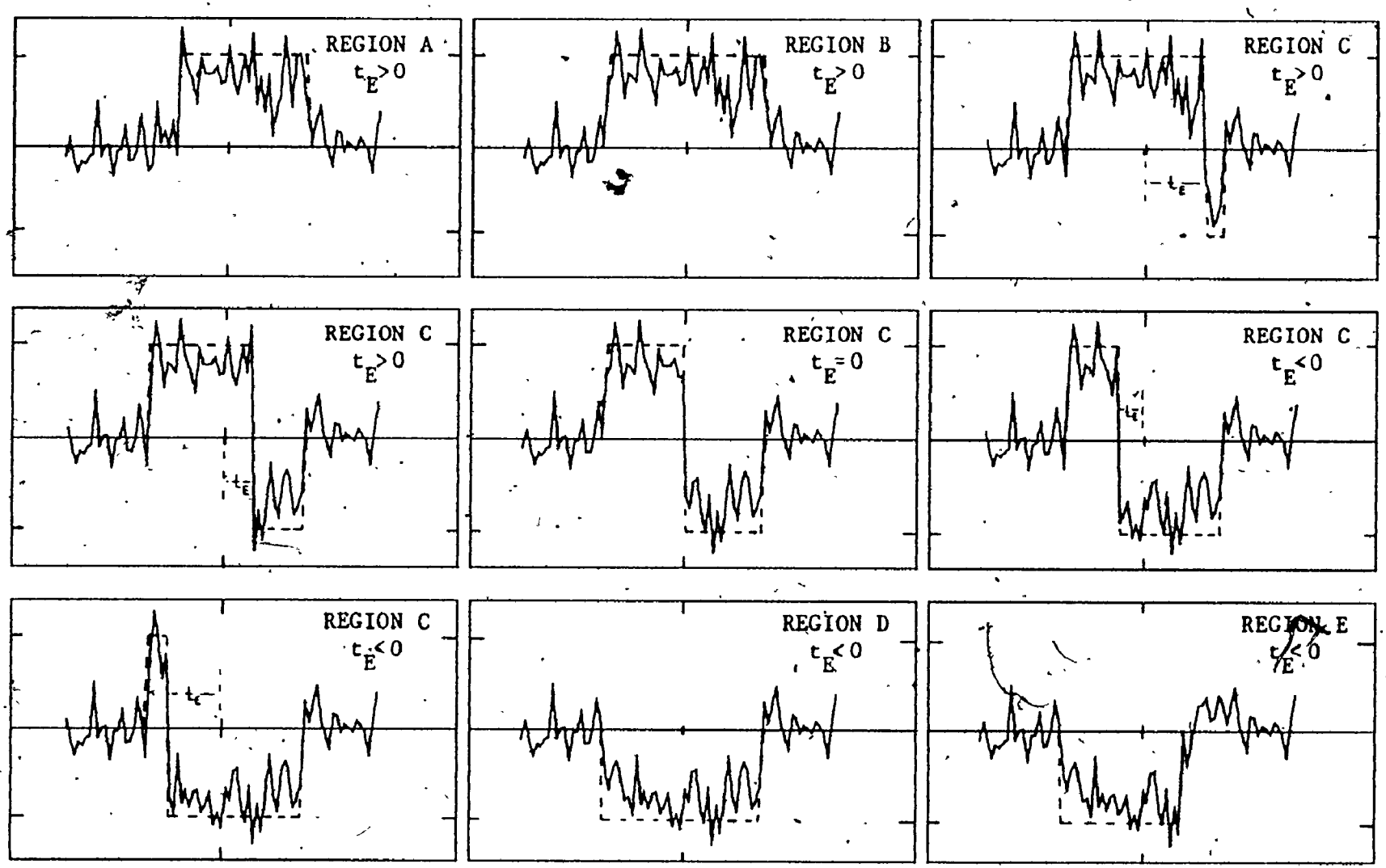

Fig. 5.4 Examples of the computer-simulated signal $s_{12}(t)$ (signal prior to integration) for $CNR_U/CNR_D = 30/10$ db (computer plottings)

Even though the trapezoidal rule is the simplest but least accurate numerical method of integrating a tabulated function, however, it is the most suitable for functions with random fluctuations.

The global truncation error R in z is given by

$$R = -\frac{N-1}{12}h^3 \cdot y''(\xi) \quad \xi\varepsilon\{x_1, x_1 + (N-1)h\} \tag{5.4}$$

The maximum value of $y''(\xi)$ which was encountered in this particular analysis was of the order of 10^3. Thus for N = 200 and h = 0.02 the maximum global truncation error is of the order of 10^{-1} (compared with the error voltage values of 0 to 2).

In order to obtain the expected value of the error voltage for a given timing error, the signal $s_{12}(t)$ is simulated and integrated a number of times, each time being supplied with different and independent sets of noise samples. Consequently, the expected value of the error voltage is simply the average of the integral values of the simulated signal $s_{12}(t)$. The simulated error detection characteristic is formed (Fig. 5.5) by repeating the whole procedure for different values of the timing error, ranging from $-\frac{1}{2}(T_P+T_W)$ to $\frac{1}{2}(T_P+T_W)$.

Simulation was performed for a system having the parameters given in Section 5.1. Moreover, the ratio L/T_I (L: number of sync bursts of the same train, T_I: integrator time constant) was chosen to be 1. If L/T_I is different from 1 the entire error detection characteristic, simply has to be multiplied by it.

The downlink gain C_2 was also varied along with the noise power n_oB to yield the proper values of the uplink/downlink carrier-to-noise ratios (CNR_U/CNR_D) as follows:

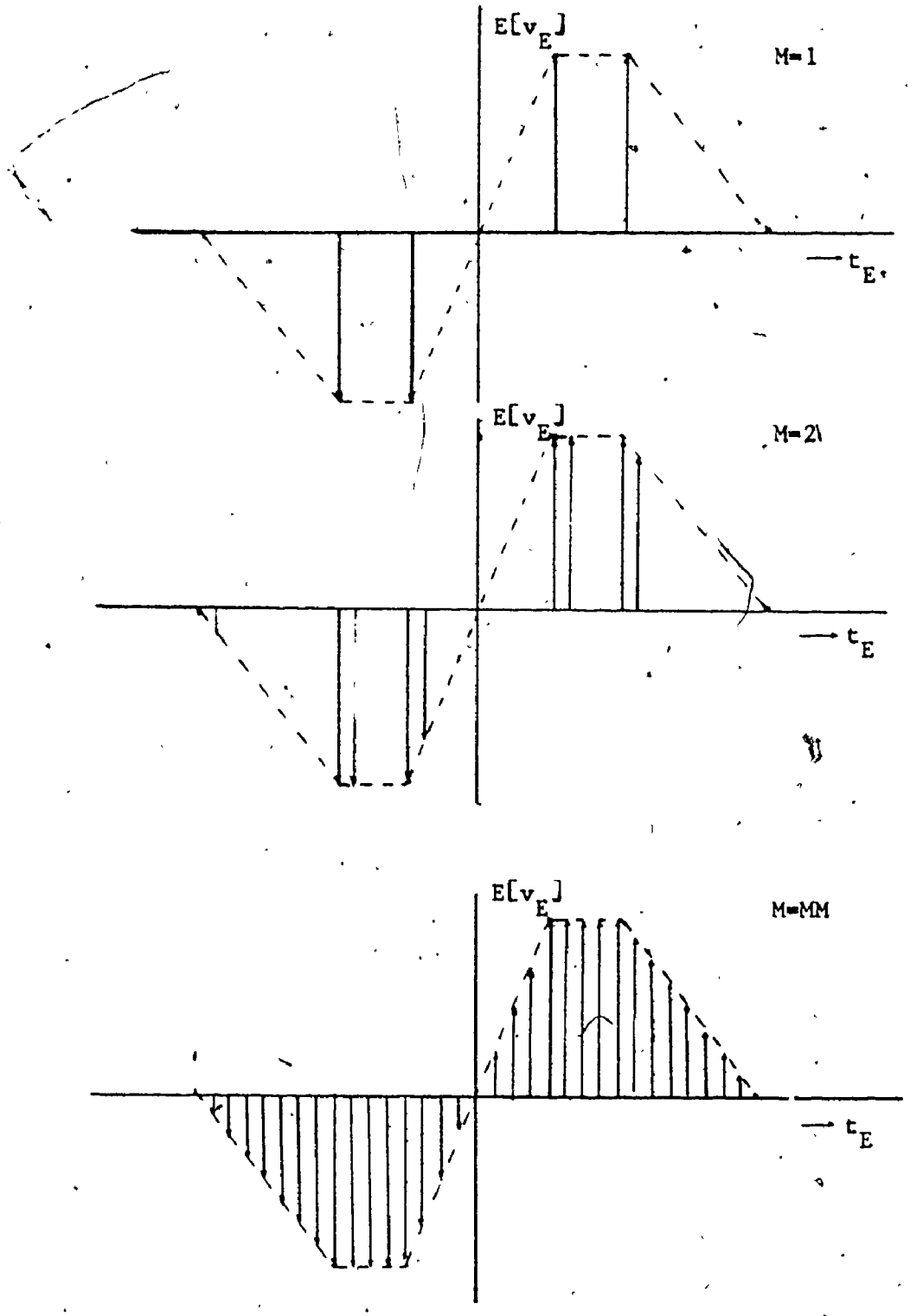

Fig. 5.5 Formation of the computer simulated first-order error detection characteristic

C_2	n_oB (in Watts)	yield	CNR_U/CNR_D in db
$10^{-1/2}$	$10^{-3}/2$		40/30
$10^{-3/4}$	$10^{-2.5}/2$		40/25
$10^{-1/2}$	$10^{-2}/2$		30/20
$10^{-3/4}$	$10^{-1.5}/2$		30/15
$10^{-1/2}$	$10^{-1}/2$		20/10
$10^{-3/4}$	$10^{-0.5}/2$		20/5
10^{-1}	$10^{0}/2$		20/0

The computer program used is listed at the end of this chapter.

The first-order error detection characteristic, based on the theory which was described in Chapter 4, is calculated through the equations (4.7) to (4.8). In Figures 5.6 to 5.12 the theoretical and simulated first-order error detection characteristics are shown for different CNR_U/CNR_D values.

A quantitative comparison between the theoretical and simulated error detection characteristics can be made by introducing the following error:

$$\text{"error"} = \frac{\sqrt{\left(\sum_{i=1}^{n} [E[v_E]^i_{theory} - E[v_E]^i_{simulation}]^2\right)}}{n} \qquad (5.5)$$

where n is the number of the simulated and integrated signals (i.e., error voltages) corresponding to n different values of the timing error. Clearly this "error" can be deduced (mostly in low CNR cases) by averaging larger number of the simulated error voltage (i.e., increasing NN, see program list).

In Figure 5.13 the above "error" is shown for different values of CNR_U/CNR_D.

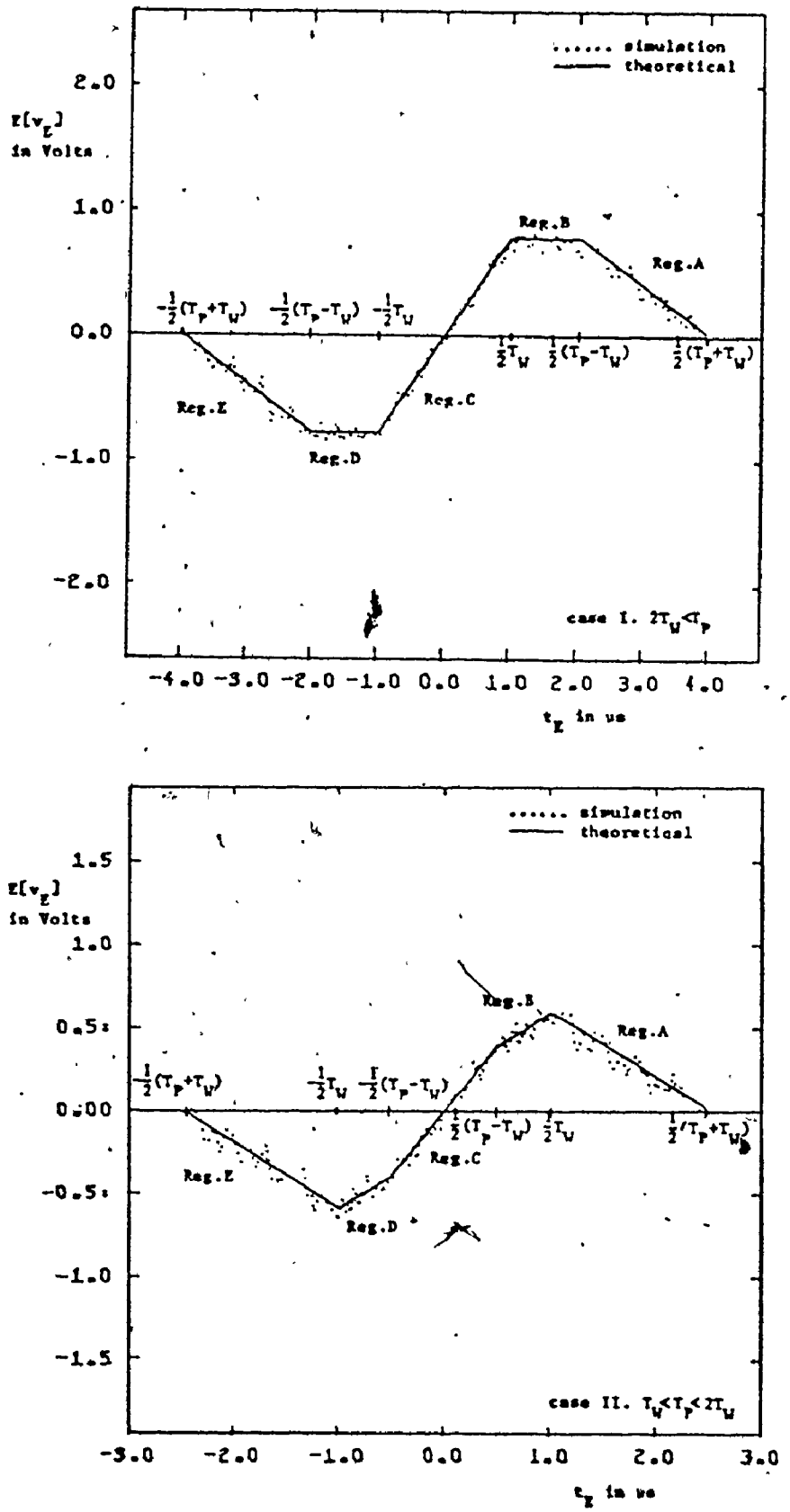

Fig. 5.6 First-order error detection characteristics CNR_U/CNR_D = 20/0 db

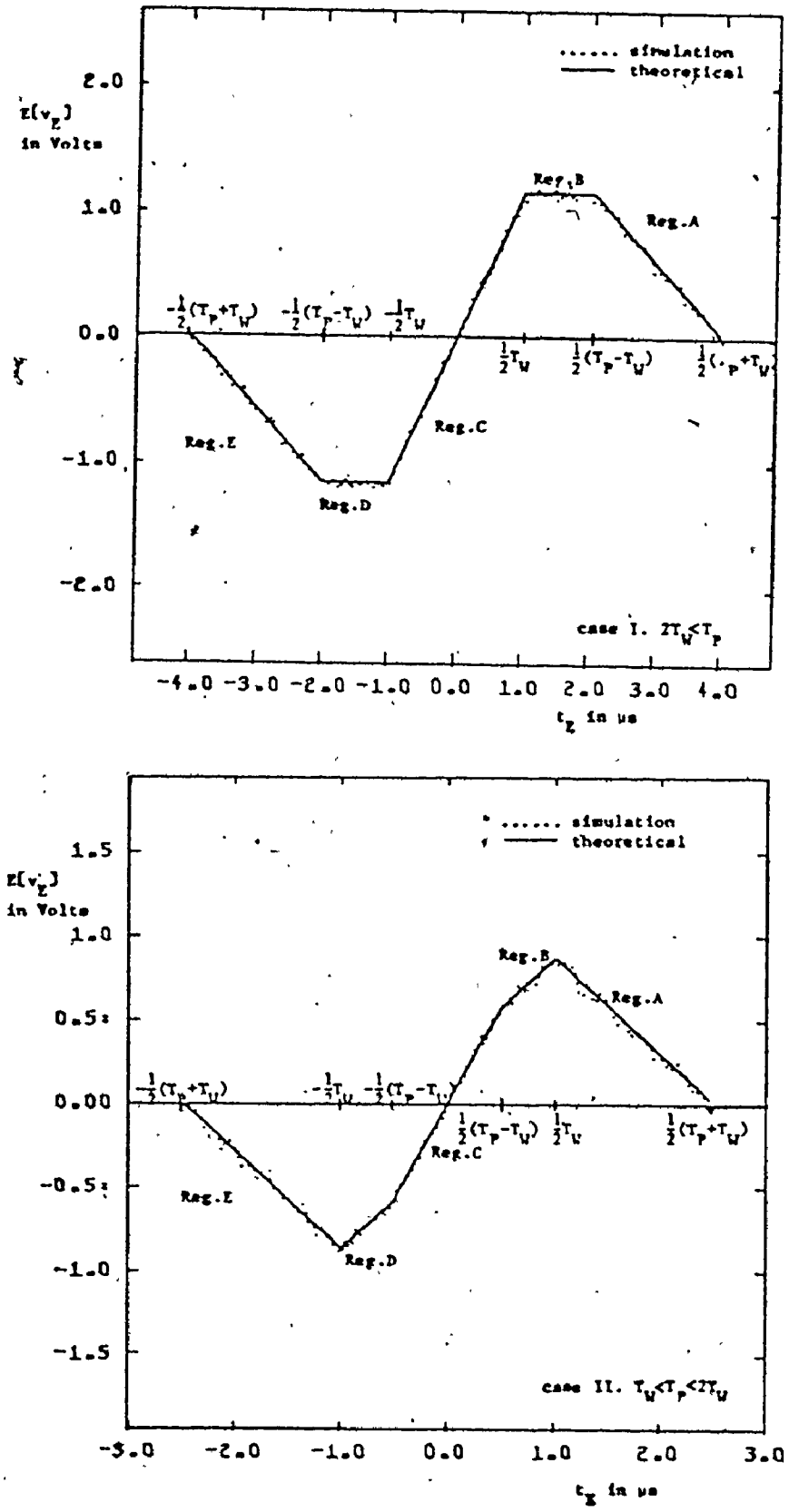

Fig. 5.7 First-order error detection characteristics CNR_U/CNR_D = 20/5 db

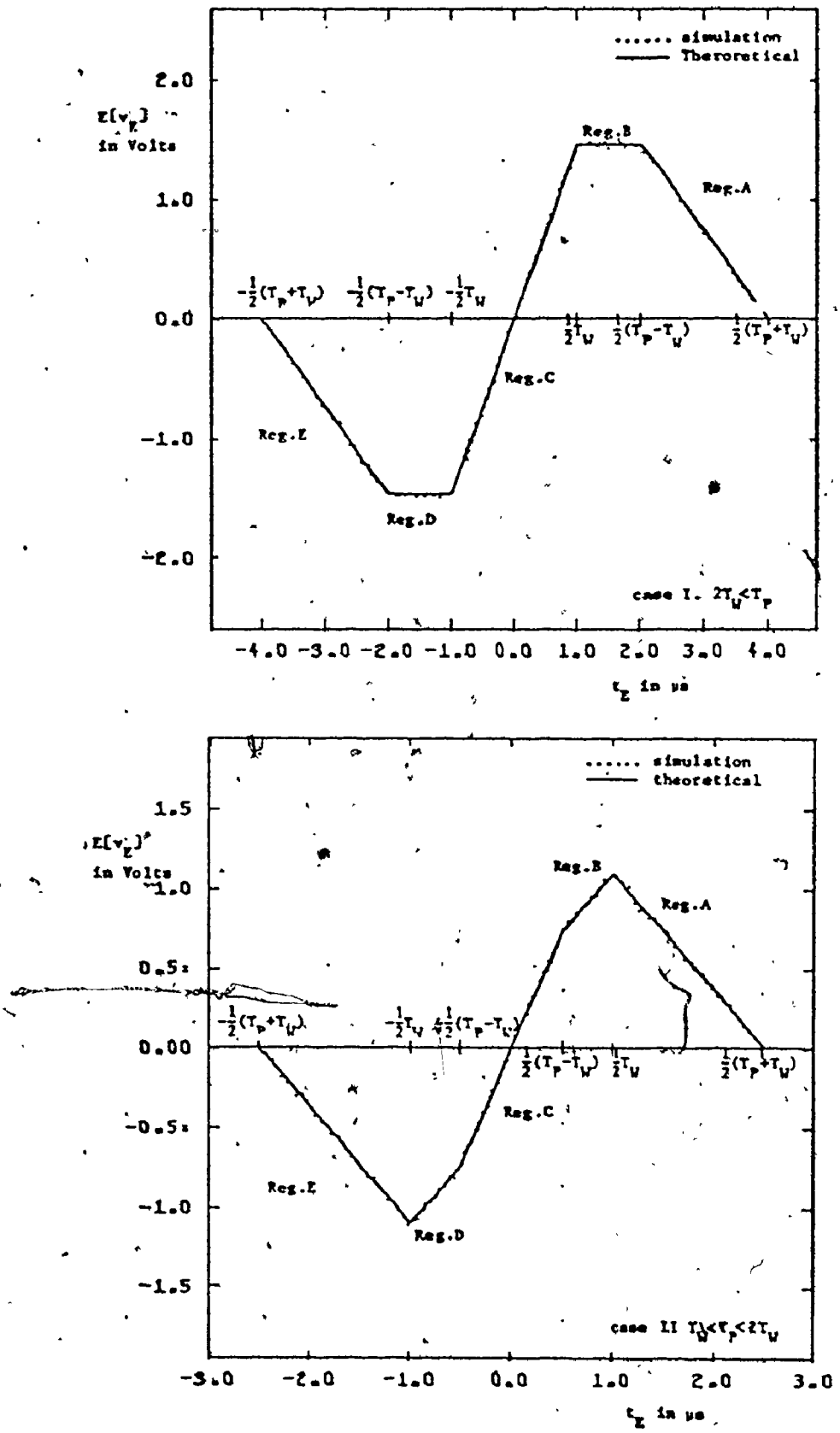

Fig. 5.8 First-order error detection characteristics CNR_{II}/CNR_{I} = 20/10 db

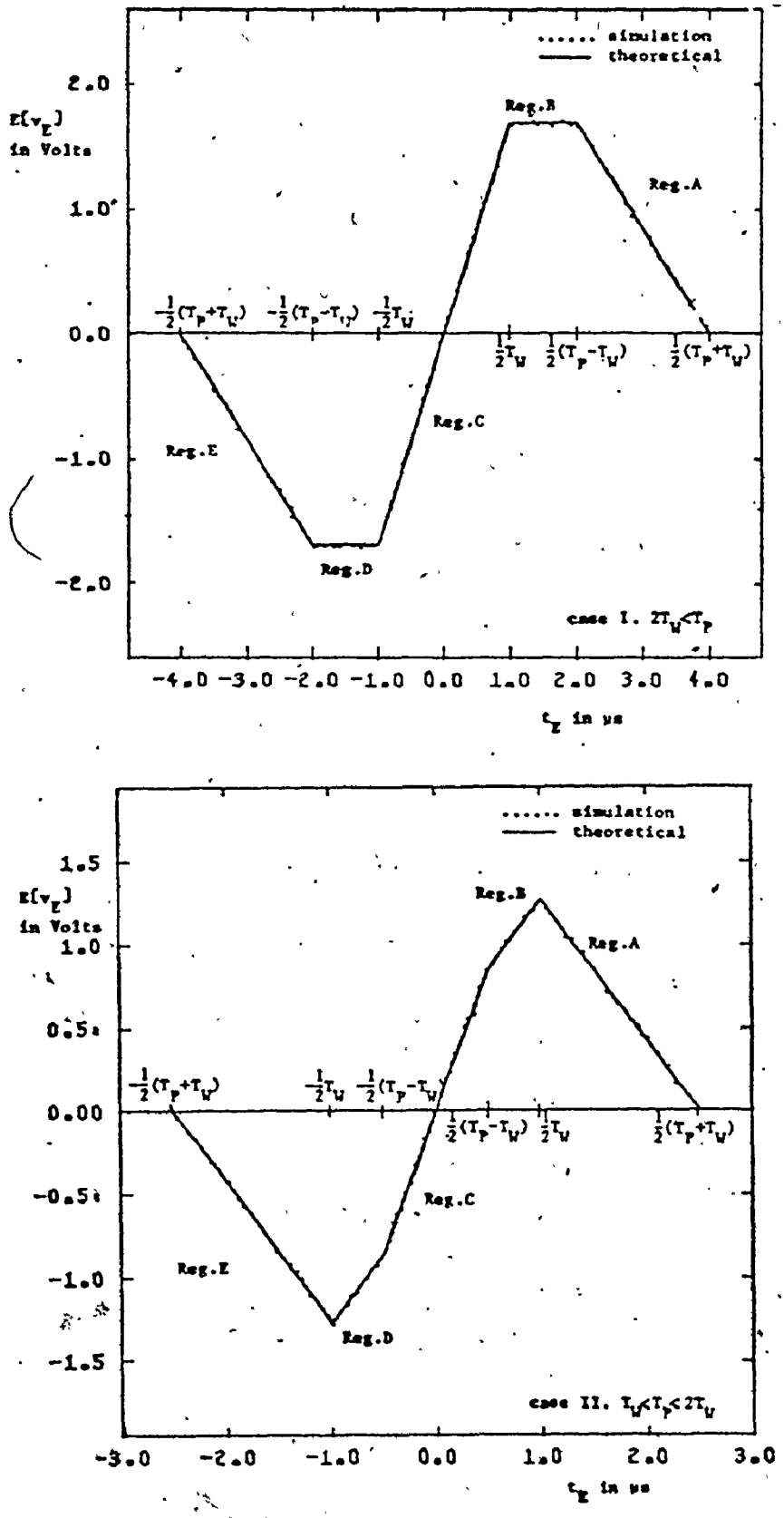

Fig. 5.9 First-order error detection characteristics
CNR_U/CNR_D = 30/15 db

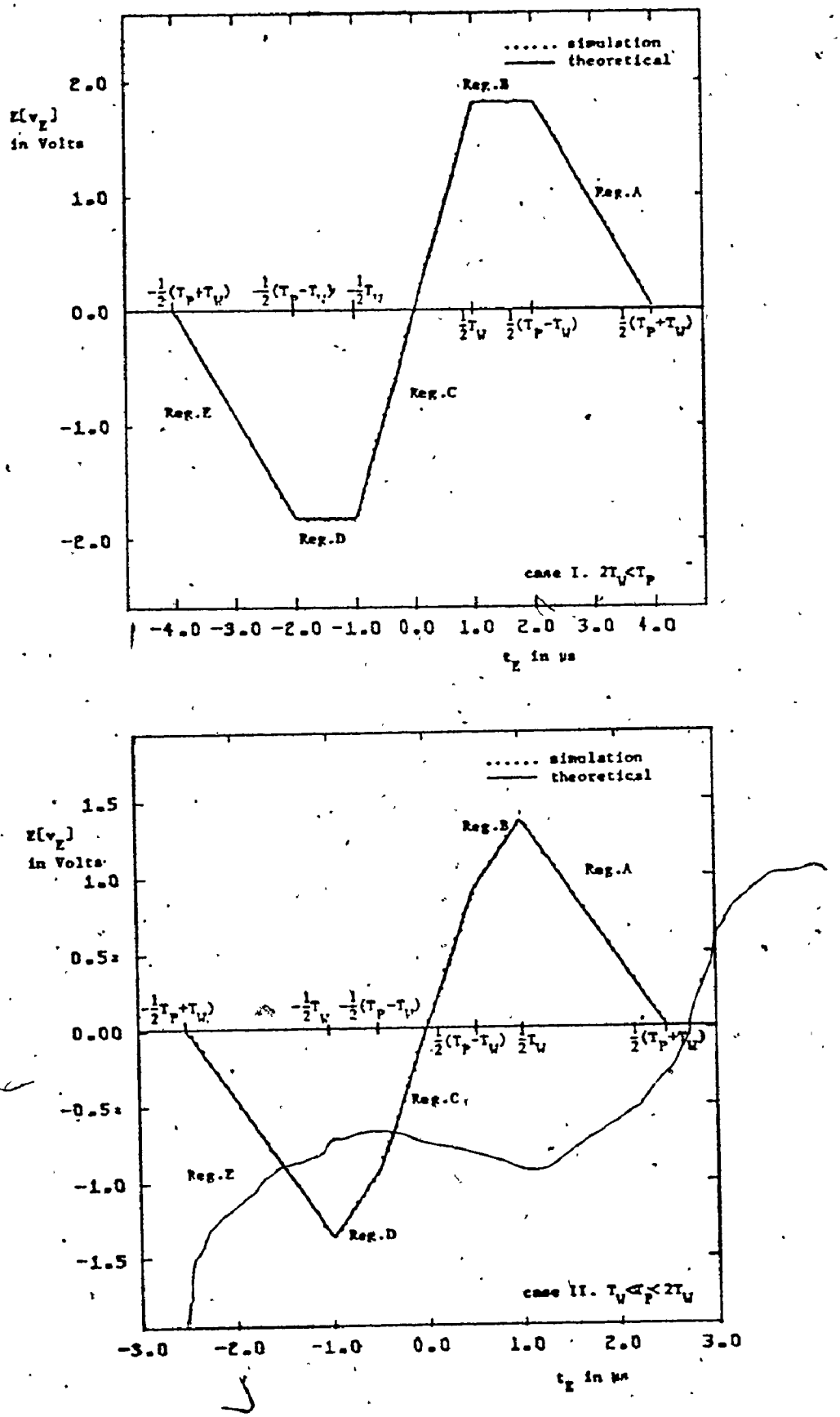

Fig. 5.10 First-order error detection characteristics
CNR_{II}/CNR_{n} = 30/20 db

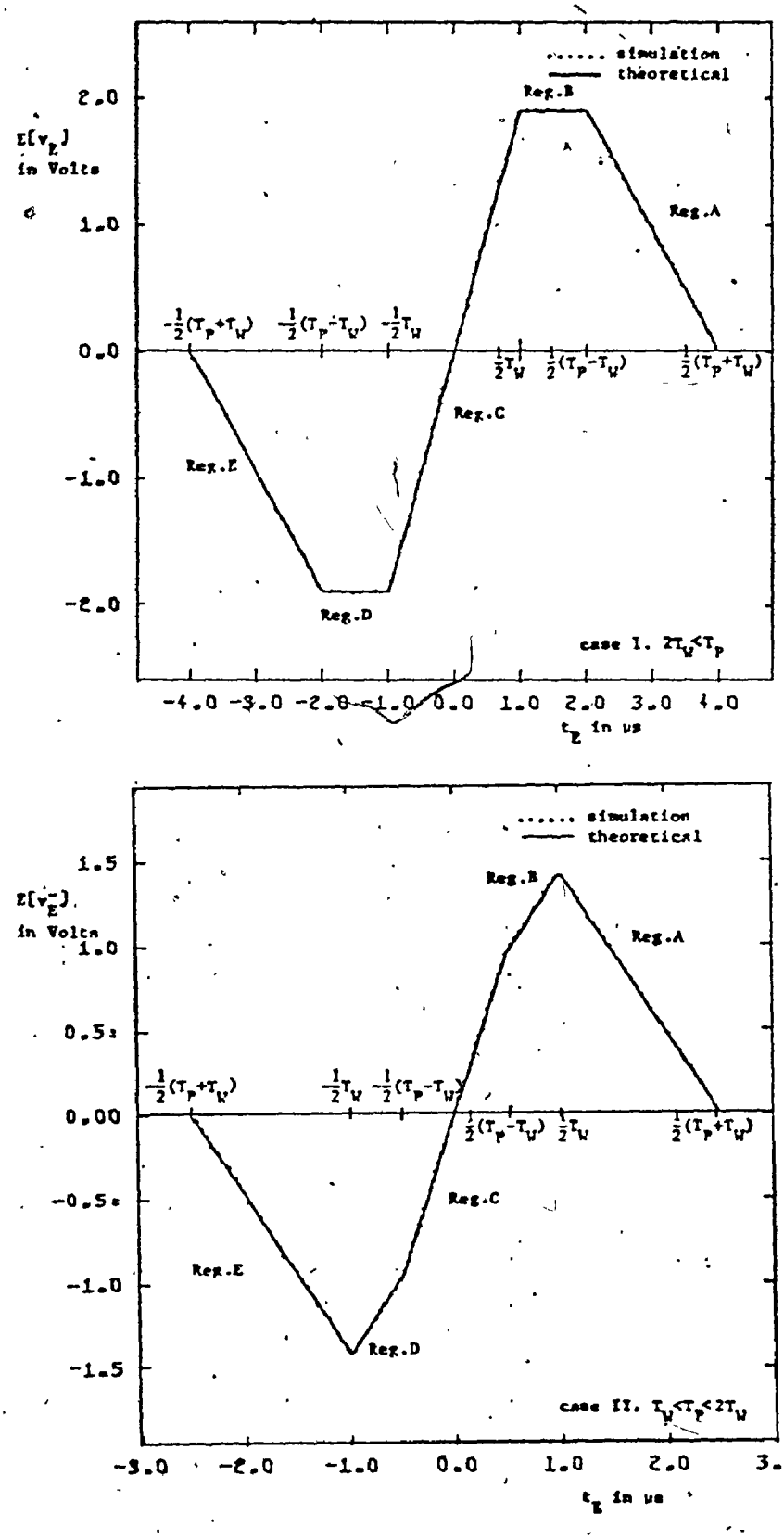

Fig. 5.11 First-order error detection characteristics
CNR_U/CNR_D = 40/25 db

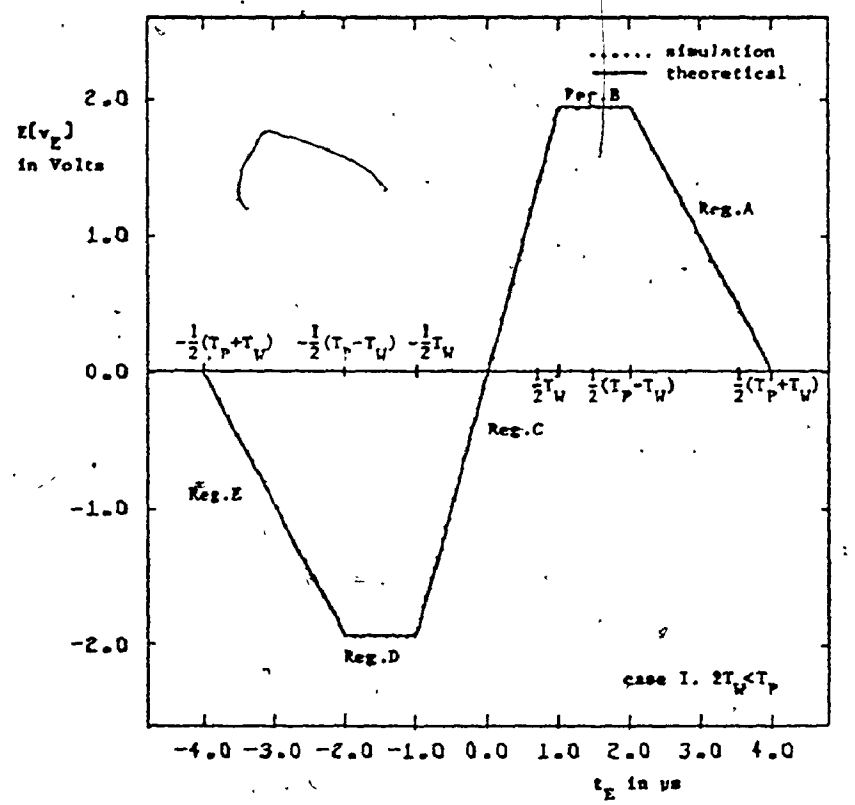

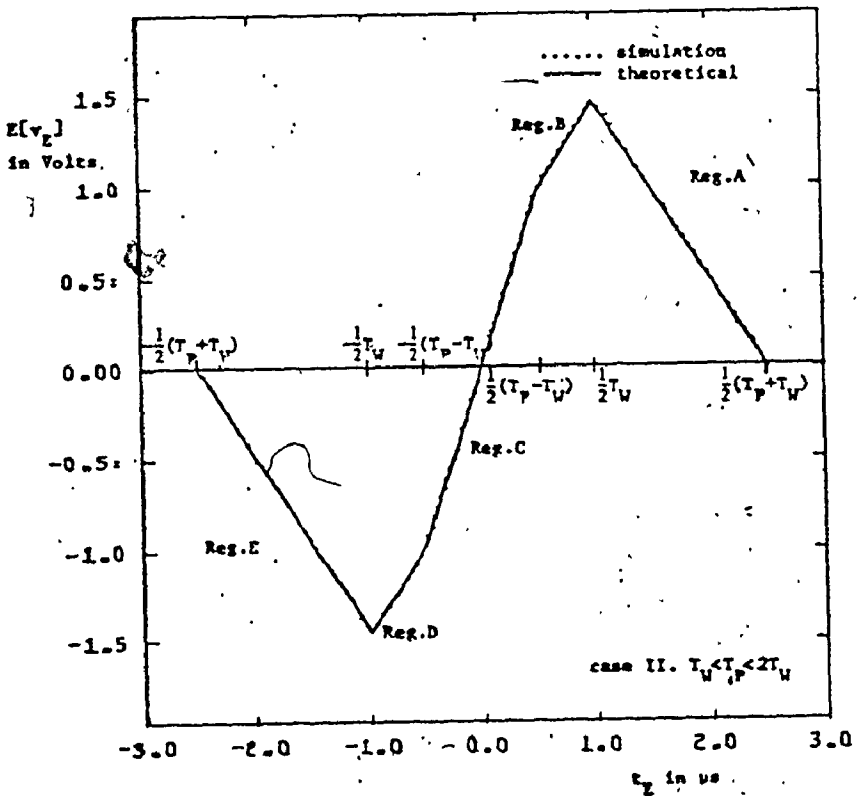

Fig. 5.12 First-order error dtèction characteristics
CNR_/CNR_ = 40/30 db

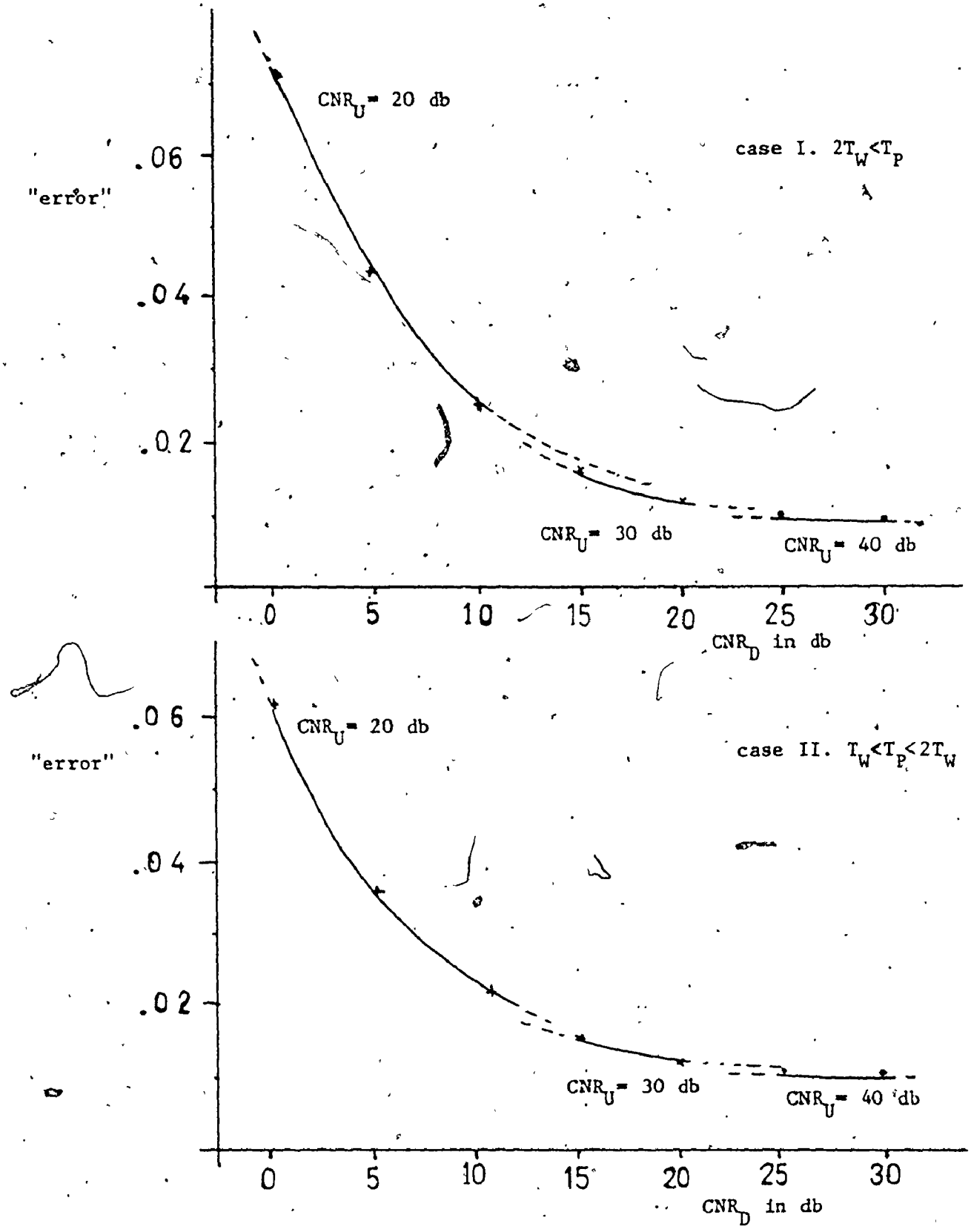

Fig. 5.13 The error between the computer-simulated and the theoretical error detection characteristics for

5.3 COMPUTATION OF THE SECOND-ORDER ERROR DETECTION CHARACTERISTIC AND ITS APPROXIMATION WITH A SMOOTH CURVE

The mean square value of the error voltage is calculated by averaging its square values, each one computed for a different and independent set of noise samples.

As in the computation of the first-order error detection characteristic, the mean square value of the error voltage can be given as a function of the timing error, yielding the second order error detection characteristic. For this, the simulation data are approximated with smooth curves as follows:

Second-order error detection characteristic. Case I.

$$\begin{aligned}
&\text{Reg. E:} && E[v_E^2] = \alpha_E t_E^2 + \beta_E t_E + \gamma_E && -\tfrac{1}{2}(T_P+T_W) < t_E < -\tfrac{1}{2}(T_P-T_W)\\
&\text{Reg. D:} && E[v_E^2] = \gamma_D && -\tfrac{1}{2}(T_P-T_W) < t_E < -\tfrac{1}{2}T_W\\
&\text{Reg. C:} && E[v_E^2] = \alpha_C t_E^2 + \gamma_C && -\tfrac{1}{2}T_W < t_E < \tfrac{1}{2}T_W \qquad (5.6)\\
&\text{Reg. B:} && E[v_E^2] = \gamma_B && \tfrac{1}{2}T_W < t_E < \tfrac{1}{2}(T_P-T_W)\\
&\text{Reg. A:} && E[v_E^2] = \alpha_A t_E^2 + \beta_A t_E + \gamma_A && \tfrac{1}{2}(T_P-T_W) < t_E < \tfrac{1}{2}(T_P+T_W)
\end{aligned}$$

Second-order error detection characteristic. Case II

$$\begin{aligned}
&\text{Reg. E:} && E[v_E^2] = \alpha_E t_E^2 + \beta_E t_E + \gamma_E && -\tfrac{1}{2}(T_P+T_W) < t_E < -\tfrac{1}{2}T_W\\
&\text{Reg. D:} && E[v_E^2] = \alpha_D t_E^2 + \beta_D t_E + \gamma_D && -\tfrac{1}{2}T_W < t_E < -\tfrac{1}{2}(T_P-T_W)\\
&\text{Reg. C:} && E[v_E^2] = \alpha_C t_E^2 + \gamma_C && -\tfrac{1}{2}(T_P-T_W) < t_E < \tfrac{1}{2}(T_P-T_W) \qquad (5.7)\\
&\text{Reg. B:} && E[v_E^2] = \alpha_B t_E^2 + \beta_B t_E + \gamma_B && \tfrac{1}{2}(T_P-T_W) < t_E < \tfrac{1}{2}T_W\\
&\text{Reg. A:} && E[v_E^2] = \alpha_A t_E^2 + \beta_A t_E + \gamma_A && \tfrac{1}{2}T_W < t < \tfrac{1}{2}(T_P+T_W)
\end{aligned}$$

The coefficients of the quadrature polynomials were computed by

means of the least square method [49], [50]. Special attention was given to the coefficient γ_C (constant term at Region C), and separate simulation was carried out for $t_E = 0$. The coefficient γ_C is quite important since it is used to calculate the ultimate timing error, i.e., the mean square value of the timing error after large number of iterations (equation (5.23)).

The coefficients of the fitted curves, corresponding to various values of the uplink/downlink carrier-to-noise ratio (CNR_U/CNR_D) are shown in Tables II and III.

The simulated second-order error detection characteristic and its approximation are shown in Figures 5.14 to 5.20 for different values of CNR_U/CNR_D.

5.4 COMPUTATION OF THE MEAN SQUARE VALUE OF THE TIMING ERROR

The timing error after n iterations is given (see equation (4.28)) as:

$$t_E(n) = t_E(n-1) - b \cdot v_E(n-1) + t_M$$

Thus,

$$t_E^2(n) = t_E^2(n-1) + b^2 \cdot v_E^2(n-1) + t_M^2 + 2t_E(n-1) \cdot t_M - 2b[t_E(n-1) + t_M]v_E(n-1) \qquad (5.8)$$

The mean square value of the error is given (see Chapter 4, Appendix B) as:

$$E[t_E^2(n)] = E_{t_E(n-1)}\{E[t_E^2(n)/v_E(n-1)]\}$$

$$= E_{t_E(n-1)}\{t_E^2(n-1) + b^2 E[v_E^2(n-1)] + t_M^2 + 2t_E(n-1) \cdot t_M - 2b(t_E(n-1) + t_M) \cdot E[v_E(n-1)]\} \qquad (5.9)$$

The mean square value of the error voltage $E[v_E^2(n-1)]$, obtained from the simulation, is given in equations (5.6) and (5.7) and its expected value

TABLE II

Coefficients of the second-order error detection characteristic

case I. $2T_W < T_P$

Fitted Curve for Region A: $E[v_E^2] = \alpha_A t_E^2 + \beta_A t_E + \gamma_A$

CNR_U/CNR_D	α_A(volts^2/μs^2)	β_A(volts^2/μs)	γ_A(volts^2)
40/30	.929	-7.46	14.98
25	.885	-7.12	14.30
30/20	.805	-6.48	13.04
15	.687	-5.55	11.20
20/10	.496	-4.04	8.19
5	.284	-2.35	4.85
0	.106	-0.92	2.00

Fitted Curve for Region B: $E[v_E^2] = \gamma_B$

CNR_U/CNR_D	γ_B(volts^2)
40/30	3.76
25	3.60
30/20	3.30
15	2.86
20/10	2.13
5	1.32
0	0.617

Fitted Curve for Region C: $E[v_E^2] = \alpha_C t_E^2 + \gamma_C$

CNR_U/CNR_D	α_C(volts^2/μs^2)	γ_C(volts^2)
40/30	3.77	$8.05 \cdot 10^{-6}$
25	3.61	$5.47 \cdot 10^{-5}$
30/20	3.30	$2.12 \cdot 10^{-4}$
15	2.87	$5.90 \cdot 10^{-4}$
20/10	2.15	$1.63 \cdot 10^{-3}$
5	1.34	$3.94 \cdot 10^{-3}$
0	0.624	$1.04 \cdot 10^{-2}$

TABLE II (Continued)

Fitted Curve for Region D: $E[v_E^2] = \gamma_D$

CNR_U/CNR_D	$\gamma_D(volts^2)$
40/30	3.77
25	3.61
30/20	3.31
15	2.88
20/10	2.18
5	1.38
0	0.687

Fitted Curve for Region E: $E[v_E^2] = \alpha_E t_E^2 + \beta_E t_E + \gamma_E$

CNR_U/CNR_D	$\alpha_E(volts^2/\mu s^2)$	$\beta_E(volts^2/\mu s)$	$\gamma_E(volts^2)$
40/30	.939	7.51	15.02
25	.900	7.20	14.39
30/20	.822	6.59	13.18
15	.715	5.72	11.46
20/10	.530	4.26	8.55
5	.333	2.68	5.40
0	.160	1.28	2.60

NOTE: The computation of the above coefficients was based on the simulation of a system with the following parameters:

Voltage level of the transmitted signal	A = 1 Volt
Total gain of the synchronization loop	$C_1 = 1$
Gain of the input amplifier	$K_6 = 1$
Input gate duration	$T_Q = 4\ \mu s$
Sync window duration	$T_W = 2\ \mu s$
FSK Sync-burst duration	$T_p = 6\ \mu s$
Integrator time constant	$T_I = 1\ \mu s$

The downlink gain C_2 was varied ($10^{-1/2}$, $10^{-3/4}$, 10^{-1}) to differentiate the CNR_U and CNR_D (see Section 5.2).

TABLE III

Coefficients of the second-order error detection characteristic

case II. $T_W < T_P < 2T_W$

Fitted Curve for Region A: $E[v_E^2] = \alpha_A t_E^2 + \beta_A t_E + \gamma_A$

CNR_U/CNR_D	α_A(volts^2/μs^2)	β_A(volts^2/μs)	γ_A(volts^2)
40/30	.939	-4.72	5.93
25	.901	-4.53	5.68
30/20	.830	-4.16	5.22
15	.725	-3.63	4.54
20/10	.551	-2.74	3.41
5	.349	-1.73	2.14
0	.166	-0.81	1.01

Fitted Curve for Region B: $E[v_E^2] = \alpha_B t_E^2 + \beta_B t_E + \gamma_B$

CNR_U/CNR_D	α_B(volts^2/μs^2)	β_B(volts^2/μs)	γ_B(volts^2)
40/30	.921	.963	.246
25	.864	.946	.228
30/20	.757	.909	.197
15	.606	.856	.150
20/10	.360	.755	.081
5	.091	.647	-.0002
0	-.127	.514	-.0416

Fitted Curve for Region C: $E[v_E^2] = \alpha_C t_E^2 + \gamma_C$

CNR_U/CNR_D	α_C(volts^2/μs^2)	γ_C(volts^2)
40/30	3.78	$8.05 \cdot 10^{-6}$
25	3.61	$5.47 \cdot 10^{-5}$
30/20	3.32	$2.12 \cdot 10^{-4}$
15	2.88	$5.90 \cdot 10^{-4}$
20/10	2.17	$1.63 \cdot 10^{-3}$
5	1.37	$3.94 \cdot 10^{-3}$
0	0.68	$1.04 \cdot 10^{-2}$

TABLE III (Continued)

Fitted Curve for Region D: $E[v_E^2] = \alpha_D t_E^2 + \beta_D t_E + \gamma_D$

CNR_U/CNR_D	α_D(volts^2/μs^2)	β_D(volts^2/μs)	γ_D(volts^2)
40/30	.924	-.968	.245
25	.867	-.944	.230
30/20	.760	-.908	.198
15	.610	-.857	.151
20/10	.365	-.760	.080
5	.094	-.648	.0001
0	-.130	-.520	-.003

Fitted Curve for Region E: $E[v_E^2] = \alpha_E t_E^2 + \beta_E t_E + \gamma_E$

CNR_U/CNR_D	α_E(volts^2/μs^2)	β_E(volts^2/μs)	γ_E(volts^2)
40/30	.948	4.72	5.87
25	.909	4.52	5.63
30/20	.834	4.16	5.17
15	.727	3.62	4.51
20/10	.550	2.74	3.42
5	.352	1.75	2.19
0	.180	0.88	1.12

NOTE: The computation of the above coefficients was based on the simulation of a system with the following parameters:

Voltage level of the transmitted signal	A = 1 Volt
Total gain of the synchronization loop	$C_1 = 1$
Gain of the input amplifier	$K_6 = 1$
Input gate duration	$T_Q = 4$ μs
Sync window duration	$T_W = 2$ μs
FSK Sync-burst duration	$T_P = 3$ μs
Integrator time constant	$T_I = 1$ μs

The downlink gain C_2 was varied ($10^{-1/2}$, $10^{-3/4}$, 10^{-1}) to differentiate the CNR_U and CNR_D (see Section 5.2).

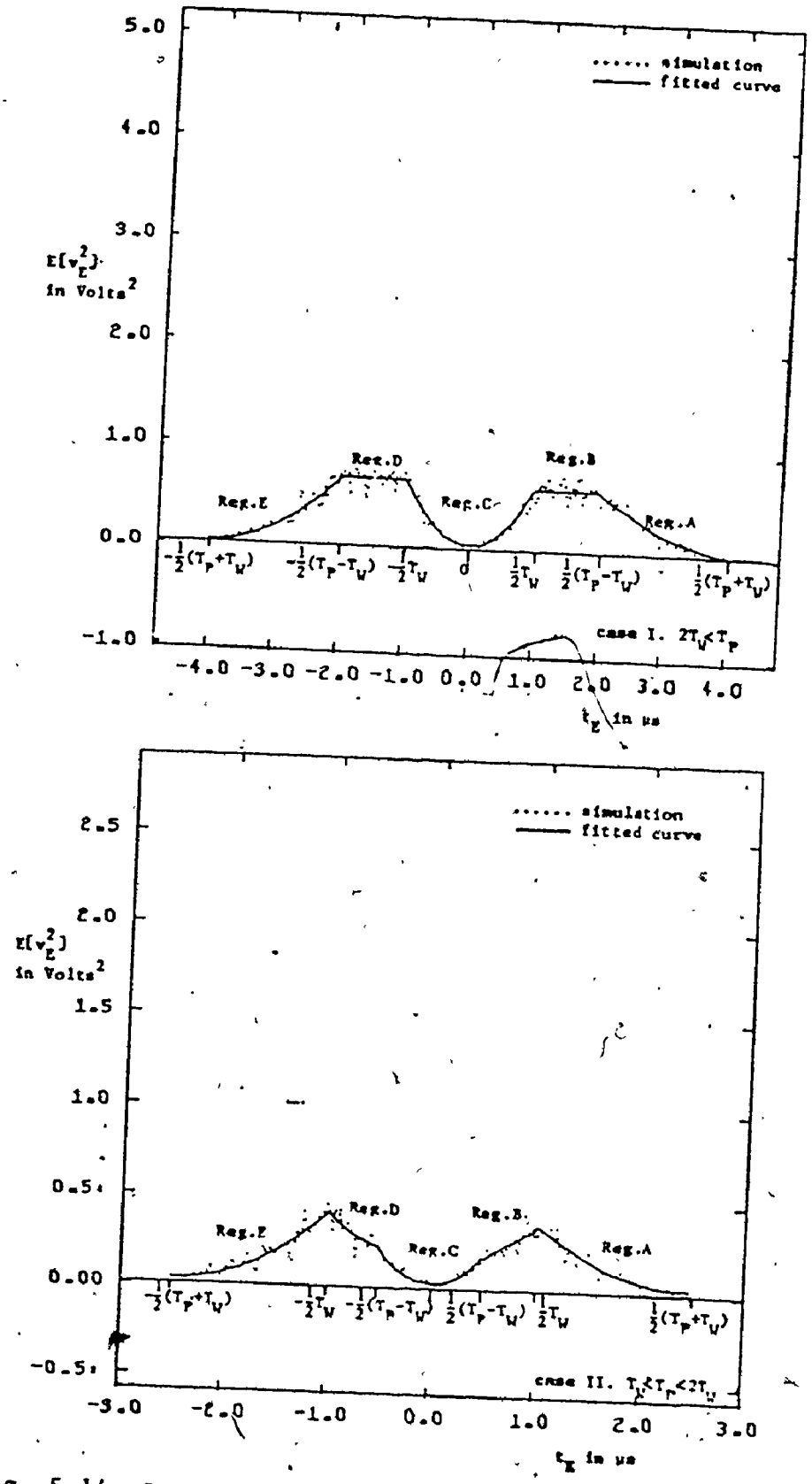

Fig. 5.14 Second-order error detection characteristics CNR_U/CNR_D = 20/0 db

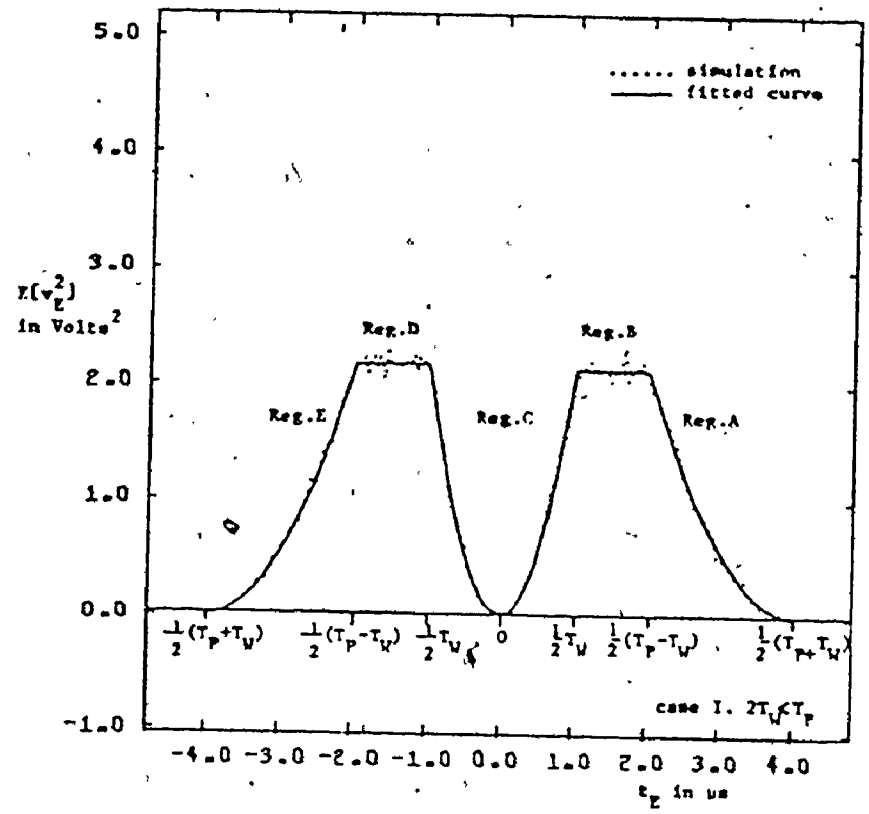

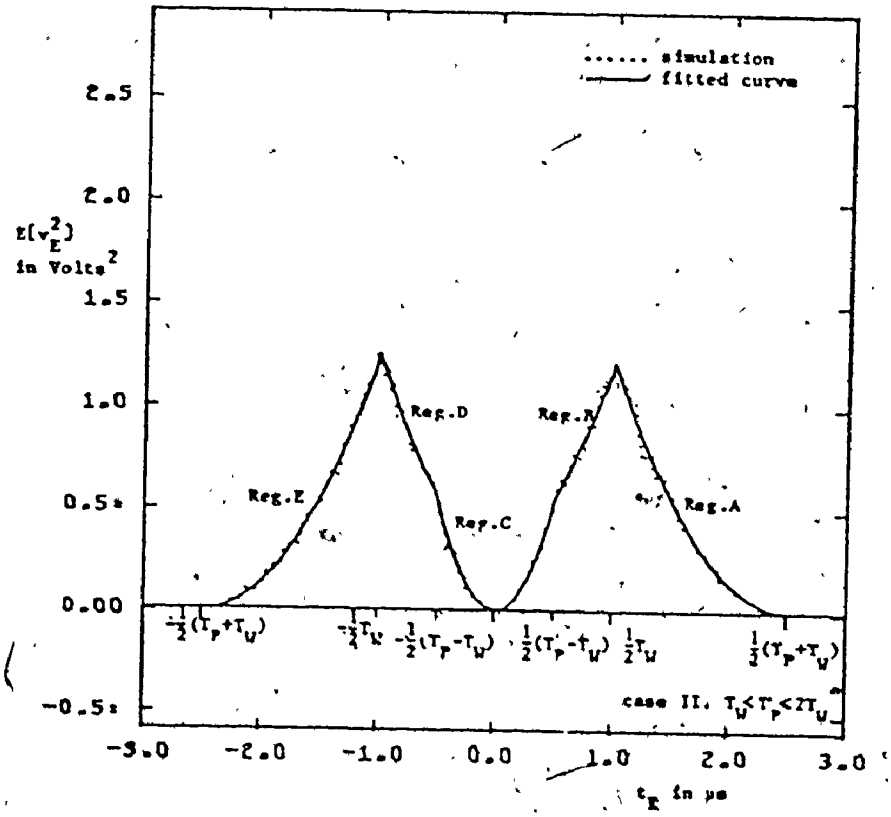

Fig. 5.16 Second-order error detection characteristics CNR_U/CNR_D = 20/10 db

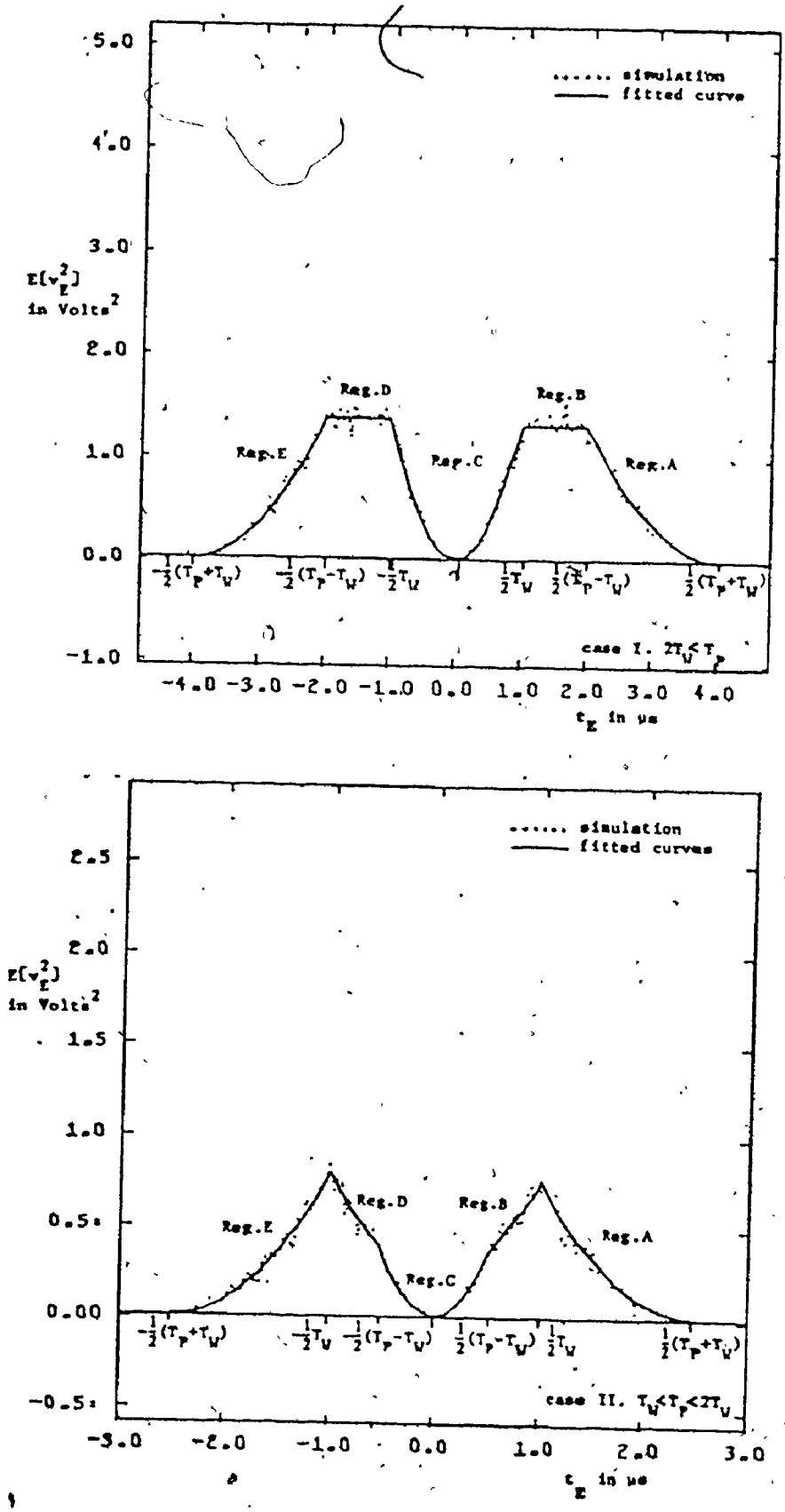

Fig. 5.15 Second-order error detection characteristics CNR_U/CNR_D = 20/5 db

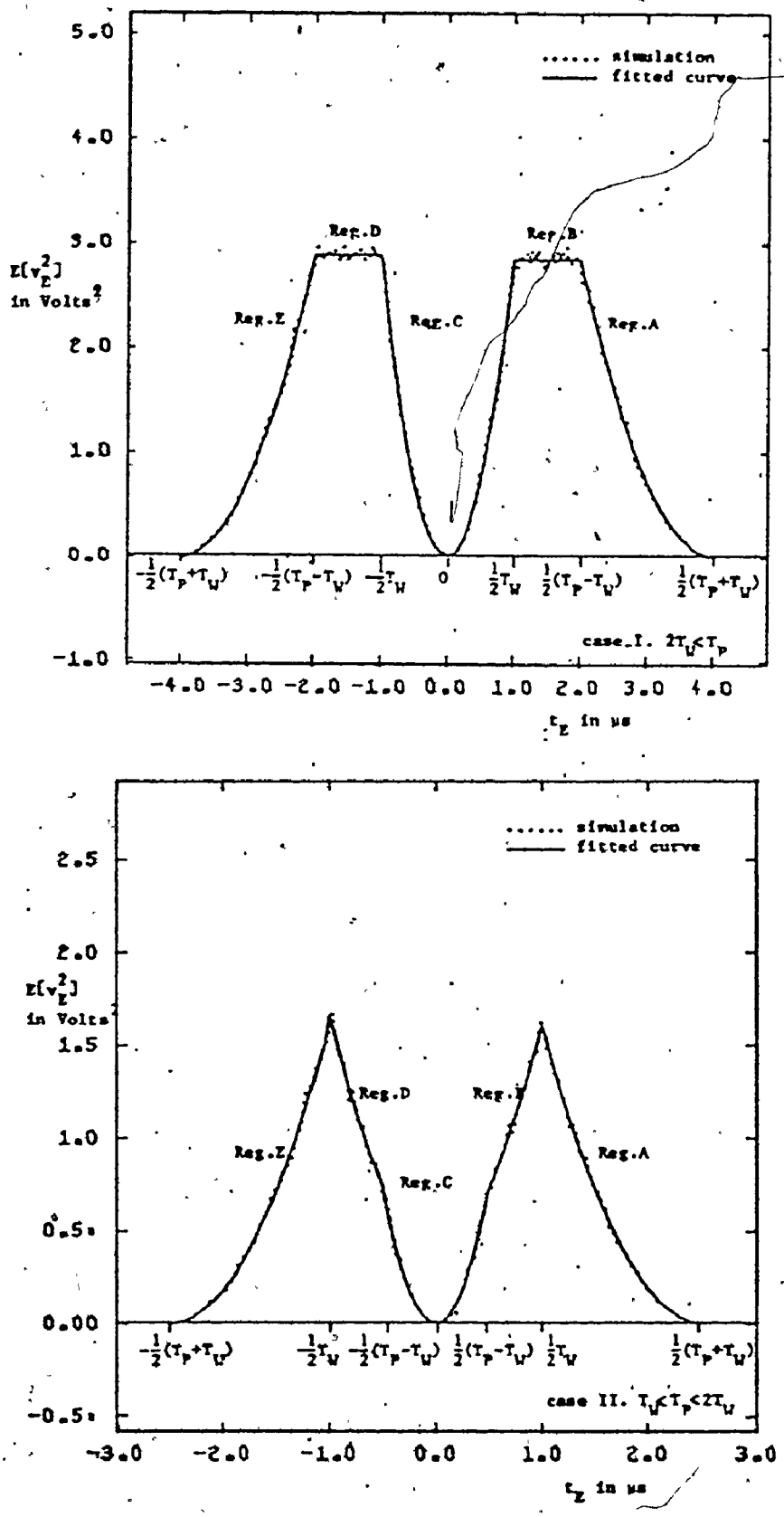

Fig. 5.17 Second-order error detection characteristics CNR_U/CNR_D = 30/15 db

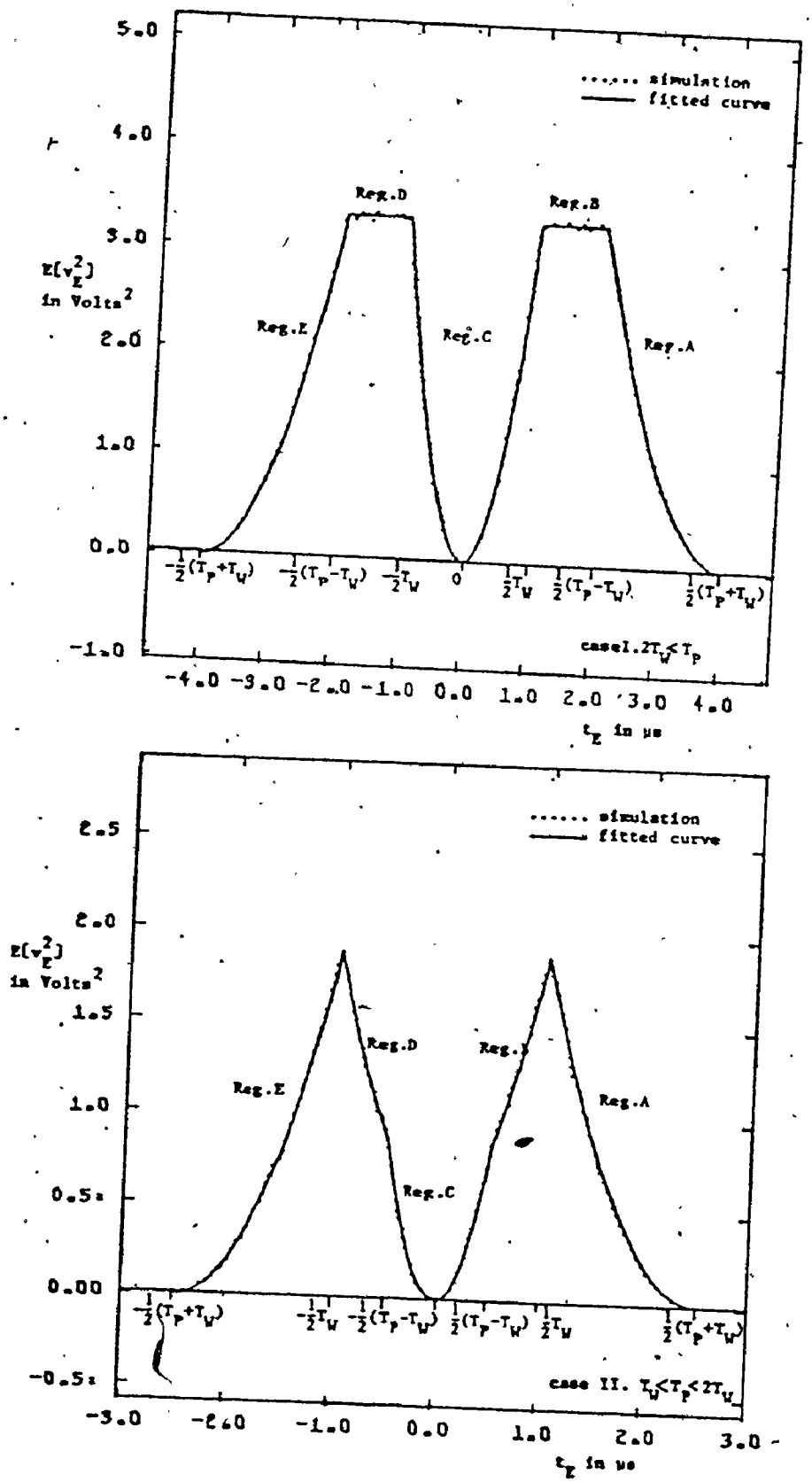

Fig. 5.18 Second-order error detection characteristics $CNR_U = CNR_D = 30/20$ db

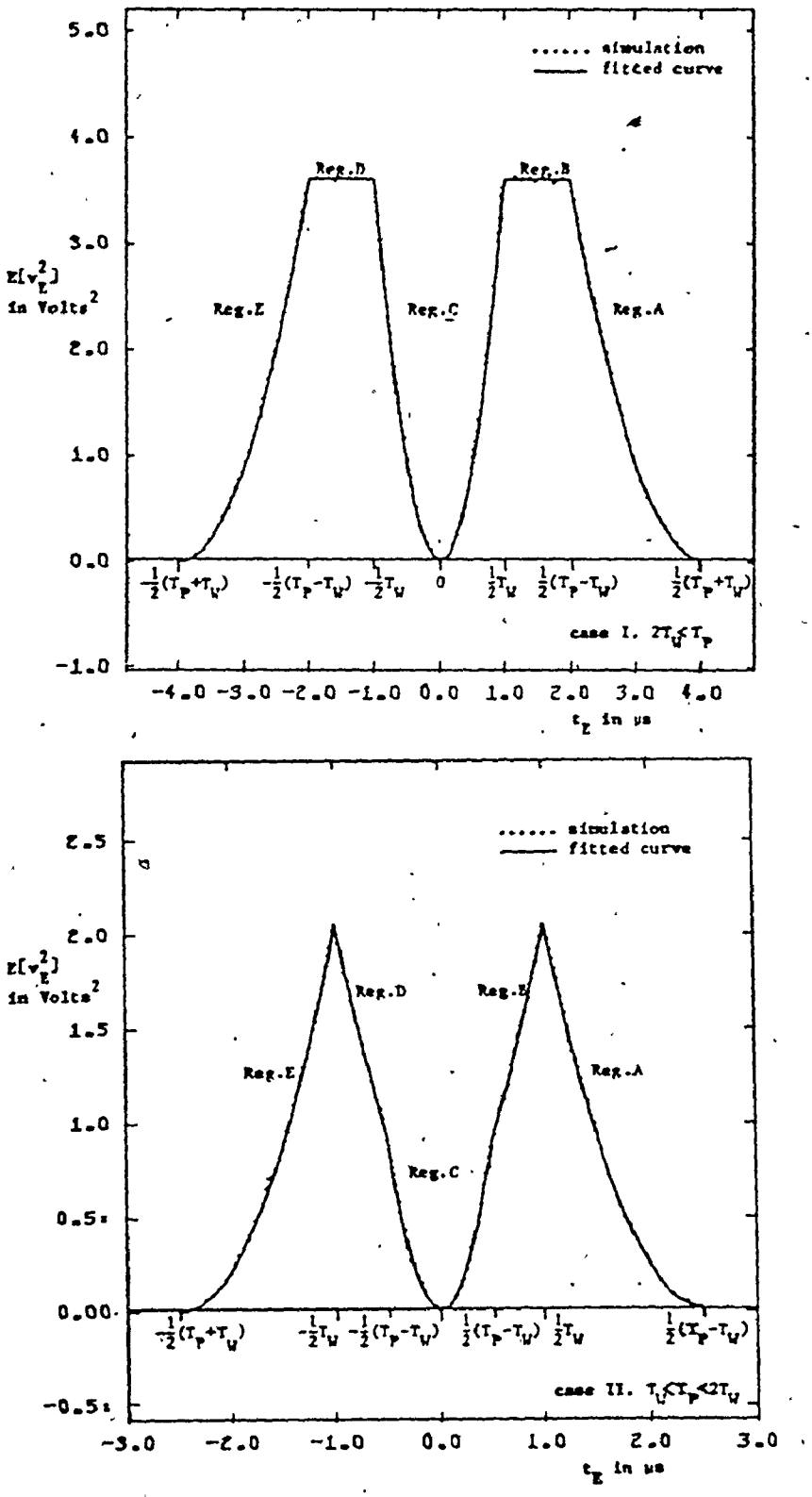

Fig. 5.19 Second-order error detection characteristics CNR_U/CNR_D = 40/25 db

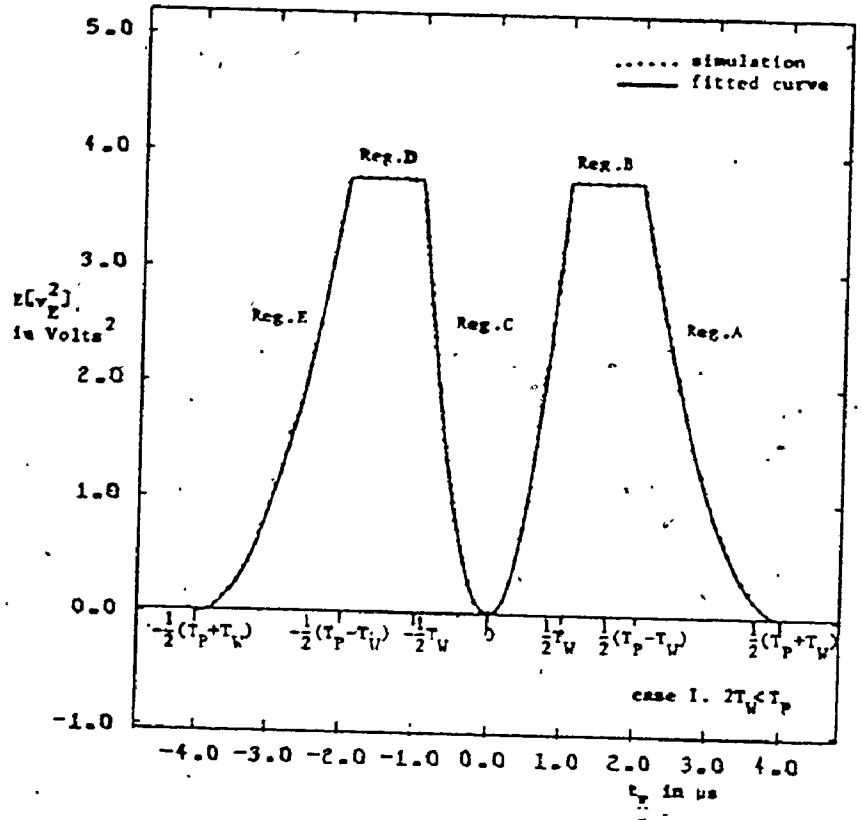

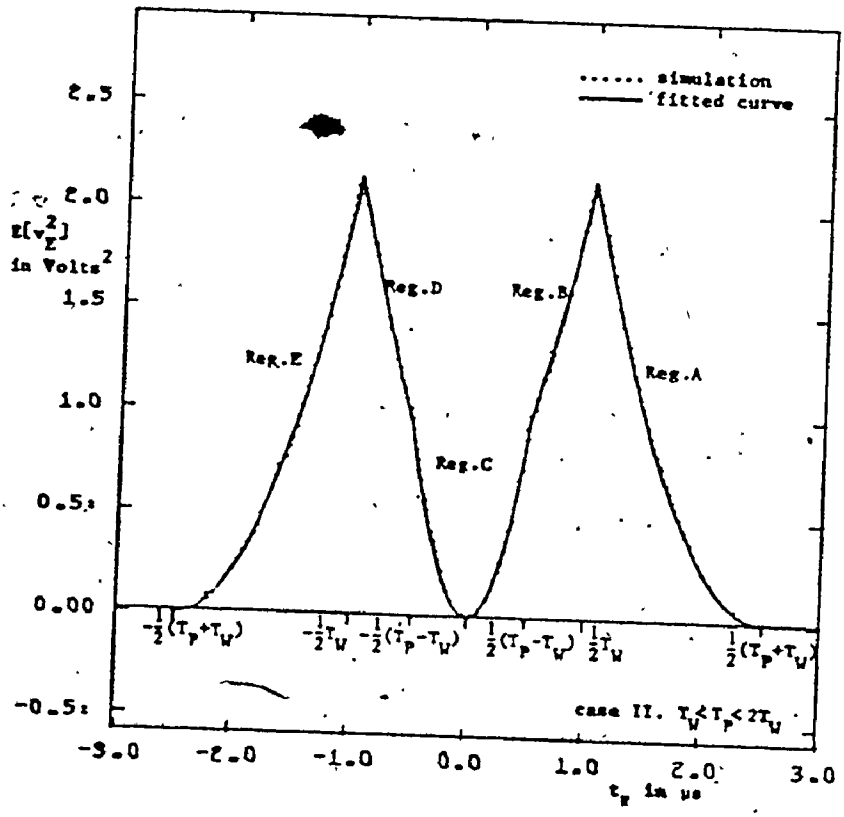

Fig. 5.20 Second-order error detection characteristics CNR_U/CNR_D = 40/30 db

$E[v_E(n-1)]$ in equations (4.7) and (4.8).

The mean square value of the timing error as a function of the number of iterations is now calculated for the Regions A, B and C and for both cases.

5.4.1 Case I. $2T_W < T_P$

5.4.1a Analysis for Region A $\frac{1}{2}(T_P-T_W) < t_E < \frac{1}{2}(T_P+T_W)$

$$E[v_{EA}^2(n)] = \alpha_A t_{EA}^2 + \beta_A t_{EA} + \gamma_A$$

$$E[v_{EA}(n)] = -C[t_{EA}(n) - \tfrac{1}{2}(T_P+T_W)] \qquad (5.10)$$

Substituting equations (5.10) to equation (5.9) we obtain:

$$\begin{aligned} E[t_{EA}^2(n)] &= E_{t_E(n-1)}\{(1 + b^2\alpha_A + 2bC)t_{EA}^2(n-1) \\ &\quad + (b^2\beta_A + 2t_M(1 + bC) + bC(T_P+T_W))t_{EA}(n-1) \\ &\quad + b^2\gamma_A + t_M^2 - bC(T_P+T_W)t_M\} \\ &= A\cdot E[t_{EA}^2(n-1)] + B\cdot E[t_{EA}(n-1)] + X \end{aligned} \qquad (5.11)$$

where $A = (1 + b^2\alpha_A + 2bC)$

$B = (b^2\beta_A + 2t_M(1+bC) + bC(T_P+T_W))$

$X = b^2\gamma_A + t_M^2 - bC(T_P+T_W)t_M$

For $n = 1$ $E[t_{EA}^2(1)] = A\cdot t_{EA}^2(0) + B\cdot E[t_{EA}(0) + X$

$n = 2$ $E[t_{EA}^2(2)] = A\cdot E[t_{EA}^2(1)] + B\cdot E[t_{EA}(1)] + X$

$= A^2\cdot t_{EA}^2(0) + AB\cdot E[t_{EA}(0)] + AX$

$+ B\cdot E[t_{EA}(1)] + X$

$n = 3$ $E[t_{EA}^2(3)] = A\cdot E[t_{EA}^2(2)] + B\cdot E[t_{EA}(2)] + X$

$= A^3\cdot t_{EA}(0) + A^2B\cdot E[t_{EA}(0)] + A^2X$

$+ AB\cdot E[t_{EA}(1)] + AX$

$+ B\cdot E[t_{EA}(2)] + X$

thus,

$$\text{For } n = r \quad E[t_{EA}^2(r)] = A^r \cdot t_{EA}^2(0) + B \cdot \sum_{n=1}^{r} A^{n-1} \cdot E[t_{EA}(r-n)] + X \cdot \sum_{n=1}^{r} A^{n-1} \qquad (5.12)$$

The expected value of the timing error after r iterations has been calculated (see equation (4.35)) as:

$$E[t_{EA}(r)] = (1+bC)^r \left[t_{EA}(0) - \frac{1}{2}(T_P+T_W) + \frac{t_M}{bC}\right] + \frac{1}{2}(T_P+T_W) - \frac{t_M}{bC}$$

Thus $\sum_{n=1}^{r} A^{n-1} \cdot E[t_{EA}(r-n)]$ can be expressed as:

$$\left[t_{EA}(0) - \frac{1}{2}(T_P+T_W) + \frac{t_M}{bC}\right] \cdot \sum_{n=1}^{r} A^{n-1} \cdot (1+bC)^{r-n} + \left[\frac{1}{2}(T_P+T_W) - \frac{t_M}{bC}\right] \cdot \sum_{n=1}^{r} A^{n-1} \qquad (5.13)$$

The above sums are the sums of the terms of geometric progress and can be derived as follows:

$$\sum_{n=1}^{r} A^{n-1}(1+bC)^{r-n} = \frac{A^r - (1+bC)^r}{A - (1+bC)}$$

$$\sum_{n=1}^{r} A^{n-1} = \frac{A^r - 1}{A - 1}$$

Finally

$$E[t_{EA}^2(r)] = A^r \cdot t_{EA}^2(0) + B \cdot \left[t_{EA}(0) - \frac{1}{2}(T_P+T_W) + \frac{t_M}{bC}\right] \frac{A^r - (1+bC)^r}{A - (1+bC)} + \left[B\left[\frac{1}{2}(T_P+T_W) - \frac{t_M}{bC}\right] + X\right] \frac{A^r - 1}{A - 1} \qquad (5.14)$$

or

$$E[t_{EA}^2(r)] = (1+b^2\alpha_A+2bC)^r t_{EA}^2(0) + [b^2\beta_A+2t_M(1+bC)+bC(T_P+T_W)]\left[t_{EA}(0) - \frac{1}{2}(T_P+T_W) + \frac{t_M}{bC}\right] \cdot \frac{(1+b^2\alpha_A+2bC)^r - (1+bC)^r}{b^2\alpha_A + bC}$$

$$+ [[b^2\beta_A + 2t_M(1+bC) + bC(T_P+T_W)][\frac{1}{2}(T_P+T_W) - \frac{t_M}{bC}]$$
$$+ b^2\gamma_A + t_M^2 - bC(T_P+T_W)t_M]\cdot\frac{(1+b^2\alpha_A+2bC)^r - 1}{b^2\alpha_A + 2bC} \qquad (5.15)$$

5.4.1.b Analysis for Region B $\frac{1}{2}T_W < t_E < \frac{1}{2}(T_P-T_W)$

$$E[v_{EB}^2(n)] = \gamma_B$$
$$E[v_{EB}(n)] = CT_W \qquad (5.16)$$

Substituting equations (5.16), equation (5.9) yields:

$$E[t_{EB}^2(n)] = E_{t_{EB}(n-1)}\{t_{EB}^2(n-1)+b^2\gamma_B+t_M^2+2t_{EB}(n-1)\cdot t_M-2bCT_W(t_{EB}(n-1)+t_M)\}$$
$$= E[t_{EB}^2(n-1)]+2(t_M-bCT_W)\cdot E[t_{EB}(n-1)]+b^2\gamma_B+t_M^2-2bCT_Wt_M$$

for n = 1 $E[t_{EB}^2(1)] = t_{EB}^2(0)+2(t_M-bCT_W)\cdot E[t_{EB}(0)]+b^2\gamma_B+t_M^2-2bCT_Wt_M$

n = 2 $E[t_{EB}^2(2)] = E[t_{EB}^2(1)]+2(t_M-bCT_W)\cdot E[t_{EB}(1)]+b^2\gamma_B+t_M^2-2bCT_Wt_M$

$= t_{EB}^2(0)+2(t_M-bCT_W)[E[t_{EB}(0)]+E[t_{EB}(1)]]+2(b^2\gamma_B+t_M^2-2bCT_Wt_M)$

n = 3 $E[t_{EB}^2(3)] = E[t_{EB}(2)]+2(t_M-bCT_W)E[t_{EB}(2)]+b^2\gamma_B+t_M^2-2bCT_Wt_M$

$= t_{EB}^2(0)+2(t_M-bCT_W)[E[t_{EB}(0)]+E[t_{EB}(1)]+E[t_{EB}(2)]$

$+ 3(b^2\gamma_B+t_M^2-2bCT_Wt_M)$

for n = r $E[t_{EB}^2(r)] = t_{EB}^2(0)+2(t_M-bCT_W)\sum_{n=1}^{r}E[t_{EB}(n-1)]+r(b^2\gamma_B+t_M^2-2bCT_Wt_M)$

The expected value of the timing error after n iterations is given by equation (4.39) as

$$E[t_{EB}(n)] = t_{EB}(0) - n(bCT_W-t_n)$$

Thus the sum $\sum_{n=1}^{r}E[t_{EB}(n-1)]$ is calculated as

$$\sum_{n=1}^{r} E[t_{EB}(n-1)] = r \cdot t_{EB}(0) - (bCT_W - t_M) \sum_{n=1}^{r} (n-1)$$

$$= r \cdot t_{EB}(0) - \frac{r(r-1)}{2} (bCT_W - t_M)$$

Thus

$$E[t_{EB}^2(r)] = t_{EB}^2(0) + 2\, r(t_M - bCT_W) t_{EB}(0) + r(r-1) \cdot (t_M - bCT_W)^2 + r(b^2 {}_B + t_M^2 - 2bCT_W t_M)$$

5.4.1.c Analysis for Region C $\quad -\frac{1}{2}T_W < t_E < \frac{1}{2}T_W$

$$E[v_{EC}^2(n)] = \alpha_C \cdot t_{EC}^2(n) + \gamma_C$$
$$E[v_{EC}(n)] = 2C \cdot t_{EC}(n) \qquad (5.19)$$

By substituting equations (5.19), equation (5.9) yields

$$E[t_{EC}^2(n)] = E_{t_{EC}(n-1)} \{(1 + b^2\alpha_C - 4bC) \cdot t_{EC}^2(n-1) + 2t_M(1-2bC)\, t_{EC}(n-1) + b^2\gamma_C + t_M^2\}$$

$$= A \cdot E[t_{EC}^2(n-1)] + B \cdot E[t_{EC}(n-1)] + X$$

where $A = 1 + b^2\alpha_C - 4bC$

$B = 2t_M(1-2bC)$ (5.20)

$X = b^2\gamma_C + t_M^2$

As in equation (5.12) the mean square value of the timing error after r iterations is given as

$$E[t_{EC}^2(r)] = A^r t_{EC}^2(0) + B \cdot \sum_{n=1}^{r} A^{n-1} \cdot E[t_{EC}(r-n)] + X \sum_{n=1}^{r} A^{n-1} \qquad (5.21)$$

The expected value of the timing error after r iterations is obtained from equation (4.42). Thus,

$$\sum_{n=1}^{r} A^{n-1} E[t_{EC}(r-n)] = (t_{EC}(0) - \frac{t_M}{bC}) \cdot \sum_{n=1}^{r} A^{n-1} (1-2bC)^{r-n} + \frac{t_M}{2bC} \sum_{n=1}^{r} A^{n-1}$$

Since $|1-2bC| < 1$ (see equation (4.43)) and $\alpha_C \approx 4C^2$ (5.22)

$\therefore\ |A| = |1 + b^2\alpha_C - 4bC| \approx |1 + 4b^2C^2 - 4bC| \approx |1 - 2bC|^2$

Thus $|A| < 1$

Consequently $\lim_{r\to\infty} \sum_{n=1}^{r} A^{n-1}\cdot(1-2bC)^{r-n} = 0$

and $\lim_{r\to\infty} \sum_{n=1}^{r} A^{n-1} = \frac{1}{1-A} = \frac{1}{4bC-b^2\alpha_C}$

Thus the mean square value after large number of iterations is given as:

$$\lim_{r\to\infty} E[t_{EC}^2(r)] = \frac{b^2\gamma_C + t_M^2 - \frac{t_M^2}{bC}}{4bC-b^2\alpha_C} \qquad (5.23)$$

5.4.2 Case II $T_W < T_P < 2T_W$

5.4.2.a Analysis for Region A $\frac{1}{2}T_W < t_E < \frac{1}{2}(T_P+T_W)$

(see equation (5.15))

5.4.2.b Analysis for Region B $\frac{1}{2}(T_P-T_W) < t_E < \frac{1}{2}T_W$

$$E[v_{EB}^2(n)] = \alpha_B\cdot t_E^2(n) + \beta_B\cdot t_E(n) + \gamma_B$$
$$E[v_{EB}(n)] = C[t_{EB}(n) + \tfrac{1}{2}(T_P-T_W)] \qquad (5.24)$$

Substituting equations (5.24), (5.9) yields

$$E[t_{EB}^2(n)] = A\cdot E[t_{EB}^2(n-1)] + B\cdot E[t_{EB}(n-1)] + X$$

where $A = 1 + b^2\alpha_C - 2bC$

$$B = b^2\beta_C + 2t_M(1-bC) - bC(T_P-T_W) \qquad (5.25)$$
$$X = b^2\gamma_B + t_M^2 - bC(T_P-T_W)t_M$$

for n = r (see equation (5.12))

$$E[t_{EB}^2(r)] = A^r \cdot t_{EB}^2(0) + B \cdot \sum_{n=1}^{r} A^{n-1} E[t_{EB}(n-r)] + X \cdot \sum_{n=1}^{r} A^{n-1}$$

The expected value of the timing error after r iterations has been calculated in equation (4.46)

$$\sum_{n=1}^{r} A^{n-1} \cdot E[t_{EB}(n-r)] = [t_{EB}(0) + \tfrac{1}{2}(T_P - T_W) - \frac{t_M}{bC}] \cdot \sum_{n=1}^{r} A^{n-1} (1-bC)^{r-n} - [\tfrac{1}{2}(T_P - T_W) - \frac{t_M}{bC}] \cdot \sum_{n=1}^{r} A^{n-1} \tag{5.26}$$

Consequently

$$E[t_{EB}(r)] = A^r t_{EB}^2(0) + B \cdot [t_{EB}(0) + \tfrac{1}{2}(T_P - T_W) - \frac{t_M}{bC}] \frac{A^r - (1-bC)^r}{A-(1-bC)} + [X - B \cdot [\tfrac{1}{2}(T_P - T_W) - \frac{t_M}{bC}]] \frac{A^r - 1}{A-1} \tag{5.27}$$

or

$$E[t_{EB}(r)] = (1+b^2\alpha_B - 2bC)^r \cdot t^2 EB(0) + [b^2\beta_C + 2t_M(1-bC) - bC(T_P - T_W)] \cdot [t_{EB}(0) + \tfrac{1}{2}(T_P - T_W) - \frac{t_M}{bC}] \cdot \frac{(1+b^2\alpha_C - 2bC)^r - (1-bC)^r}{b^2\alpha_C - bC} + [[b^2\gamma_B + t_M^2 - bC(T_P - T_W) t_M] - [b^2\beta_C + 2t_M(1-bC) - bC(T_P - T_W)] \cdot [\tfrac{1}{2}(T_P - T_W) - \frac{t_M}{bC}] \cdot \frac{(1+b^2\alpha_C - 2bC)^r - 1}{b^2\alpha_C - 2bC} \tag{5.28}$$

5.4.2.c Analysis for Region C, $-\frac{1}{2}(T_P - T_W) < t_E < \frac{1}{2}(T_P - T_W)$ (see equation (5.23))

5.5 NUMERICAL RESULTS

The number of iterations required for transition from Region A to Region B and for transition from Region B to Region C can be calculated

from the equations given in Section 4.5. The number of iterations required for convergence to the origin can be also calculated from equation (4.42) by having the dependent on the number of iterations term $(1-2bC)^r [t_{EC}(0) - \frac{t_M}{2bC}]$ to be insignificant compared with the steady state timing error $t_M/2bC$.

Results for different carrier-to-noise ratios, the timing circuits constant b, the change in path delay due to satellite motion t_M and the initial timing error at Region A $t_{EA}(0)$ are given in Tables IV to IX (Case I) and X to XV (Case II). It is seen that generally high CNR and large values of the timing circuits constant b yield faster synchronization. However, the total number of iterations required to achieve synchronization (Tables XVI and XVII (Case I) and XVIII and XIX (Case II) has a minimum value when $bC \approx .5$.

The mean square timing error can be calculated from equations given in Section 5.4, the number of iterations calculated previously and the coefficients α_A, β_A, γ_A, etc. calculated by the simulation.

The ultimate rms timing error (i.e., the rms timing error at Region C after large number of iterations) is given in Table XX and plotted in Figures 5.21, 5.22, and 5.22a as a function of the timing circuits constant b and the normalized carrier-to-noise ratio. (Note that $CNR_N \approx CNR_D$, see also equation 4.14a).

T A B L E IV

(case I)

NUMBER OF ITERATIONS REQUIRED TO ACHIEVE SYNCHRONIZATION

INITIAL TIMING ERROR AT REGION A $t_{FA}(0) = 3.2$ μs
CHANGE IN PATH DELAY DUE TO SATELLITE MOTION $t_M = 18$ ns

NO OF ITERATIONS REQUIRED FOR TRANSMISSION FROM REG. A TO REG. B

CRFU/CRFD	b = 0.0	.1	.2	.3	.4	.5	.6	.7
20 / 0.	***	39	15	10	7	6	5	4
20 / 5.	70	22	10	7	5	4	4	3
20 /10.	43	16	8	5	4	4	3	3
30 /15.	35	14	7	5	4	3	3	3
30 /20.	31	13	6	4	4	3	3	2
40 /25.	30	12	6	4	3	3	3	2
40 /30.	29	12	6	4	3	3	3	2

NO OF ITERATIONS REQUIRED FOR TRANSMISSION FROM REG. B TO REG. C

CRFU/CRFD	b = 0.0	.1	.2	.3	.4	.5	.6	.7
20 / 0.	***	16	7	4	4	3	2	2
20 / 5.	25	10	5	3	2	2	1	2
20 /10.	18	8	3	3	2	1	1	1
30 /15.	15	7	3	2	1	1	1	1
30 /20.	14	6	3	2	1	1	1	1
40 /25.	12	6	3	2	2	1	1	1
40 /30.	12	6	3	2	2	1	1	1

NO OF ITERATIONS REQUIRED FOR CONVERGENCE TO THE OFFSET

CRFU/CRFD	b = 0.0	.1	.2	.3	.4	.5	.6	.7
20 / 0.	***	71	39	27	19	15	13	10
20 / 5.	90	51	26	17	13	9	7	5
20 /10.	74	41	21	13	9	6	4	3
30 /15.	66	36	18	11	8	5	2	5
30 /20.	63	34	17	10	6.	4	3	7
40 /25.	61	33	16	10	6	3.	4	8
40 /30.	60	32	15	9	5	3	5	8

(NOTE: *** denotes no convergence with satellite motion)

T A B L E V

(case I)

NUMBER OF ITERATIONS REQUIRED TO ACHIEVE SYNCHRONIZATION

INITIAL TIMING ERROR AT REGION A $t_{EA}(0)$= 3.2 μs
CHANGE IN PATH DELAY DUE TO SATELLITE MOTION t_M= 25 ns

NO OF ITERATIONS REQUIRED FOR TRANSITION FROM REG. A TO REG. B

CNR0/CNR1	b = .0	.1	.2	.3	.4	.5	.6	.7
20 / 0.	***	55	17	10	8	6	5	5
20 / 5.	***	26	11	7	5	4	4	3
20 /10.	64	18	9	6	4	4	3	3
30 /15.	46	15	7	5	4	3	3	3
30 /20.	40	14	7	5	4	3	3	2
40 /25.	37	13	6	4	4	3	3	2
40 /30.	33	13	6	4	3	3	3	2

NO OF ITERATIONS REQUIRED FOR TRANSITION FROM REG. B TO REG. C

CNR0/CNR1	b = .0	.1	.2	.3	.4	.5	.6	.7
20 / 0.	***	19	7	5	3	3	2	1
20 / 5.	***	11	4	3	3	2	1	2
20 /10.	20	8	4	2	2	1	1	1
30 /15.	17	7	3	2	1	1	1	1
30 /20.	15	6	3	2	1	1	1	1
40 /25.	14	6	3	2	1	1	1	1
40 /30.	14	6	3	2	2	1	1	1

NO OF ITERATIONS REQUIRED FOR CONVERGENCE TO THE DESIRED

CNR0/CNR1	b = .0	.1	.2	.3	.4	.5	.6	.7
20 / 0.	***	55	37	25	19	14	12	10
20 / 5.	***	47	26	17	11	9	7	4
20 /10.	69	39	20	12	9	6	4	3
30 /15.	61	34	18	11	7	5	2	5
30 /20.	58	32	15	9	6	4	3	7
40 /25.	56	31	15	9	6	3	4	8
40 /30.	56	30	15	9	5	3	4	8

(NOTE: *** denotes no convergence with satellite motion)

TABLE VI

(case I)

NUMBER OF ITERATIONS REQUIRED TO ACHIEVE SYNCHRONIZATION

INITIAL TIMING ERROR AT REGION A $t_{EA}(0) = 3.0$ μs
CHANGE IN PATH DELAY DUE TO SATELLITE MOTION $t_M = 18$ ns

NO OF ITERATIONS REQUIRED FOR TRANSITION FROM REG. A TO REG. B

CKEU/CNEO	b = .05	.1	.2	.3	.4	.5	.6	.7
20 / 0.	128	27	11	7	6	5	4	3
20 / 5.	45	16	8	5	4	3	3	3
20 /10.	30	12	6	4	3	3	2	2
30 /15.	25	11	5	4	3	3	2	2
30 /20.	22	10	5	4	3	2	2	2
40 /25.	21	9	5	3	3	2	2	2
40 /30.	21	9	5	3	3	2	2	2

NO OF ITERATIONS REQUIRED FOR TRANSITION FROM REG. B TO REG. C

CKEU/CNEO	b = .15	.1	.2	.3	.4	.5	.6	.7
20 / 0.	46	17	8	5	3	2	2	2
20 / 5.	25	10	4	3	2	2	1	1
20 /10.	18	8	4	3	2	1	2	1
30 /15.	15	6	3	2	2	1	1	1
30 /20.	14	6	3	1	1	2	1	1
40 /25.	13	6	3	2	1	1	1	1
40 /30.	12	6	2	2	1	1	1	1

NO OF ITERATIONS REQUIRED FOR CONVERGENCE TO THE DESIRED

CKEU/CNEO	b = .25	.1	.2	.3	.4	.5	.6	.7
20 / 0.	119	70	38	26	20	15	12	10
20 / 5.	89	51	27	18	13	9	7	5
20 /10.	74	41	20	13	9	6	4	3
30 /15.	66	36	18	11	7	4	3	5
30 /20.	63	34	17	10	7	3	4	6
40 /25.	61	33	15	10	6	3	5	6
40 /30.	60	32	16	9	6	3	5	7

T A B L E VII

(case I)

NUMBER OF ITERATIONS REQUIRED TO ACHIEVE SYNCHRONIZATION

INITIAL TIMING ERROR AT REGION A $t_{EA}(0) = 3.0$ ps
CHANGE IN PATH DELAY DUE TO SATELLITE MOTION $t_M = 25$ ns

NO OF ITERATIONS REQUIRED FOR TRANSITION FROM REG. A TO REG. B

CNFU/CNFD	b = .0	.1	.2	.3	.4	.5	.6	.7
20 / 0.	***	34	12	8	6	5	4	4
20 / 5.	72	18	8	5	4	3	3	3
20 /10.	39	13	6	4	3	3	2	2
30 /15.	30	11	5	4	3	3	2	2
30 /20.	27	10	5	4	3	2	2	2
40 /25.	25	10	5	3	3	2	2	2
40 /30.	24	10	5	3	3	2	2	2

NO OF ITERATIONS REQUIRED FOR TRANSITION FROM REG. A TO REG. C

CNFU/CNFD	b = .0	.1	.2	.3	.4	.5	.6	.7
20 / 0.	***	19	8	5	3	2	2	1
20 / 5.	30	11	5	3	2	2	1	1
20 /10.	20	8	4	3	2	1	2	1
30 /15.	17	7	4	2	2	1	1	1
30 /20.	15	7	3	1	1	2	1	1
40 /25.	14	6	3	2	1	1	1	1
40 /30.	14	6	3	2	1	1	1	1

NO OF ITERATIONS REQUIRED FOR CONVERGENCE TO THE REGION

CNFU/CNFD	b = .0	.1	.2	.3	.4	.5	.6	.7
20 / 0.	***	65	36	24	19	15	12	10
20 / 5.	81	48	25	17	12	9	7	5
20 /10.	68	39	20	12	9	6	3	3
30 /15.	61	34	17	11	7	4	3	5
30 /20.	58	32	16	10	6	3	4	5
40 /25.	57	31	15	9	6	3	4	5
40 /30.	55	30	14	9	6	3	5	7

(NOTE: *** denotes no convergence with satllite motion)

T A B L E VIII

(case I)

NUMBER OF ITERATIONS REQUIRED TO ACHIEVE SYNCHRONIZATION

INITIAL TIMING ERROR AT REGION A $t_{EA}(0) = 2.8$ μs
CHANGE IN PATH DELAY DUE TO SATELLITE MOTION $t_M = 18$ ns

NO OF ITERATIONS REQUIRED FOR
EQUATION FROM REG. A TO REG. B

CNFU/CNFD	b = .0	.1	.2	.3	.4	.5	.6	.7
20 / 0.	58	19	8	6	4	4	3	3
20 / 5.	30	12	6	4	3	3	2	2
20 /10.	21	9	4	3	3	2	2	2
30 /15.	18	8	4	3	2	2	2	2
30 /20.	16	7	4	3	2	2	2	2
40 /25.	15	7	4	3	2	2	2	2
40 /30.	15	7	4	3	2	2	2	2

NO OF ITERATIONS REQUIRED FOR
EQUATION FROM REG. B TO REG. C

CNFU/CNFD	b = .0	.1	.2	.3	.4	.5	.6	.7
20 / 0.	46	17	9	4	4	2	2	2
20 / 5.	25	10	4	3	2	1	2	1
20 /10.	18	8	4	3	1	2	1	1
30 /15.	14	6	3	2	2	1	1	1
30 /20.	14	6	3	2	2	1	1	1
40 /25.	13	6	2	1	2	1	1	1
40 /30.	12	5	2	1	1	1	1	1

NO OF ITERATIONS REQUIRED FOR
CONVERGENCE TO THE OPTIMUM

CNFU/CNFD	b = .0	.1	.2	.3	.4	.5	.6	.7
20 / 0.	119	70	38	26	19	15	12	10
20 / 5.	90	51	27	17	13	10	7	5
20 /10.	74	40	21	13	9	6	4	3
30 /15.	67	37	18	11	7	5	2	5
30 /20.	62	34	16	10	6	4	3	7
40 /25.	61	32	16	10	5	3	3	8
40 /30.	60	32	16	10	5	3	4	9

T A B L E IX

(case I)

NUMBER OF ITERATIONS REQUIRED TO ACHIEVE SYNCHRONIZATION

INITIAL TIMING ERROR AT REGION A $t_{EA}(0) = 2.8$ us
CHANGE IN PATH DELAY DUE TO SATELLITE MOTION $t_M = 25$ ns

NO OF ITERATIONS REQUIRED FOR TRANSITION FROM REG. A TO REG. B

CNFU/CNFD	b = .0	.1	.2	.3	.4	.5	.6	.7
20 / 0.	***	23	9	6	4	4	3	3
20 / 5.	42	13	6	4	3	3	2	2
20 /10.	26	10	5	3	3	2	2	2
30 /15.	21	8	4	3	2	2	2	2
30 /20.	18	8	4	3	2	2	2	2
40 /25.	17	7	4	3	2	2	2	2
40 /30.	17	7	4	3	2	2	2	2

NO OF ITERATIONS REQUIRED FOR TRANSITION FROM REG. B TO REG. C

CNFU/CNFD	b = .0	.1	.2	.3	.4	.5	.6	.7
20 / 0.	***	19	7	5	4	2	2	2
20 / 5.	30	11	5	3	2	1	2	1
20 /10.	20	8	3	3	1	2	1	1
30 /15.	16	7	3	2	2	1	1	1
30 /20.	15	6	3	2	2	1	1	1
40 /25.	15	6	3	2	2	1	1	1
40 /30.	14	6	2	1	1	1	1	1

NO OF ITERATIONS REQUIRED FOR CONVERGENCE TO THE ORIGIN

CNFU/CNFD	b = .0	.1	.2	.3	.4	.5	.6	.7
20 / 0.	***	65	37	24	18	15	12	9
20 / 5.	81	47	25	17	12	9	6	5
20 /10.	68	38	20	12	9	6	4	3
30 /15.	62	34	17	11	7	5	2	5
30 /20.	59	32	16	9	6	4	3	7
40 /25.	56	31	15	9	5	3	3	8
40 /30.	55	30	15	9	6	3	4	9

(NOTE: *** denotes no convergence with satellite motion)

TABLE X

(case II)

NUMBER OF ITERATIONS REQUIRED TO ACHIEVE SYNCHRONIZATION

INITIAL TIMING ERROR AT REGION A $t_{EA}(0)$= 1.8 μs
CHANGE IN PATH DELAY DUE TO SATELLITE MOTION t_M= 18 ns

NO OF ITERATIONS REQUIRED FOR TRANSITION FROM REG. A TO REG. B

CNRJ/CNRD	b =.0E	.1	.2	.3	.4	.5	.6	.7
20 / 0.	***	38	14	9	6	5	4	4
20 / 5.	82	20	9	6	4	4	3	3
20 /10.	43	15	7	5	4	3	3	2
30 /15.	33	12	6	4	3	3	2	2
30 /20.	29	11	6	4	3	3	2	2
40 /25.	27	11	5	4	3	3	2	2
40 /30.	26	11	5	4	3	2	2	2

NO OF ITERATIONS REQUIRED FOR TRANSITION FROM REG. B TO REG. C

CNRJ/CNRD	b =.0E	.1	.2	.3	.4	.5	.6	.7
20 / 0.	***	16	6	3	3	2	2	1
20 / 5.	28	9	3	2	2	1	1	1
20 /10.	18	6	3	1	1	1	1	1
30 /15.	15	6	2	2	1	1	1	1
30 /20.	13	5	2	1	1	1	1	1
40 /25.	13	5	2	1	1	1	1	1
40 /30.	12	4	2	1	1	1	1	1

NO OF ITERATIONS REQUIRED FOR CONVERGENCE TO THE ORIGIN

CNRJ/CNRD	b =.0E	.1	.2	.3	.4	.5	.6	.7
20 / 0.	***	71	38	25	20	15	13	10
20 / 5.	69	36	24	16	12	9	7	5
20 /10.	60	27	19	12	9	6	4	3
30 /15.	55	22	16	11	7	5	3	5
30 /20.	53	18	15	10	6	4	4	7
40 /25.	31	21	14	9	6	3	5	8
40 /30.	50	19	14	9	6	3	5	9

(NOTE: *** denotes no convergence with satellite motion)

T A B L E XI

(case II)

NUMBER OF ITERATIONS REQUIRED TO ACHIEVE SYNCHRONIZATION

INITIAL TIMING ERROR AT REGION A $t_{EA}(0) = 1.8$ μs
CHANGE IN PATH DELAY DUE TO SATELLITE MOTION $t_M = 25$ ns

NO OF ITERATIONS REQUIRED FOR TRANSITION FROM REG. A TO REG. B

CNFJ/CNFD	b = .05	.1	.2	.3	.4	.5	.6	.7
20 / 0.	***	66	15	9	7	5	5	4
20 / 5.	***	25	9	6	5	4	3	3
20 /10.	92	17	7	5	4	3	3	2
30 /15.	51	14	6	4	3	3	2	2
30 /20.	41	13	6	4	3	3	2	2
40 /25.	38	12	6	4	3	3	2	2
40 /30.	36	12	5	4	3	3	2	2

NO OF ITERATIONS REQUIRED FOR TRANSITION FROM REG. B TO REG. C

CNFJ/CNFD	b = .05	.1	.2	.3	.4	.5	.6	.7
20 / 0.	***	21	7	4	2	2	1	1
20 / 5.	***	10	4	2	1	1	1	1
20 /10.	25	7	3	2	1	1	1	1
30 /15.	18	6	3	2	1	1	1	1
30 /20.	16	5	2	1	1	1	1	1
40 /25.	14	5	2	1	1	1	1	1
40 /30.	14	5	3	1	1	1	1	1

NO OF ITERATIONS REQUIRED FOR CONVERGENCE TO THE ORIGIN

CNFJ/CNFD	b = .05	.1	.2	.3	.4	.5	.6	.7
20 / 0.	***	65	37	25	19	15	11	10
20 / 5.	***	47	26	17	12	9	7	5
20 /10.	50	29	18	12	8	6	4	3
30 /15.	48	24	16	10	7	4	2	5
30 /20.	46	23	14	9	6	4	4	7
40 /25.	45	20	14	9	6	3	4	8
40 /30.	44	21	13	8	5	3	5	8

(NOTE: *** denotes no convergence with satellite motion)

T A B L E XII

(case II)

NUMBER OF ITERATIONS REQUIRED TO ACHIEVE SYNCHRONIZATION

INITIAL TIMING ERROR AT REGION A $t_{EA}(0) = 1.6\ \mu s$
CHANGE IN PATH DELAY DUE TO SATELLITE MOTION $t_M = .18$ ns

NO OF ITERATIONS REQUIRED FOR TRANSITION FROM REG. A TO REG. B

CREJ/CNFD	b = .0	.1	.2	.3	.4	.5	.6	.7
20 / 0.	***	22	9	6	4	4	3	3
20 / 5.	40	13	6	4	3	3	2	2
20 /10.	25	10	5	3	3	2	2	2
30 /15.	20	8	4	3	2	2	2	2
30 /20.	18	8	4	3	2	2	2	2
40 /25.	17	7	4	3	2	2	2	2
40 /30.	16	7	4	3	2	2	2	2

NO OF ITERATIONS REQUIRED FOR TRANSITION FROM REG. B TO REG. C

CREJ/CNFD	b = .0	.1	.2	.3	.4	.5	.6	.7
20 / 0.	***	17	6	3	3	2	2	1
20 / 5.	28	9	4	2	2	1	1	1
20 /10.	18	6	2	2	1	1	1	1
30 /15.	14	6	3	1	1	1	1	1
30 /20.	13	5	2	1	1	1	1	1
40 /25.	12	5	2	1	1	1	1	1
40 /30.	12	5	2	1	1	1	1	1

NO OF ITERATIONS REQUIRED FOR CONVERGENCE TO THE ORIGIN

CREJ/CNFD	b = .0	.1	.2	.3	.4	.5	.6	.7
20 / 0.	***	71	39	26	20	15	12	10
20 / 5.	68	36	24	16	12	9	7	5
20 /10.	60	27	19	12	9	6	4	3
30 /15.	56	19	16	11	7	5	3	5
30 /20.	52	21	15	10	6	4	4	7
40 /25.	51	15	14	9	6	3	5	8
40 /30.	50	18	14	9	6	3	5	9

(NOTE: *** denotes no convergence with satellite motion)

T A B L E XIII

(case II)

NUMBER OF ITERATIONS REQUIRED TO ACHIEVE SYNCHRONIZATION

INITIAL TIMING ERROR AT REGION A $t_{EA}(0) = 1.6$ μs
CHANGE IN PATH DELAY DUE TO SATELLITE MOTION $t_M = 25$ ns

NO OF ITERATIONS REQUIRED FOR TRANSITION FROM REG. A TO REG. B

CNRJ/CNED	b =.05	.1	.2	.3	.4	.5	.6	.7
20 / 0.	***	31	10	6	5	4	3	3
20 / 5.	93	15	6	4	3	3	2	2
20 /10.	36	11	5	3	3	2	2	2
30 /15.	26	9	4	3	2	2	2	2
30 /20.	23	8	4	3	2	2	2	2
40 /25.	21	8	4	3	2	2	2	2
40 /30.	20	8	4	3	2	2	2	2

NO OF ITERATIONS REQUIRED FOR TRANSITION FROM REG. B TO REG. C

CNRJ/CNED	b =.05	.1	.2	.3	.4	.5	.6	.7
20 / 0.	***	21	6	4	2	2	2	1
20 / 5.	50	10	4	3	2	1	1	1
20 /10.	24	7	3	2	1	1	1	1
30 /15.	19	6	3	2	1	1	1	1
30 /20.	16	6	2	1	1	1	1	1
40 /25.	15	5	2	1	1	1	1	1
40 /30.	14	5	2	1	1	1	1	1

NO OF ITERATIONS REQUIRED FOR CONVERGENCE TO THE ORIGIN

CNRJ/CNED	b =.05	.1	.2	.3	.4	.5	.6	.7
20 / 0.	***	65	36	25	18	14	12	10
20 / 5.	47	38	23	15	11	8	6	5
20 /10.	50	29	18	12	8	6	4	3
30 /15.	47	25	16	10	7	4	2	5
30 /20.	46	22	14	9	6	4	3	7
40 /25.	45	21	14	9	6	3	4	8
40 /30.	45	21	13	8	5	3	5	8

(NOTE: *** denotes no convergence with satellite motion)

T A B L E XIV

(case II)

NUMBER OF ITERATIONS REQUIRED TO ACHIEVE SYNCHRONIZATION

INITIAL TIMING ERROR AT REGION A $\tau_{EA}(0) = 1.4$ μs
CHANGE IN PATH DELAY DUE TO SATELLITE MOTION $t_M = 18$ ns

NO OF ITERATIONS REQUIRED FOR TRANSITION FROM REG. A TO REG. B

CNPJ/CNRO	b = .05	.1	.2	.3	.4	.5	.6	.7
20 / 0.	58	13	5	4	3	2	2	2
20 / 5.	21	8	4	3	2	2	2	1
20 /10.	14	6	3	2	2	2	1	1
30 /15.	12	5	3	2	2	1	1	1
30 /20.	11	5	3	2	2	1	1	1
40 /25.	10	5	2	2	1	1	1	1
40 /30.	10	4	2	2	1	1	1	1

NO OF ITERATIONS REQUIRED FOR TRANSITION FROM REG. B TO REG. C

CNPJ/CNRO	b = .05	.1	.2	.3	.4	.5	.6	.7
20 / 0.	94	16	7	3	2	2	2	1
20 / 5.	28	9	3	2	2	1	1	1
20 /10.	18	6	3	2	1	1	1	1
30 /15.	14	6	2	1	1	1	1	1
30 /20.	12	5	2	1	1	1	1	1
40 /25.	12	4	3	1	1	1	1	1
40 /30.	11	5	2	1	1	1	1	1

NO OF ITERATIONS REQUIRED FOR CONVERGENCE TO THE ORIGIN

CNPJ/CNRO	b = .05	.1	.2	.3	.4	.5	.6	.7
20 / 0.	57	57	34	24	18	14	12	10
20 / 5.	69	37	24	16	12	9	7	5
20 /10.	60	27	19	12	9	6	4	3
30 /15.	55	20	16	11	7	5	3	5
30 /20.	53	15	15	10	6	4	4	7
40 /25.	51	19	14	9	6	3	5	8
40 /30.	51	14	14	9	6	3	5	9

T A B L E XV

(case II)

NUMBER OF ITERATIONS REQUIRED TO ACHIEVE SYNCHRONIZATION

INITIAL TIMING ERROR AT REGION A $t_{EA}(0) = 1.4$ μs
CHANGE IN PATH DELAY DUE TO SATELLITE MOTION $t_M = 25$ ns

NO. OF ITERATIONS REQUIRED FOR
RESOLUTION FROM REG. A TO REG. B

CNRJ/CNRD	b=.01	.1	.2	.3	.4	.5	.6	.7
20 / 0.	***	16	6	4	3	2	2	2
20 / 5.	34	9	4	3	2	2	2	1
20 /10.	19	6	3	2	2	2	1	1
30 /15.	14	5	3	2	2	1	1	1
30 /20.	13	5	3	2	2	1	1	1
40 /25.	12	5	2	2	2	1	1	1
40 /30.	11	5	2	2	1	1	1	1

NO. OF ITERATIONS REQUIRED FOR
RESOLUTION FROM REG. B TO REG. C

CNRJ/CNRD	b=.01	.1	.2	.3	.4	.5	.6	.7
20 / 0.	***	22	7	4	3	2	2	1
20 / 5.	50	10	4	2	2	1	1	1
20 /10.	24	8	3	2	1	1	1	1
30 /15.	19	6	2	2	1	1	1	1
30 /20.	16	6	2	1	1	1	1	1
40 /25.	15	5	3	1	1	1	1	1
40 /30.	15	5	3	1	1	1	1	1

NO OF ITERATIONS REQUIRED FOR
CONVERGENCE TO THE ORIGIN

CNRJ/CNRD	b=.01	.1	.2	.3	.4	.5	.6	.7
20 / 0.	***	66	37	25	19	15	12	10
20 / 5.	47	38	23	15	11	8	6	5
20 /10.	50	28	18	12	8	6	4	3
30 /15.	47	25	16	10	7	4	2	5
30 /20.	46	22	14	9	6	4	4	7
40 /25.	45	22	14	9	6	3	4	8
40 /30.	44	22	13	8	5	3	5	8

(NOTE: *** denotes no convergence with satellite motion)

T A B L E XVI

(case I)

TOTAL NUMBER OF ITERATIONS REQUIRED TO ACHIEVE SYNCHRONIZATION

CHANGE IN PATH DELAY DUE TO SATELLITE MOTION t_M= 18 ns

INITIAL TIMING ERROR AT REGION A $t_{EA}(0)$= 3.2 μs

CNPU/CNED	b = .0	.1	.2	.3	.4	.5	.6	.7
20 / 0.	***	126	61	41	30	24	20	16
20 / 5.	185	83	41	27	20	15	12	10
20 /10.	135	65	32	21	15	11	8	7
30 /15.	116	57	28	18	13	9	6	9
30 /20.	106	53	26	16	11	8	7	10
40 /25.	103	51	25	16	11	7	8	11
40 /30.	101	50	24	15	10	7	9	11

INITIAL TIMING ERROR AT REGION A $t_{EA}(0)$= 3.0 μs

CNPU/CNED	b = .0	.1	.2	.3	.4	.5	.6	.7
20 / 0.	293	114	57	38	29	22	19	15
20 / 5.	159	77	39	26	19	14	11	9
20 /10.	122	61	30	20	14	10	8	6
30 /15.	106	53	26	17	12	8	6	8
30 /20.	99	50	25	15	11	7	7	9
40 /25.	95	48	23	15	10	6	8	9
40 /30.	93	47	23	14	10	6	9	10

INITIAL TIMING ERROR AT REGION A $t_{EA}(0)$= 2.8 μs

CNPU/CNED	b = .0	.1	.2	.3	.4	.5	.6	.7
20 /.0.	233	106	54	36	27	21	17	15
20 / 5.	145	73	37	24	18	14	11	8
20 /10.	113	57	29	19	13	10	7	6
30 /15.	99	51	25	16	11	8	5	8
30 /20.	92	47	23	15	10	7	6	10
40 /25.	89	45	22	14	9	6	6	11
40 /30.	87	44	22	14	9	6	7	12

(NOTE: *** denotes no convergence with satellite motion)

TABLE XVII

(case I)

TOTAL NUMBER OF ITERATIONS REQUIRED TO ACHIEVE SYNCHRONIZATION

CHANGE IN PATH DELAY DUE TO SATELLITE MOTION t_M = 25 ns

INITIAL TIMING ERROR AT REGION A $t_{EA}(0)$ = 3.2 μs

CNPU/CNPD	b = .05	.1	.2	.3	.4	.5	.6	.7
20 / 0.	***	138	61	40	30	23	19	16
20 / 5.	***	84	41	27	19	15	12	9
20 /10.	153	65	32	20	15	11	8	7
30 /15.	124	56	28	18	12	9	6	9
30 /20.	113	52	25	16	11	8	7	10
40 /25.	107	50	24	15	11	7	8	11
40 /30.	105	49	24	15	10	7	9	11

INITIAL TIMING ERROR AT REGION A $t_{EA}(0)$ = 3.0 μs

CNPU/CNPD	b = .05	.1	.2	.3	.4	.5	.6	.7
20 / 0.	***	116	56	37	28	22	18	15
20 / 5.	183	77	39	25	16	14	11	9
20 /10.	127	60	30	19	14	10	7	6
30 /15.	108	52	26	17	12	8	6	8
30 /20.	100	49	24	15	10	7	7	8
40 /25.	96	47	23	14	10	6	7	8
40 /30.	93	46	22	14	10	6	9	10

INITIAL TIMING ERROR AT REGION A $t_{EA}(0)$ = 2.8 μs

CNPU/CNPD	b = .05	.1	.2	.3	.4	.5	.6	.7
20 / 0.	***	107	53	35	26	21	17	14
20 / 5.	153	71	36	24	17	13	10	8
20 /10.	114	56	28	18	13	10	7	6
30 /15.	99	49	24	16	11	8	5	8
30 /20.	92	46	23	14	10	7	6	10
40 /25.	88	44	22	14	9	6	6	11
40 /30.	86	43	21	13	9	6	7	12

(NOTE: *** denotes no convergence with satellite motion)

T A B L E XVIII

(case II)

TOTAL NUMBER OF ITERATIONS
REQUIRED TO ACHIEVE SYNCHRONIZATION

CHANGE IN PATH DELAY DUE TO SATELLITE MOTION t_M = 18 ns

INITIAL TIMING ERROR AT REGION A $t_{EA}(0)$ = 1.8 μs

CNRJ/CNRD	b=.0E	.1	.2	.3	.4	.5	.6	.7
20 / 0.	***	125	58	38	29	22	19	15
20 / 5.	179	65	36	24	18	14	11	9
20 /10.	121	48	29	18	14	10	8	6
30 /15.	103	40	24	17	11	9	6	8
30 /20.	95	34	23	15	10	8	7	10
40 /25.	91	37	21	14	10	7	8	11
40 /30.	88	34	21	14	10	6	8	12

INITIAL TIMING ERROR AT REGION A $t_{EA}(0)$ = 1.6 μs

CNRJ/CNRD	b=.0E	.1	.2	.3	.4	.5	.6	.7
20 / 0.	***	110	54	35	27	21	17	14
20 / 5.	136	58	34	22	17	13	10	8
20 /10.	103	43	26	17	13	9	7	6
30 /15.	90	33	23	15	10	8	6	8
30 /20.	83	3*	21	14	9	7	7	10
40 /25.	80	27	20	13	9	6	8	11
40 /30.	78	30	20	13	9	6	8	12

INITIAL TIMING ERROR AT REGION A $t_{EA}(0)$ = 1.4 μs

CNRJ/CNRD	b=.0E	.1	.2	.3	.4	.5	.6	.7
20 / 0.	209	86	46	31	23	18	16	13
20 / 5.	118	54	31	21	16	12	10	7
20 /10.	92	39	25	16	12	9	6	5
30 /15.	81	31	21	14	10	7	5	7
30 /20.	76	25	20	13	9	6	6	9
40 /25.	73	28	19	12	8	5	7	10
40 /30.	72	23	19	12	8	5	7	11

(NOTE: *** denotes no convergence with satellite motion)

T A B L E XIX

(case II)

TOTAL NUMBER OF ITERATIONS REQUIRED TO ACHIEVE SYNCHRONIZATION

CHANGE IN PATH DELAY DUE TO SATELLITE MOTION t_M= 25 ns

INITIAL TIMING ERROR AT REGION A $t_{EA}(0)$= 1.8 μs

CNRU/CNRD	b =.05	.1	.2	.3	.4	.5	.6	.7
20 / 0.	***	152	59	38	28	22	17	15
20 / 5.	***	82	39	25	18	14	11	9
20 /10.	167	53	28	19	13	10	8	6
30 /15.	117	44	25	16	11	8	5	8
30 /20.	103	41	22	14	10	8	7	10
40 /25.	97	37	22	14	10	7	7	11
40 /30.	96	38	21	13	9	7	8	11

INITIAL TIMING ERROR AT REGION A $t_{EA}(0)$= 1.6 μs

CNRU/CNRD	b =.05	.1	.2	.3	.4	.5	.6	.7
20 / 0.	***	117	52	35	25	20	17	14
20 / 5.	190	63	33	22	15	12	9	8
20 /10.	110	47	26	17	12	9	7	6
30 /15.	92	40	23	15	10	7	5	8
30 /20.	85	36	20	13	9	7	7	10
40 /25.	81	34	20	13	9	6	7	11
40 /30.	79	34	19	12	8	6	8	11

INITIAL TIMING ERROR AT REGION A $t_{EA}(0)$= 1.4 μs

CNRU/CNRD	b =.05	.1	.2	.3	.4	.5	.6	.7
20 / 0.	***	104	50	33	25	19	16	13
20 / 5.	131	57	31	20	15	11	9	7
20 /10.	93	42	24	15	11	9	6	5
30 /15.	80	36	21	14	10	6	4	7
30 /20.	75	33	19	12	9	6	6	9
40 /25.	72	32	19	12	9	5	6	10
40 /30.	70	32	19	11	7	5	7	10

(NOTE: *** denotes no convergence with satellite motion)

TABLE XX

Ultimate value of the timing error (in ns)
(rms timing error at Reg. C after large number of iterations)

Change in path delay due to satellite motion $t_M = 0$

CNR_U/CNR_D	b = .2	.3	.4	.5	.6	.7	(μs/volt)
20/0	37.8	47.3	55.9	64.0	71.9	79.7	
20/5	19.5	24.7	29.6	34.3	39.2	44.3	
20/10	11.3	14.5	17.5	20.7	24.1	27.8	
30/15	6.5	8.3	10.2	12.2	14.5	17.2	
30/20	3.8	4.9	6.0	7.3	8.7	10.5	
40/25	1.9	2.5	3.0	3.7	4.5	5.5	
40/30	0.7	0.9	1.2	1.4	1.7	2.1	

Change in path delay due to satellite motion $t_M = 18$ ns

CNR_U/CNR_D	b = .2	.3	.4	.5	.6	.7	(μs/volt)
20/0	19.8	89.3	79.7	78.5	81.2	86.1	
20/5	79.2	56.8	48.4	46.0	46.8	49.4	
20/10	61.3	42.6	34.7	31.6	31.2	32.6	
30/15	53.3	36.2	28.3	24.4	22.8	22.9	
30/20	49.3	33.1	25.3	20.9	18.5	17.4	
40/25	47.4	31.7	23.9	19.3	16.4	14.6	
40/30	46.3	30.9	23.2	18.6	15.5	13.4	

Change in path delay due to satellite motion $t_M = 25$ ns

CNR_U/CNR_D	b = .2	.3	.4	.5	.6	.7	(μs/volt)
20/0	162.4	115.4	96.7	89.9	89.1	91.6	
20/5	108.4	75.2	60.9	54.7	52.8	53.7	
20/10	84.4	57.5	45.2	39.2	36.6	36.4	
30/15	73.7	49.6	38.1	31.8	28.4	27.1	
30/20	68.4	45.8	34.6	28.2	24.3	22.0	
40/25	65.8	43.9	33.0	26.6	22.4	19.6	
40/30	64.3	42.9	32.1	25.7	21.5	18.4	

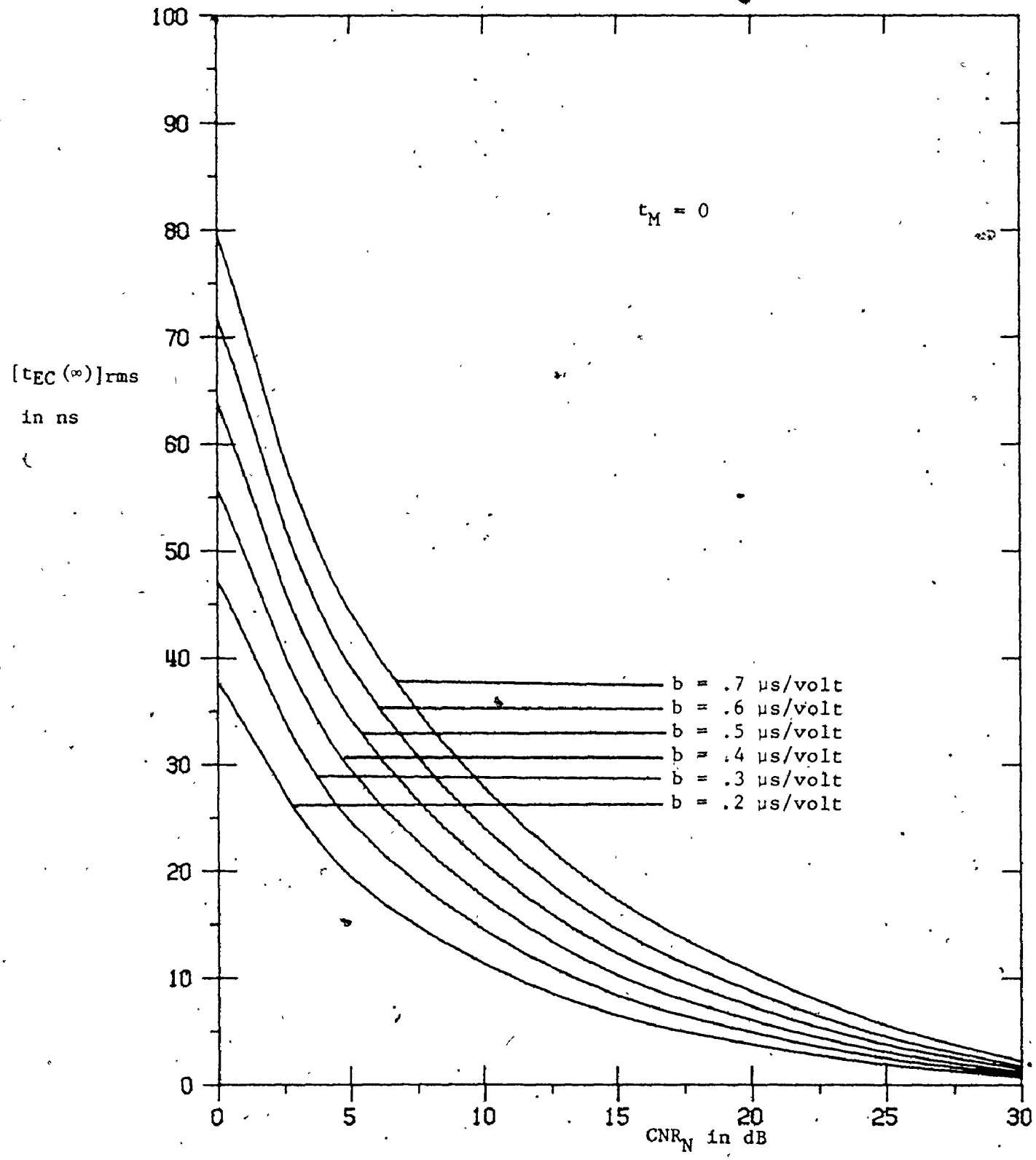

Fig. 5.21 The rms value of the timing error at Reg. C after large number of iterations (ultimate value of the timing error) vs. CNR_N and the timing circuits constant b ($t_M = 0$)

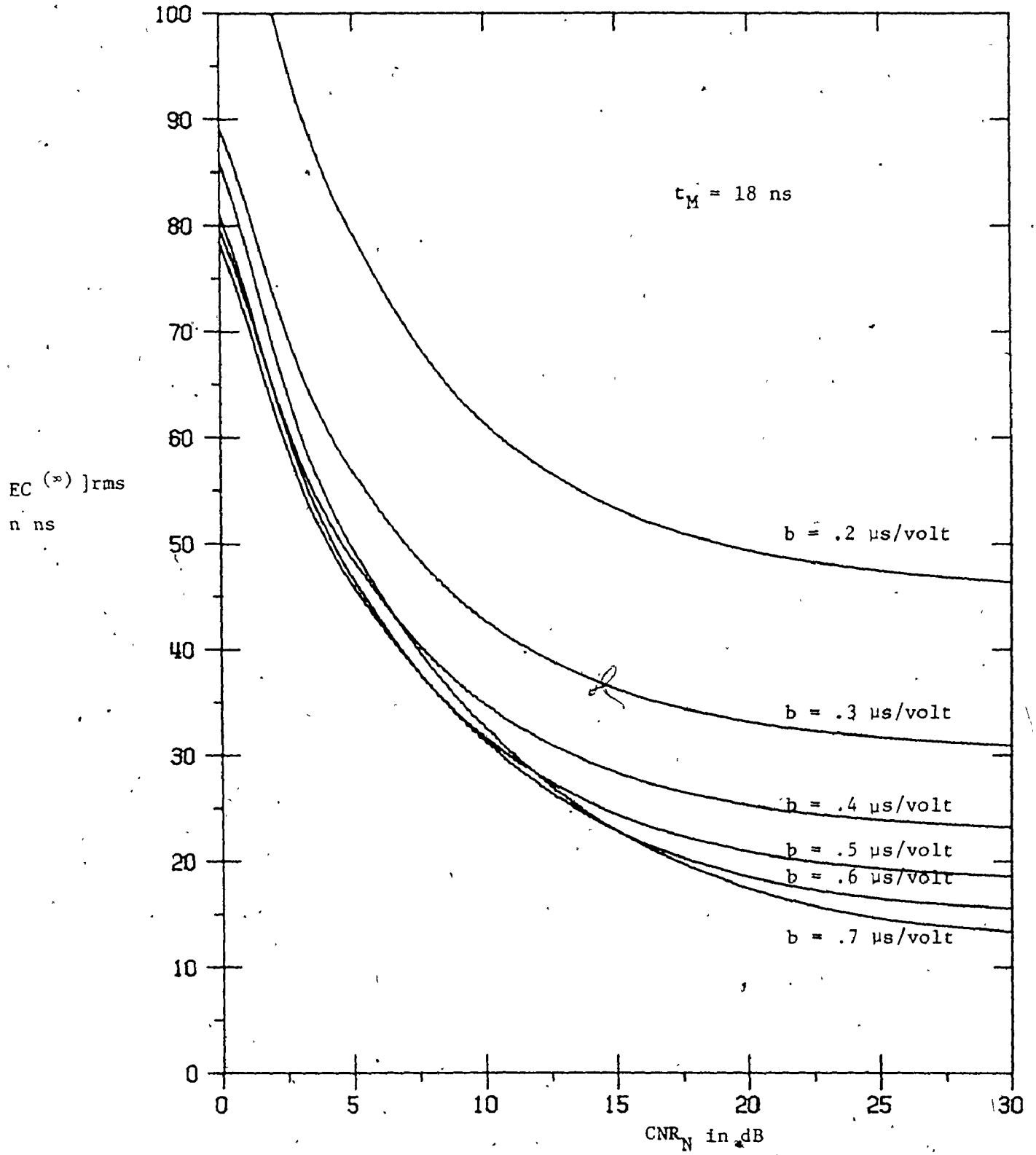

Fig. 5.22 The rms value of the timing error at Reg. C after large number of iterations (ultimate value of the timing error) vs. CNR_N and the timing circuits constant b (t_M = 18 ns)

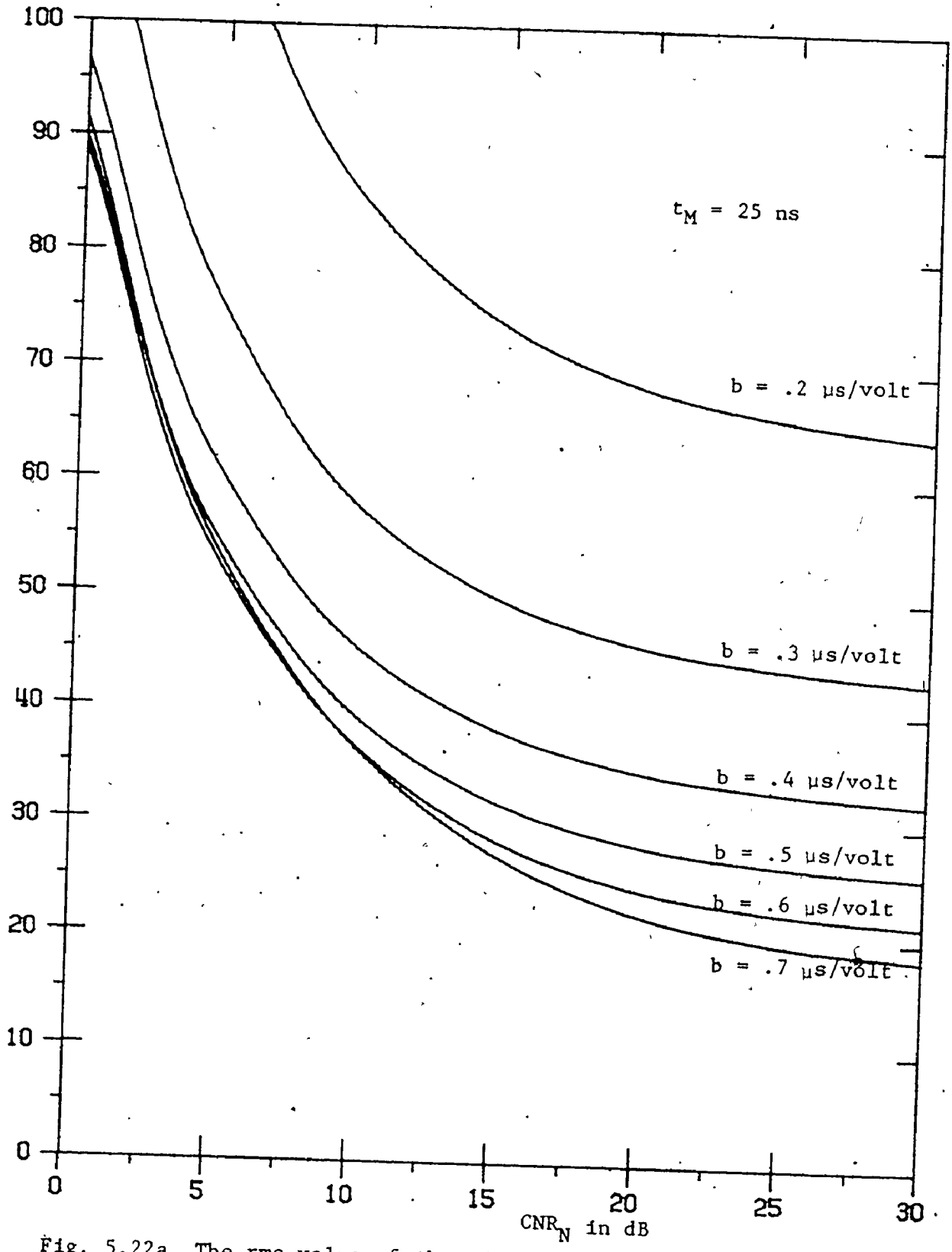

Fig. 5.22a The rms value of the timing error at Reg. C after large number of iterations (ultimate value of the timing error) vs. CNR_N and the timing circuits constant b (t_M = 25 ns)

```
LABEL,TAPE2,P,D=HI,L=      ,T=999,NORING,VSN=-214.          READ/-214.
FTN(OPT=2)
LGO.
/*      6-00 END OF RECORD
        PROGRAM MTN (INPUT,OUTPUT,PUNCH,TAPE5=INPUT,TAPE6=OUTPUT,
       ,TAPE7=PUNCH,TAPE2)
        DIMENSION XI1(200),XI2(200),YI1(200),YI2(200)
        DIMENSION YEVE1(200),XEVE2(200),YEVE1(200),YEVE2(200)
        DIMENSION TE(200),Y(1000),EVE1(200),EVE2(200),TEVE1(200)
        DIMENSION  X(200),          EEVE2(200),XTE(40),YEVE2(40)
        COMMON /TT/ A,C1,C2,K6,NT1,NT2
        REAL K6
C-------------------------------------------------------------------
CC-    THIS PROGRAM SIMULATES THE SIGNAL S12(T) PRIOR              -
CC-    TO INTEGRATION, THE EXPECTED VALUE, AND THE MEAN SQUARE     -
CC-    VALUE OF ITS INTEGRAL (I.E. THE ERROR VOLTAGE)              -
CC-    IT ALSO CALCULATES THE EXPECTED VALUE OF THE ERROR          -
CC-    VOLTAGE OBTAINED FROM THE THEORY                            -
CC-    AND APPROXIMATES SMOOTH CURVES FOR THE SECOND-ORDER         -
CC-    ERROR DETECTION CHARACTERISTICS                             -
C-------------------------------------------------------------------
        DATA TO,TP,TW/4.,2.,2./
        DATA N,NN,MM/200,22,40/
        DATA A,C1,K6/1.,1.,1./
C          N=NUMBER OF SAMPLES FORMING THE SIGNAL S12(T) PRIOR
CC C       TO INTEGRATION
CCC        TO= INPUT GATE DURATION
CCC        TP= PSK SYNC BURST DURATION
CCC        TW= SYNC WINDOW DURATION
CCC        C1= TOTAL GAIN OF THE SYNCHRONIZATION LOOP
CCC        K6= GAIN OF THE INPUT AMPLIFIER (EARTH STATION)
C          A= VOLTAGE LEVEL OF THE PSK SYNC BURST
        C2=.1
        PN=.5
        SPN=SQRT(PN)
C          C2,PPN   APPROPRIATE VALUES OF THE UPLINK LOOP GAIN
CC         AND THE MEAN NOISE POWER  YIELDING THE ABOVE CNRU/CNRD S
        H=TO/FLOAT(N)
C          H= THE STEPSIZE BETWEEN TWO SUCCESSIVE SAMPLES
        DT=(TO-TW)/2.
        DT1=TW
        NT=P+MM
C*********************
C     CALCULATE THE DC STAMT C
CC          C=(A*C1)*F(CNR)      WHERE  F(CNR) IS AFUNCTION OF THE
CC            CARRIER-TO-NOISE RATIO AND VARIES FROM .1 (FOR CNR=10 DB)
C             TO  1. (FOR VERY HIGH CNR)
        PI=ACOS(-1.)
         CNRD=(C1*A)**2/(K6**2*PN)/2.
        CNRU=(C1*A)**2/(C2**2*PN)/2.
        CNRN=(CNRU*CNRD)/(CNRU+CNRD)
        IF (CNRN.GT.6TE.) GO TO 1100
             C=(A*C1)*SQRT(PI)*(EXP(-CNRN)*CHYP(CNRN)-1.)/SQRT(CNRN)/2.
        GO TO 1200
 1100       C=(C1*A)*(1.-SQRT(PI)/SQRT(CNRN)/2.)
 1200 CONTINUE
C*********************
```

```
      DO 5555 LSW=1,2
C        LSW= 1  CORRESPONDS TO CASE I.  2*TW<TP
C        LSW= 2  CORRESPONDS TO CASE II.   TW<TP<2*TW
      IF(LSW.EQ.2) TP=3
      DT2=TP/2
      TE(1)=-(TP+TW)/2.
      IF (LSW.EQ.2)  GO TO 101
      TE(1+   MM)=-(TP-TW)/2.
      TE(1+2*MM)=-TW/2.
      TE(1+3*MM)=TW/2.
      TE(1+4*MM)=(TP-TW)/2.
      GO TO 102
  101 CONTINUE
                    TE(1+   MM)=-TW/2.
                    TE(1+2*MM)=-(TP-TW)/2.
                    TE(1+3*MM)=(TP-TW)/2.
                    TE(1+4*MM)=TW/2.
  102 CONTINUE
C*$$**********************************************************************
            DO 1000 M=1,MM
      IF (M.EQ.MM)  GO TO 104
      IF (LSW.EQ.2)  GO TO 103
      TE(M+1)=TE(M)+TW/FLOAT(MM)
      TE(1+M+   MM)=TE(M+   MM)+(TP/2.-TW)/FLOAT(MM)
      TE(1+M+2*MM)=TE(M+2*MM)+TW/FLOAT(MM)
      TE(1+M+3*MM)=TE(M+3*MM)+(TP/2.-TW)/FLOAT(MM)
      TE(1+M+4*MM)=TE(M+4*MM)+TW/FLOAT(MM)
      GO TO 104
  103 CONTINUE
                   TE(M+1)=TE(M)+TP/2./FLOAT(MM)
                    TE(1+M+   MM)=TE(M+   MM)+(TW-TP/2.)/FLOAT(MM)
                    TE(1+M+2*MM)=TE(M+2*MM)+(TP   -TW)/FLOAT(MM)
                    TE(1+M+3*MM)=TE(M+3*MM)+(TW-TP/2.)/FLOAT(MM)
                    TE(1+M+4*MM)=TE(M+4*MM)+TP/2./FLOAT(MM)
  104 CONTINUE
      DTA1=(TW-TP)/2.+TE(1+4*MM)
      DTA2=(TP+TW)/2.-TE(1+4*MM)
      DTB1=(TW-TP)/2.+TE(1+3*MM)
      DTB2=TW/2.     -TE(M+3*MM)
      DTC1=TW/2.     +TE(M+2*MM)
      DTC2=TW/2.     -TE(M+2*MM)
      DTD1=TW/2.     +TE(M+MM)
      DTD2=(TW-TP)/2.-TE(M+MM)
      DTE1=(TP+TW)/2.+TE(M)
      DTE2=(TW-TP)/2.-TE(M)
      SPA1=0.
      SPB1=0.
      SPC1=0.
      SPD1=0.
      SPE1=0.
      SPA2=0.
      SPB2=0.
      SPC2=0.
      SPD2=0.
      SPE2=0.
```

```
      DO 2000 LL=1,NN
C*      READ IN NORMALIZED SAMPLES (ZERO MEAN,MEAN POWER=1) OF GAUSSIAN NOI
        READ  (2) (XI1(I),XI2(I),XII1(I),XII2(I),
     ,YI1(I),YI2(I),YII1(I),YII2(I),I=1,N)
        IF (EOF(2)) 2001,2002
 2001 REWIND 2
 2002 CONTINUE
C**   X OR Y
C         X= IN-PHASE NOISE COMPONENT
C         Y= QUADRATURE NOISE COMPONENT
C**   I OR II
C         I   CORRESPONDS TO THE WA FREQUENCY-PART OF THE FSK SYNC BURST
C         II  CORRESPONDS TO THE WB FREQUENCY-PART OF THE FSK SYNC BURST
C**   1 OR 2
C         1   CORRESPONDS  TO THE UPLINK NOISE
C         2   CORRESPONDS  TO THE DOWNLINK NOISE
C         (SEE CHAPTER 3)
C
C*      MULTIPLY WITH SQR  TO OBTAIN GAUSSIAN NOISE SAMPLES
C*      WITH THE PROPER MEAN POWER
        DO 222 I=1,N
        XI1 (I)=SQR*XI1 (I)
        YI1 (I)=SQR*YI1 (I)
        XI2 (I)=SQR*XI2 (I)
        YI2 (I)=SQR*YI2 (I)
        XII1(I)=SQR*XII1(I)
        YII1(I)=SQR*YII1(I)
        XII2(I)=SQR*XII2(I)
        YII2(I)=SQR*YII2(I)
 222    CONTINUE

C** R E G I O N  A
C         REGION A     (TP-TW)/2 < TE < (TP+TW)/2     FOR CASE I.
C                  OR      TW/2 < TE < (TP+TW)/2     FOR CASE II.
C*      DETERMINE THE LIMITS NT1,NT2 FOR FUNC1  (DOWNLINK NOISE)
        NT1=1
        NT2=DT/H
C           CALL FUNC1 TO SUPPLY THE ARRAY X( ) WITH SIGNAL SAMPLES
C           FROM NT1=1 TO NT2=DT/H
C*      FUNC1=K6*(SQR*(YI2**2+YII2**2)-SQRT(XII2**2+YII2**2))
        CALL FUNC1  (XI2,YI2,YII2,YII2,NN,X)
C*      DETERMINE THE LIMITS NT1,NT2 FOR FUNC4  (UPLINK PLUS DOWNLINK NOISE
        NT1=NT2+1
        NT2=(DT+DTA1)/H
C           CALL FUNC4 TO SUPPLY THE ARRAY X( ) WITH SIGNAL SAMPLES
C           FROM NT1 TO NT2
C*      FUNC4=SQRT((C2*XI1+K6*XI2)**2+(C2*YI1+K6*YI2)**2)
C*           -SQRT((C2*XII1+K6*XII2)**2+(C2*YII1+K6*YII2)**2)
        CALL FUNC4  (XI1,YI1,XI2,YI2,XII1,YII1,XII2,YII2,NN,X)
C*      DETERMINE THE LIMITS NT1,NT2 FOR FUNC2  (SIGNAL PLUS NOISE)
        NT1=NT2+1
        NT2=(DT+DTA1+DTA2)/H
C           CALL FUNC2 TO SUPPLY THE ARRAY X( ) WITH SIGNAL SAMPLES
C           FROM NT1 TO NT2
C*      FUNC2=SQRT((C1*A+C2*XI1+K6*XI2)**2+(C2*YI1+K6*YI2)**2)
C*           -SQRT((C2*XII1+K6*XII2)**2+(C2*YII1+K6*YII2)**2)
        CALL FUNC2  (XI1,YI1,XI2,YI2,XII1,YII1,XII2,YII2,NN,X)
C*      DETERMINE THE LIMITS NT1,NT2 FOR FUNC1  (DOWNLINK NOISE)
```

```
      NT1=NT2+1
      NT2=N
C           CALL FUNC1 TO SUPPLY THE ARRAY X( ) WITH SIGNAL SAMPLES
C           FROM NT1 TO NT2=N
      CALL FUNC1  (XI2,YI2,XII2,YII2,NN,X)
C*     NOW THE ARRAY X( )  CONTAINES THE SAMPLED SIGNAL S12(T)
CCCC
CCCC        INTEGRATE THE SAMPLED SIGNAL  S12(T) AND OBTAIN
C           ITS INTEGRAL VALUE
      CALL ZINT(H,X,N,Z)
      SRA1=SRA1+Z
      SRA2=SRA2+Z**2

C** R E G I O N  B
CCC         REGION B              TW/2 < TE < (TP-TW)/2     FOR CASE I.
CCC                  OR   -(TP-TW)/2 < TE < TW/2           FOR CASE II.
C*     REPEAT FOR REGION  B
      NT1=1
      NT2=DT/H
      CALL FUNC1  (XI2,YI2,XII2,YII2,NN,X)
      IF (LSW.EQ.1)  GO TO 2301
      NT1=NT2+1
          NT2=(DT+DTB1)/H
      CALL FUNC4 (XI1,YI1,XI2,YI2,XII1,YII1,XII2,YII2,NN,X)
      NT1=NT2+1
          NT2=(DT+DTB1+DT2)/H
      CALL FUNC2 (XI1,YI1,XI2,YI2,XII1,YII1,XII2,YII2,NN,X)
      NT1=NT2+1
          NT2=(DT+DTB1+DT2+DTB2)/H
      CALL FUNC3 (XI1,YI1,XI2,YI2,XII1,YII1,XII2,YII2,NN,X)
      GO TO 2302
 2301 CONTINUE
      NT1=NT2+1
          NT2=(DT+ DT1)/H
      CALL FUNC2  (XI1,YI1,XI2,YI2,XII1,YII1,XII2,YII2,NN,X)
 2302 CONTINUE
      NT1=NT2+1
      NT2=N
      CALL FUNC1  (XI2,YI2,XII2,YII2,NN,X)
      CALL ZINT(H,X,N,Z)
      SRB1=SRB1+Z
      SRB2=SRB2+Z**2

C** R E G I O N  C
C           REGION C              -TW/2 < TE < TW/2          FOR CASE I.
CCC                  OR   -(TP-TW)/2 < TE < (TP-TW)/2      FOR CASE II.
C*     REPEAT FOR REGION  C
      NT1=1
      NT2=DT/H
      CALL FUNC1  (XI2,YI2,XII2,YII2,NN,X)
      NT1=NT2+1
          NT2=(DT+DTC1)/H
      CALL FUNC2  (XI1,YI1,XI2,YI2,XII1,YII1,XII2,YII2,NN,X)
      NT1=NT2+1
          NT2=(DT+DTC1+DTC2)/H
      CALL FUNC3  (XI1,YI1,XI2,YI2,XII1,YII1,XII2,YII2,NN,X)
      NT1=NT2+1
      NT2=N
      CALL FUNC1  (XI2,YI2,XII2,YII2,NN,X)
      CALL ZINT(H,X,N,Z)
```

```
      SRC1=SRC1+Z
      SRC2=SRC2+Z**2
C*      REPEAT FOR REGION  D

C** R E G I O N  D
C           REGION D      -(TP-TW)/2 < TE < -TW/2          FOR CASE I.
C                     OR  -(TP+TW)/2 < TE < -TW/2      FOR CASE II.
      NT1=1
      NT2=DT/H
      CALL FUNC1  (XI2,YI2,XII2,YII2,NN,X)
      IF (LSW.EQ.1)  GO TO 1201
      NT1=NT2+1
      NT2=(DT+DTD1)/H
      CALL FUNC2 (XI1,YI1,XI2,YI2,XII1,YII1,XII2,YII2,NN,X)
      NT1=NT2+1
           NT2=(DT+DTD1+DT2)/H
      CALL FUNC3 (XI1,YI1,XI2,YI2,XII1,YII1,XII2,YII2,NN,X)
      NT1=NT2+1
           NT2=(DT+DTD1+DT2+DTD2)/H
      CALL FUNC4 (XI1,YI1,XI2,YI2,XII1,YII1,XII2,YII2,NN,X)
      GO TO 1202
 1201 CONTINUE
      NT1=NT2+1
           NT2=(DT+DT1)/H
      CALL FUNC3  (XI1,YI1,XI2,YI2,XII1,YII1,XII2,YII2,NN,X)
 1202 CONTINUE
      NT1=NT2+1
      NT2=N
      CALL FUNC1  (XI2,YI2,XII2,YII2,NN,X)
      CALL ZINT(H,X,N,Z)
      SRD1=SRD1+Z
      SRD2=SRD2+Z**2

C** R E G I O N  E
C           REGION E      -(TP+TW)/2 < TE < -(TP-TW)/2   FOR CASE I.
C                     OR      -TW/2 < TE < -(TP-TW)/2 FOR CASE II.
C*      REPEAT FOR REGION  E
      NT1=1
      NT2=DT/H
      CALL FUNC1  (XI2,YI2,XII2,YII2,NN,X)
      NT1=NT2+1
           NT2=(DT+DTE1)/H
      CALL FUNC3  (XI1,YI1,XI2,YI2,XII1,YII1,XII2,YII2,NN,X)
      NT1=NT2+1
           NT2=(DT+DTE1+DTE2)/H
      CALL FUNC4  (XI1,YI1,XI2,YI2,XII1,YII1,XII2,YII2,NN,X)
      NT1=NT2+1
      NT2=N
      CALL FUNC1  (XI2,YI2,XII2,YII2,NN,X)
      CALL ZINT(H,X,N,Z)
      SRE1=SRE1+Z
      SRE2=SRE2+Z**2
 2000   CONTINUE
      EVE1(M+0*MM)=SRA1/FLOAT(N)
      EVE1(M+3*MM)=SRB1/FLOAT(N)
      EVE1(M+2*MM)=SRC1/FLOAT(N)
      EVE1(M+ *MM)=SRD1/FLOAT(N)
      EVE1(M)     =SRE1/FLOAT(N)
      EVE2(M+0*MM)=SRA2/FLOAT(N)
      EVE2(M+3*MM)=SRB2/FLOAT(N)
```

```
      EVE2(M+2*MM)=SEC2/FLOAT(NN)
      EVE2(M+  MM)=SEC2/FLOAT(NN)
      EVE2(M)     =SEE2/FLOAT(NN)
 1000 CONTINUE
C*       NOW THE ARRAYS EVE1( ) AND EVE2( ) CONTAIN THE EXPECTED
C        VALUE (FIRST AND SECOND MOMENTS) OF THE ERROR VOLTAGE
C*       THE ARRAY TE( ) CONTAINS THE CORRESPONDING VALUES
C        OF THE TIMING ERROR
C*$$$$$$$$$$$$$$$$$$$$$$$$$$$$$$$$$$$$$$$$$$$$$$$$$$$$$$$$$$$$$$$$$$$$$$$$
C*$$$$$$$$$$$$$$$$$$$$$$$$$$$$$$$$$$$$$$$$$$$$$$$$$$$$$$$$$$$$$$$$$$$$$$$$
C   C U R V E   F I T T I N G
      DO 6000 K=1,2
      DO 6001 I=1,MM
      KK=4*(K-1)*MM+I
      XTE(I)=TE(KK)
 6001 YEVE2(I)=EVE2(KK)
      CALL QUALSQ (XTE,YEVE2,MM,ALPHA,BETA,GAMMA)
      DO 6002 I=1,MM
      KK=4*(K-1)*MM+I
 6002 AEVE2(KK)=ALPHA*TE(KK)*TE(KK)+BETA*TE(KK)+GAMMA
 6000 CONTINUE
      IF (LSW.EQ.2) GO TO 6222
      DO 6100 K=1,3,2
      SS=0.0
      DO 6101 I=1,MM
      KK=K*MM+I
 6101 SS=SS+EVE2(KK)
      GAMMA=SS/FLOAT(MM)
      WRITE (6,70)GAMMA
      DO 6102 I=1,MM
      KK=K*MM+I
 6102 AEVE2(KK)=GAMMA
 6100 CONTINUE
      GO TO 6111
 6222 CONTINUE
      DO 6200 K=1,3,2
      DO 6201 I=1,MM
      KK=K*MM+I
      XTE(I)=TE(KK)
 6201 YEVE2(I)=EVE2(KK)
      CALL QUALSQ (XTE,YEVE2,MM,ALPHA,BETA,GAMMA)
      DO 6202 I=1,MM
      KK=K*MM+I
 6202 AEVE2(KK)=ALPHA*TE(KK)*TE(KK)+BETA*TE(KK)+GAMMA
 6200 CONTINUE
 6111 CONTINUE
      DO 666  I=1,MM
      XTE(I)=TE(2*MM+I)
  666 YEVE2(I)=EVE2(2*MM+I)
      CALL PARLSQ (XTE,YEVE2,MM,ALPHA,GAMMA)
      DO 6666 I=1,MM
 6666 AEVE2(2*MM+I)=ALPHA*TE(2*MM+I)**2+GAMMA
C        THE ARRAY AEVE2( ) CONTAINS THE VALUES OF THE
C        FITTED CURVES FOR THE MEAN SQUARE (SECOND MOMENT)
C        OF THE ERROR VOLTAGE
C*$$$$$$$$$$$$$$$$$$$$$$$$$$$$$$$$$$$$$$$$$$$$$$$$$$$$$$$$$$$$$$$$$$$$$$$$
```

```
C*******************
CC       CALCULATE THE THEORETICAL EXPECTED VALUE
CC       OF THE ERROR VOLTAGE
C     (SEE CHAPTER 4)
      IF (LSW.EQ.2) GO TO 1111
      GO TO 2222
 1111 CONTINUE
      DO 111 M=1,MM
      TEVE1(M      )=-C*(TE(M      )+(TP+TW)/2.)
      TEVE1(M+  MM)= C*(TE(M+  MM)-(TP-TW)/2.)
      TEVE1(M+2*MM)=2.*C*TE(M+2*MM)
      TEVE1(M+3*MM)= C*(TE(M+3*MM)+(TP-TW)/2.)
      TEVE1(M+4*MM)=-C*(TE(M+4*MM)-(TP+TW)/2.)
  111 CONTINUE
      GO TO 3333
 2222 CONTINUE
      DO 110 M=1,MM
      TEVE1(M      )=-C*(TE(M      )+(TP+TW)/2.)
      TEVE1(M+  MM)=-C*W
      TEVE1(M+2*MM)=2.*C*TE(M+2*MM)
      TEVE1(M+3*MM)= C*W
      TEVE1(M+4*MM)=-C*(TE(M+4*MM)-(TP+TW)/2.)
  110 CONTINUE
 3333 CONTINUE
C*******************
 5555 CONTINUE
      STOP
      END
```

CPTOT 389

```
      SUBROUTINE FUNC1 (XI2,YI2,XII2,YII2,NN,X)
      REAL K6
      COMMON /TT/ A,C1,C2,K6,NT1,NT2
      DIMENSION X(1),XI2(1),YI2(1),XII2(1),YII2(1)
      DO100 I=NT1,NT2
100   X(I)=K6*(SQRT(XI2( I )**2+YI2( I )**2)
     --SQRT(XII2( I )**2+YII2( I )**2))
      RETURN
      END


      SUBROUTINE FUNC2  (XI1,YI1,XI2,YI2,XII1,YII1,XII2,YII2,NN,X)
      REAL K6
      COMMON /TT/ A,C1,C2,K6,NT1,NT2
      DIMENSION X(1),XI2(1),YI2(1),XII2(1),YII2(1)
      DIMENSION XI1(1),YI1(1),XII1(1),YII1(1)
      DO100 I=NT1,NT2
100   X(I)=SQRT((C1*A+C2*XI1( I )+K6*XI2( I ))**2
     ++(C2*YI1( I )+K6*YI2( I ))**2)
     --SQRT((C2*XII1( I )+K6*XII2( I ))**2
     ++(C2*YII1( I )+K6*YII2( I ))**2)
      RETURN
      END


      SUBROUTINE FUNC3  (XI1,YI1,XI2,YI2,XII1,YII1,XII2,YII2,NN,X)
      REAL K6
      COMMON /TT/ A,C1,C2,K6,NT1,NT2
      DIMENSION X(1),XI2(1),YI2(1),XII2(1),YII2(1)
      DIMENSION XI1(1),YI1(1),XII1(1),YII1(1)
      DO100 I=NT1,NT2
100   X(I)=SQRT((C2*XI1( I )+K6*XI2( I ))**2
     +          +(C2*YI1( I )+K6*YI2( I ))**2)
     --SQRT((C1*A+C2*XII1( I )+K6*XII2( I ))**2
     +          +(C2*YII1( I )+K6*YII2( I ))**2)
      RETURN
      END


      SUBROUTINE FUNC4  (XI1,YI1,XI2,YI2,XII1,YII1,XII2,YII2,NN,X)
      REAL K6
      COMMON /TT/ A,C1,C2,K6,NT1,NT2
      DIMENSION X(1),XI2(1),YI2(1),XII2(1),YII2(1)
      DIMENSION XI1(1),YI1(1),XII1(1),YII1(1)
      DO100 I=NT1,NT2
100   X(I)=SQRT((C2*XI1( I )+K6*XI2( I ))**2
     +          +(C2*YI1( I )+K6*YI2( I ))**2)
     --SQRT((C2*XII1( I )+K6*XII2( I ))**2
     +      +(C2*YII1( I )+K6*YII2( I ))**2)
      RETURN
      END
```

```
      SUBROUTINE QUALSQ (XTE,YEVE2,MM,ALPHA,BETA,GAMMA)
      DIMENSION XTE(1),YEVE2(1),A(3),B(3),C(3),D(3),E(3,3)
C-----------------------------------------------------------------
CCC         THIS SUBROUTINE CALCULATES THE COEFFICIENTS
CCC         OF A COMPLETE SECOND DEGREE POLYNOMIAL USING
CCC         THE LEAST SQUARES METHOD
C-----------------------------------------------------------------
      SX=0.0   $  SX2=0.0   $  SX3=0.0   $  SX4=0.0   $  SX2Y=0.0
      SXY=0.0  $  SY=0.0
      DO 100 I=1,MM
      X=XTE(I)
      Y=YEVE2(I)
      SX=SX+X
      SX2=SX2+X**Y
      SX3=SX3+X**X**X
      SX4=SX4+X**X**X**X
      SX2Y=SX2Y+X**X**Y
      SXY=SXY+X**Y
      SY=SY+Y
  100 CONTINUE
      A(1)=SX4$          A(2)=SX3$          A(3)=SX2
      B(1)=SX3$          B(2)=SX2$          B(3)=SX
      C(1)=SX2$          C(2)=SX $          C(3)=FLOAT(MM)
      D(1)=SX2Y$         D(2)=SXY$          D(3)=SY
      DO 200 K=1,3
      E(K,1)=A(K)
      E(K,2)=B(K)
  200 E(K,3)=C(K)
      DEN  =(E(1,1)*(E(2,2)*E(3,3)-E(2,3)*E(3,2))
     -      -E(1,2)*(E(2,1)*E(3,3)-E(2,3)*E(3,1))
     -      +E(1,3)*(E(2,1)*E(3,2)-E(3,1)*E(2,2)))
      DO 300 K=1,3
  300 E(K,1)=D(K)
      ALPHA=(E(1,1)*(E(2,2)*E(3,3)-E(2,3)*E(3,2))
     -      -E(1,2)*(E(2,1)*E(3,3)-E(2,3)*E(3,1))
     -      +E(1,3)*(E(2,1)*E(3,2)-E(3,1)*E(2,2)))/DEN
      DO 400 K=1,3
      E(K,1)=A(K)
  400 E(K,2)=D(K)
      BETA =(E(1,1)*(E(2,2)*E(3,3)-E(2,3)*E(3,2))
     -      -E(1,2)*(E(2,1)*E(3,3)-E(2,3)*E(3,1))
     -      +E(1,3)*(E(2,1)*E(3,2)-E(3,1)*E(2,2)))/DEN
      DO 500 K=1,3
      E(K,2)=B(K)
  500 E(K,3)=D(K)
      GAMMA=(E(1,1)*(E(2,2)*E(3,3)-E(2,3)*E(3,2))
     -      -E(1,2)*(E(2,1)*E(3,3)-E(2,3)*E(3,1))
     -      +E(1,3)*(E(2,1)*E(3,2)-E(3,1)*E(2,2)))/DEN
      WRITE (6,1) ALPHA,BETA,GAMMA
    1 FORMAT(//,' ALPHA=',F18.9,'  BETA=',F18.9,'  GAMMA=',F18.9)
      RETURN
      END
```

```
      SUBROUTINE PARLSQ (XTE,YEVE2,MM,ALPHA,GAMMA)
      DIMENSION XTE(1),YEVE2(1)
C-----------------------------------------------------------------
CC          THIS SUBROUTINE CALCULATES THE COEFFICIENTS
CC          OF A PARABOLA USING THE LEAST SQUARES METHOD
CC          AND A WEIGHTING FUNCTION W(.)=1/((ABS(X(.))+.005)
C-----------------------------------------------------------------
      SW=0.0
      SX2YW=0.0
      SYW=0.0
      SX2W=0.0
      SX4W=0.0
      DO 100 I=1,MM
      X=XTE(I)
      Y=YEVE2(I)
      W=1./(ABS(X)+.005)
      SW=SW+W
      SX2YW=SX2YW+X*X*Y*W
      SYW=SYW+Y*W
      SX2W=SX2W+X*X*W
      SX4W=SX4W+X**4*W
  100 CONTINUE
      DEN=SW*SX4W-SX2W*SX2W
      ALPHA=(SW*SX2YW-SYW*SX2W)/DEN
      GAMMA=(SYW*SX4W-SX2YW*SX2W)/DEN
      WRITE (6,1) ALPHA,GAMMA
    1 FORMAT (//,'  ALPHA=',F15.7,5X,'  GAMMA=',F15.7)
      RETURN
      END

      SUBROUTINE ZINT(H,X,N,Z)
      DIMENSION X(1)
C-----------------------------------------------------------------
CC          THIS SUBROUTINE CALCULATES THE INTEGRAL VALUE
CC          OF A TABULATED FUNCTION USING THE TRAPEZOIDAL RULE
C-----------------------------------------------------------------
      NN=N-1
      S=.5*H*(X(1)+X(N))
      DO 100 I=2,NN
  100 S=S+H*X(I)
      Z=S
      RETURN
      END

      FUNCTION CHYP(Z)
      REAL K,N
C-----------------------------------------------------------------
CC          THIS SUBROUTINE CALCULATES THE CONFLUENT
CC          HYPERGEOMETRIC FUNCTION 1F1(3/2,1,Z)
C-----------------------------------------------------------------
      A=1.5   $  B=1.   $  N=1.   $  S=1.
      K=A*Z   $  S=S+K
      DO 100 L=1,1000
      A=A+1.  $  B=B+1.  $  N=N+1.
      K=A*K*Z/(B*N)
      S=S+K
  100 CONTINUE
      CHYP=S
      RETURN
      END
```

CHAPTER 6

SUMMARY AND RECOMMENDATIONS

6.1 SUMMARY

The fine synchronization of an earth station to the switching sequence of an SDMA/SS-TDMA satellite system using non-coherent FSK was studied.

Detailed analysis of the synchronization loop was provided. It was shown that the timing error between the earth station and satellite time bases, defined by the sync-window modulation on-board the satellite can be interpreted as an error voltage obtained at the receiver. The relation between the error voltage and the timing error (error detection characteristic) was derived.

The first-order statistics of the error voltage in a noisy environment were evaluated, and the ratio of the expected value of the error voltage to its noise-free value was given as a function of the uplink and downlink carrier-to-noise ratios.

The timing analysis showed that the timing circuits can always provide a reduction in the timing error after each transmission, thus the average timing error can be reduced to zero (assuming stationary satellite) and exact synchronization can be achieved.

It was shown that the performance of the synchronization loop depends on both the carrier-to-noise ratio and the timing circuits constant. The number of iterations required to achieve synchronization was calculated as a function of the timing circuits constant and the carrier-to-noise ratio.

A computer program was developed to simulate and integrate the detected signal. Agreement with theory was demonstrated. The computer simulation program also provided the second-order statistics of the error voltage. Finally, with the aid of the second-order error detection characteristic, the mean square value of the timing error was evaluated.

6.2 RECOMMENDATIONS FOR FURTHER STUDY

Optimization of the parameters of the synchronization loop such as sync-window duration, sync-pulse duration, timing-circuit constant so as to yield fast and accurate synchronization should be carried out.

Faster synchronization can be achieved if a microprocessor is employed: if the values of the error voltage of two or more successive iterations are known, the timing error between the satellite and earth station time bases can be calculated by the microprocessor being properly programmed. Then, by shifting the earth station time base by this amount, synchronization is completed.

REFERENCES

[1] Morgan, W. L., "Communication satellites and new technology", Microwave Systems News, (Technology), April/May, 1974, Vol. 4, No. 2, pp. 64-68.

[2] Pritchard, W. L. and Bargellini, P. L., "Trends in technology for communications satellites", Astronautics and Aeronautics, April, 1972, pp. 36-42.

[3] Maloney, E. D., "Advanced electron tubes for next generation satellite telecommunications", Microwave Journal, May and July, 1976.

[4] Schmidt, W. G., "An on-board switched multiple-access system for millimeter-wave satellites", Proceedings INTELSAT/IEE Conf. on Digital Satallite Communications, 1969, pp. 399-407.

[5] Rozec, X. and Assal, F., "Microwave switch matrix for communications satellites", IEEE Conf. on Communications, 1976 (ICC '76), Philadelphia, Pennsylvania, June 14-16, 1976, pp. 35-13 to 35-17.

[6] Schmidt, W. G., Cooperman, R. S., Kaiser, J., Shimasaki, N., "Multiple-access technology: present and near-future", COMSAT Laboratories technical memorandum, Report no. CL-19-71, April 5, 1971.

[7] "A review of satellite systems technology", by the Satellite Committee of the Aerospace and Electronics Systems Group IEEE, September 1972, p. 43.

[8] Schwartz,J. W.,'Aein, J. M., Kaiser, J.,' "Modulation techniques for multiple-access to a hard-limiting satellite repeater", Proceedings IEEE, Vol. 54, No. 5, May 1966, pp. 763-777.

[9] Werth, A. M., "SPADE: a pcm.fdma demand-assignment system for satellite-communications", Proceedings INTELSAT/IEE International Conference on Digital Satellite Communications, 1969, pp. 51-68.

[10] Gabbard, O. G., Kaul, P., "Time division multiple access", EASCON '74, pp. 179-183.

[11] Abramson, N., "Packet switching with satellites", 1973 National Computer Conference AFIPS Conference Proceedings, Vol. 42, AFIPS Press 1973, pp. 695-702.

[12] Abramson, N., "Another alternative for computer communications: ALOHA system", Fall, 1970, Joint Computer Conference, AFIPS Conference Proceedings, Vol. 37, pp. 281-285.

[13] Kleinrock, L. and Lam, S. S., "Packet switching in a slotted satellite system", 1973 National Computer Conference, AFIPS Conference Proceedings, Vol. 42, AFIPS Press 1973, pp. 703-710.

[14] Schmidt, W. G. and Cooperman, R., "A Satellite-switched sdma/tdma system for a wideband multibeam satellite", IEEE International Conference on Communications, 1973 (ICC '73), Seattle, Washington, June 11-13, 1973, pp. 12-7 to 12-12.

[15] Hulteberg, R. M., Jean, F. H., Jones, M. E., "Time division multiple access for military communications satellites", IEEE Trans. on Aerospace and Electronics Systems, December 1965, Vol. AES-1, No. 3, pp. 273-282.

[16] Sekimoto, T. and Puente, J. G., "A satellite time-division multiple access experiment", IEEE Trans. on Communications Technology, Vol. COM-16, No. 4, August, 1968, pp. 581-588.

[17] Gabbard, O. G., "Design of a satellite time-division multiple access burst synchronizer", IEEE Trans. on Communications Technology, Vol. COM-16, No. 4, August, 1968, pp. 589-596.

[18] Schremp, W. and Sekimoto, T., "Unique word detection in digital burst communications", IEEE Trans on Communications Technology, Vol. COM-16, No. 4, August, 1968, pp. 597-605.

[19] Shimasaki, N. and Rapuano, R., "Synchronization for a communications distribution center on-board a satellite", International Conference on Communications, 1971 (ICC '71), Montreal, Canada, June 14-16, 1971, pp. 42-20 to 42-25.

[20] Rapuano, R. A., Shimasaki, N., "Synchronization of earth stations to a satellite switched sequence", AIAA 4th Communications Satellite System Conference, Washington, D.C., April 24-26, 1972, AIAA paper No. 72-545.

[21] Carter, C.R., deBuda, R., Haykin, S. S., "A new system synchronization technique for the switching satellite", IEEE Transactions on Communications (accepted for publication).

[22] Carter, C. R., "Synchronization of earth stations to a communications switching satellite", Ph.D. thesis, Department of Electrical Engineering, McMaster University, Hamilton, Ontario, 1974.

[23] Carter, C. R. and Haykin, S. S., "A new synchronization technique for switched tdma satellite systems", IEEE Trans. on Communications Systems, Vol. COM-22, No. , May, 1974, pp. 710-713.

[24] Carter, C. R. and Haykin, S. S., "Fine search synchronization for a switching satellite", Proceedings IEE, Vol. 122, No. 1, January, 1975, pp. 37-43.

[25] Carter, C. R. and Haykin, S. S., "Tracking mode synchronization for a switching satellite", Proceedings IEE, Vol. 122, No. 8, August, 1975, pp. 775-779.

[26] Carter, C. R. and Haykin, S. S., "A laboratory model for the switching satellite synchronization loop", NTC '74, San Diego California, December 2-4, 1974, pp. 134-139.

[27] Carter, C. R. and Haykin, S. S., "A comparison of the signals used for synchronizing to a switching satellite", IEEE Canadian Communications and Power Conference, Montreal, Canada, November 7-8, 1974, pp. 28-29.

[28] Schwartz, M., "Information Transmission, Modulation and Noise", (McGraw-Hill, 1970), pp. 433-434.

[29] Schwartz, M., Bennett, W., Stein, S., "Communications Systems and Techniques", (McGraw-Hill, 1966), pp. 285-286.

[30] ibid., p. 316.

[31] Carter, C. R., Ph.D. thesis, op. cit., p. 98.

[32] Abramowitz, M. and Stegun, I. A., "Handbook of Mathematical Functions", Dover Publications, New York, p. 504.

[33] Carter, C. R., Ph.D. thesis, op. cit., pp. 99-100.

[34] Lubowe, A. G., "Path length variation in a synchronous satellite communications link", Bell System Technical Journal, December, 1968,

pp. 2139-2144.

[35] Blanc-Lapierre, A. and Forter, B., "Theory of Random Functions", Gordon and Breach, 1967, p. 57.

[36] ibid., p. 66.

[37] ibid., p. 123.

[38] Schwartz, M., Bennett, W. and Stein, S., op. cit., p. 14.

[39] ibid., pp. 4 and 7.

[40] Woodward, P. M., "Probability and Information Theory with Applications to RADAR", Pergamon Press, p. 20.

[41] Papoulis, A., "Probability, Random Variables, and Stochastic Processes", McGraw-Hill, 1965, pp. 195-196.

[42] Bechmann, P., "Elements of Applied Probability Theory", Harcourt, Brace and World, 1968, p. 74.

[43] Rice, C. O., "Mathematical analysis of random noise", Bell System Technical Journal, Vol. 23, pp. 228-333, July, 1944, and Vol. 24, pp. 96-157, January, 1945, (reprinted in: N. Wax, "Selected Papers on Noise and Stochastic Processes", Dover Publications, New York, 1954).

[44] Gradshteyn, I. S. and Ryzhik, I. M., "Tables of Integrals, Series and Products", Academic Press, New York, 1965, p. 716.

[45] Spiegel, M. R., "Mathematical Handbook of Formulas and Tables", Schaum's outline series, McGraw-Hill, 1968, p. 138.

[46] Papoulis, A., op. cit., pp. 207-209.

[47] ibid., p. 178.

[48] Scarborough, J. B., "Numerical Mathematical Analysis", 6th edition, 1966, the John's Hopkins Press, p. 142.

[49] ibid., p. 482.

[50] Pennington, R. H., "Introductory Computer Methods and Numerical Analysis", The McMillan Company, New York, 1965, p. 374.